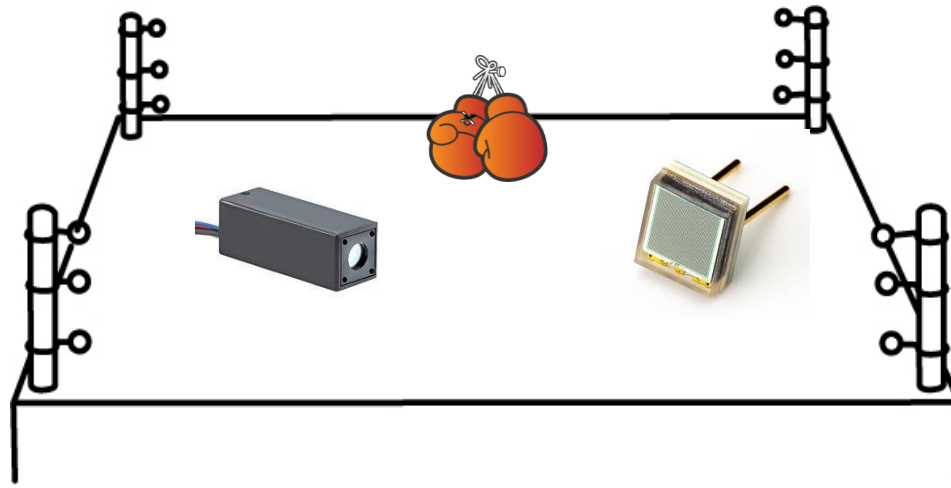


Journée thématique du réseau Photodétecteurs IN2P3

SiPM, PMT, quel photodétecteur utiliser ?



Introduction

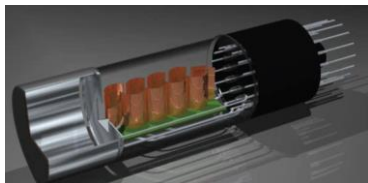
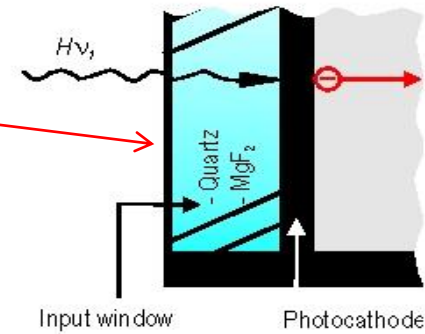
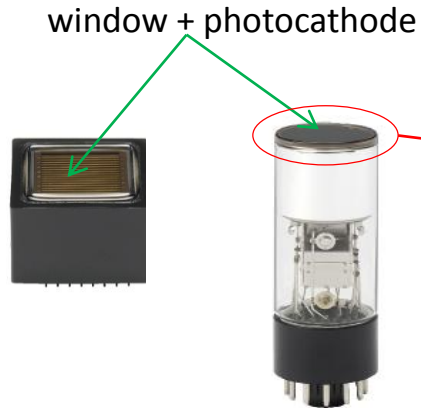
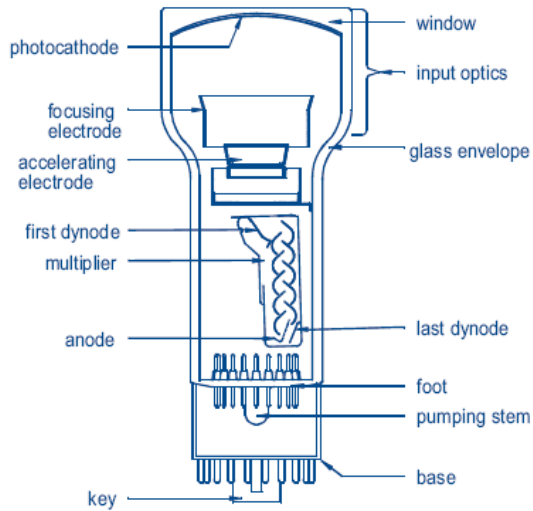
A decorative vertical element on the left side of the slide, consisting of numerous thin, overlapping lines in various colors (red, orange, yellow, green, cyan, blue, purple, magenta) that create a sense of motion and depth.

Outline

Basics, properties and news concerning the:

- PMTs
- MCP-PMTs
- SiPMs





Photoelectron multiplication: secondary emission of electrons by the dynodes
The HV is supplied through a resistive voltage divider

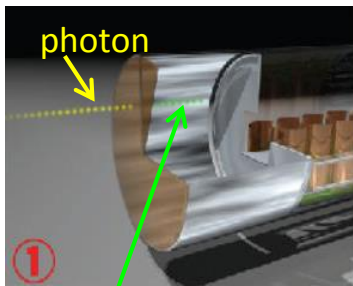
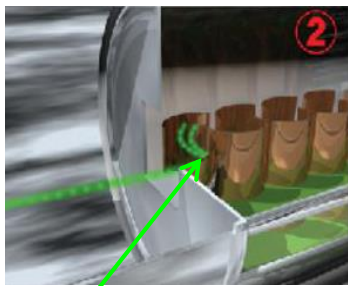
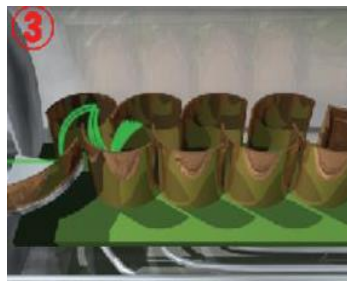


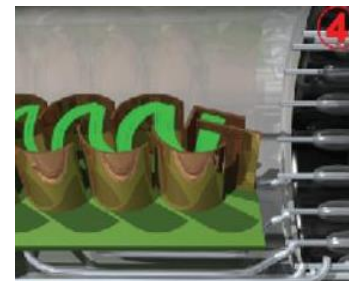
photo-electron

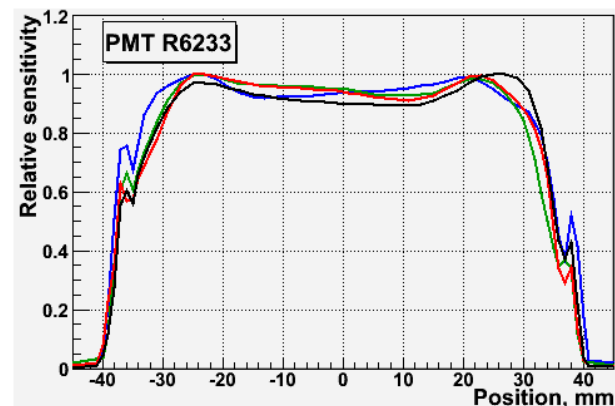
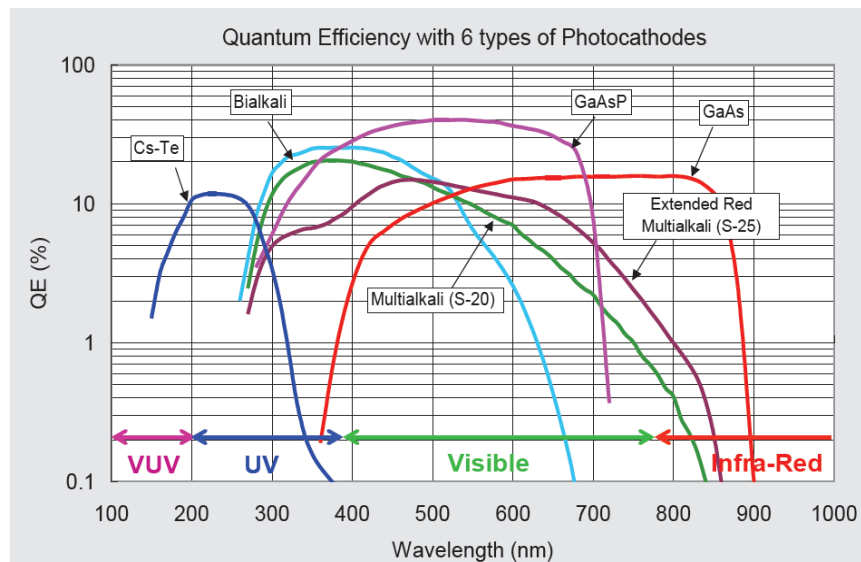


impact on the first dynode



multiplication by n dynodes and signal on the anode

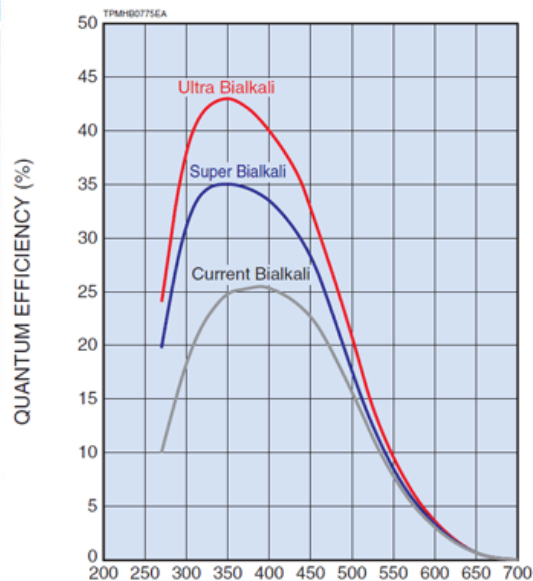




O. Kalekin, RICH 2010

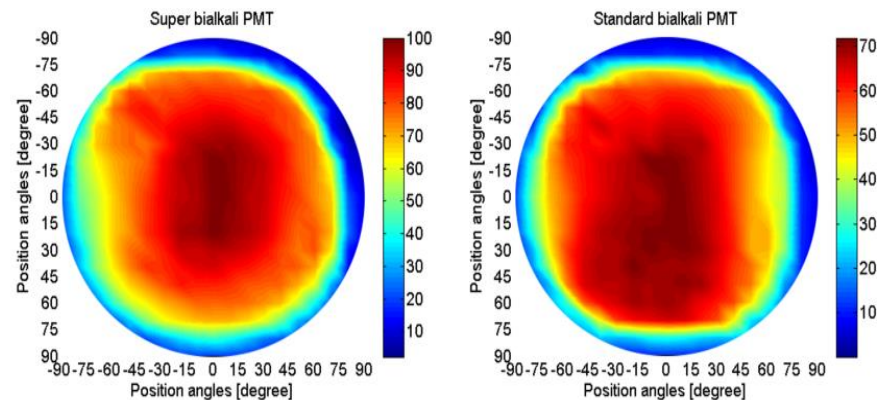
Homogeneity of the photocathode deposition *and* variations in collection efficiency (depends on the PC geometry)

UBA (Ultra Bialkali) & SBA (Super Bialkali) PHOTOMULTIPLIER TUBE SERIES



HAMAMATSU, PMT catalogue

Detection efficiency uniformity



E. Leonora, Photodet2012

Large water Cherenkov and scintillator detectors for long baseline neutrino oscillations, proton decay, supernova and solar **neutrinos experiments**

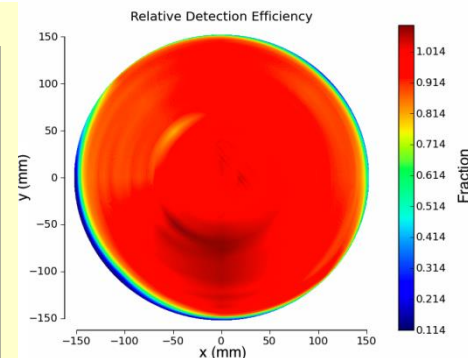
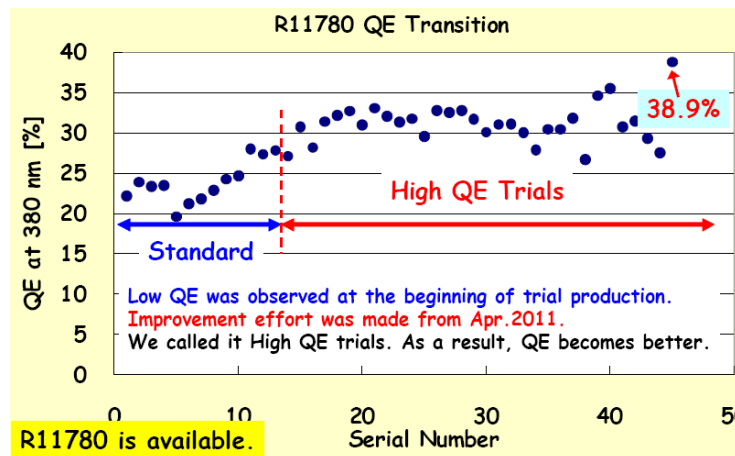
Need for PMT with:

- ✓ large-area
- ✓ high Q ϵ in UV

R11780 (12-inch)



Y. Yoshizawa, Photodet 2012



J. Brack, arXiv:1210.2765v2

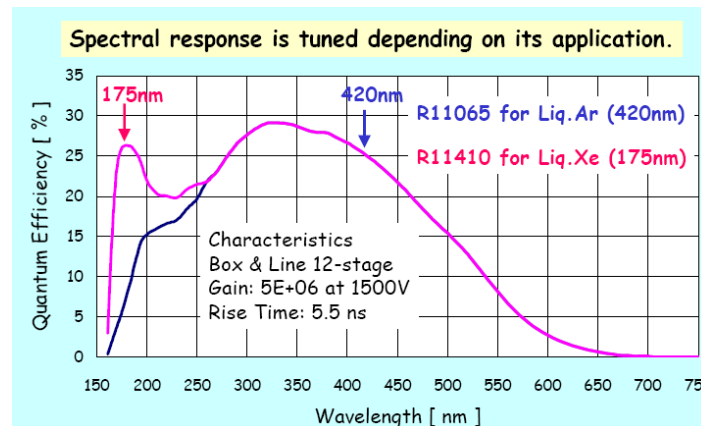
Scintillation detector for **Dark Matter experiments** (scintillation light from Xe nuclear recoil resulting from the scattering of WIMPs*) - low-background detectors + proximity of the PMTs to the active scintillation region → background dominated by PMT radioactivity → need for Ultra low background PMT working at low temp

3- inch metal bulb PMT



Extremely low radioactivity
(radiopure composition)

Low temp: Liquid Ar (- 186 °C)

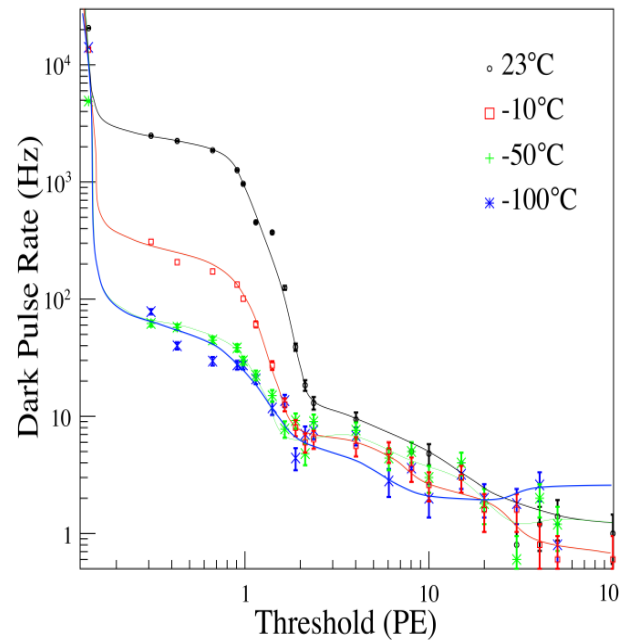
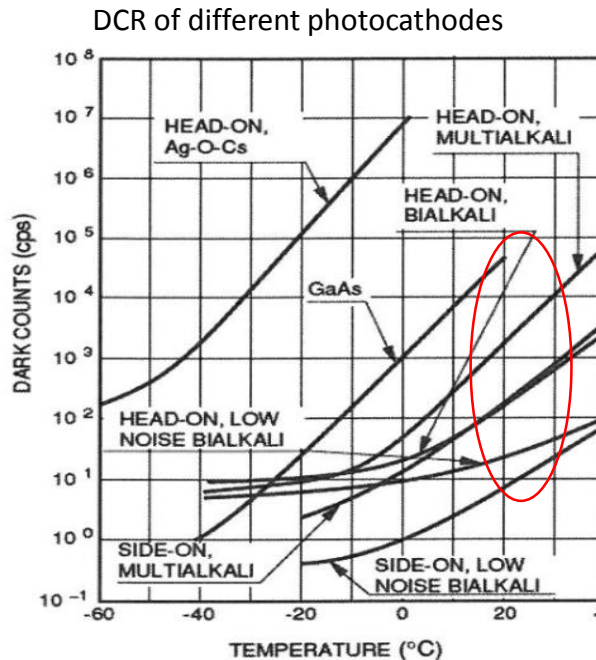
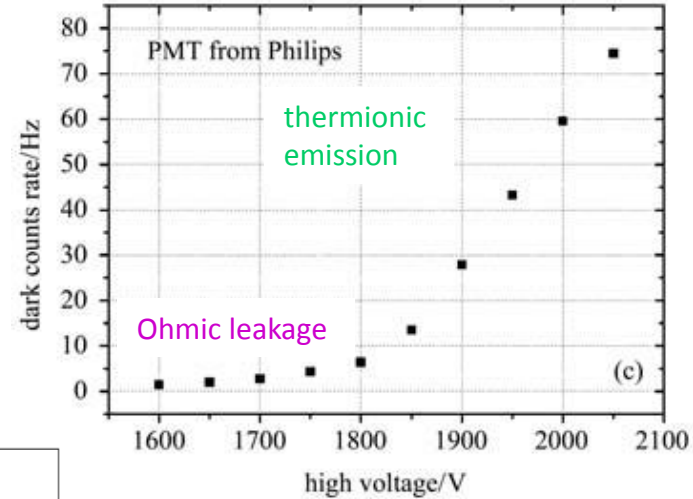


G. Fiorillo, NNN14

* WIMP: weakly Interacting Massive Particles

Dark current (I_d): current when photomultiplier is operated in complete darkness

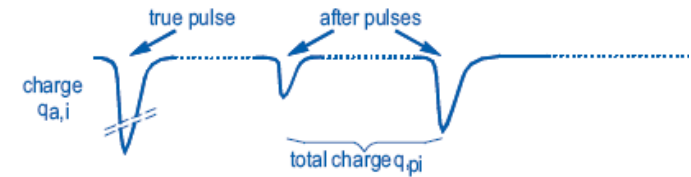
- due to leakage currents between electrodes and insulating surfaces (ohmic leakage)
- depends on the cathode type, the cathode area, and the temperature (thermionic emission)
- is highest for cathodes with high sensitivity at long wavelengths (low work function)
- increases considerably if exposed to daylight



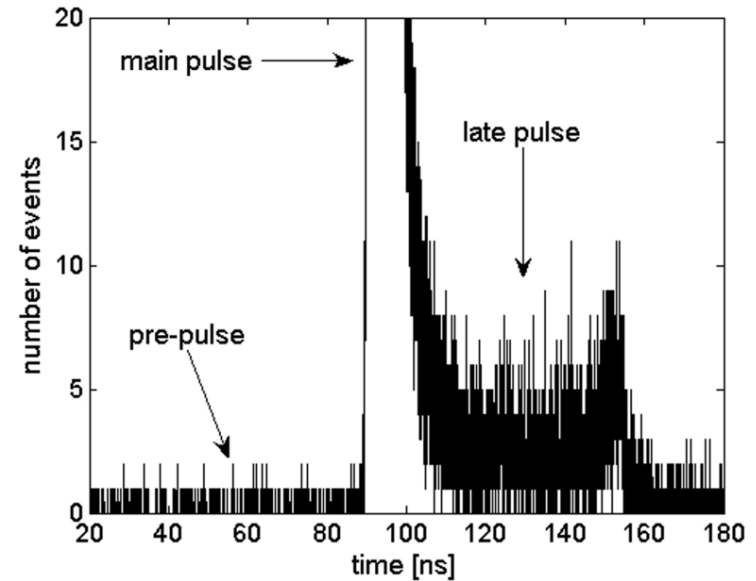
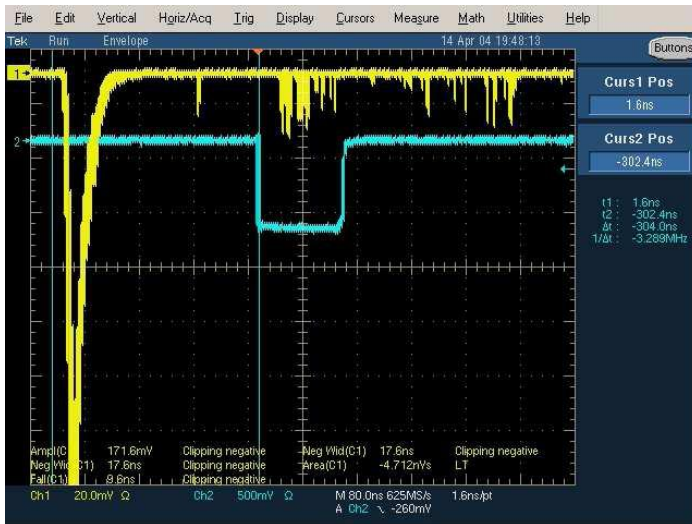
I_d needs to be minimized for low intensities measurements
 → cooling

Afterpulses: small signals, few p.e level, that appear after the main pulse

- short delay afterpulses (up to several tens of ns after the signal) caused by the elastic scattering of the electrons from the first dynode.
- long delay afterpulses (several tens of ns to several μ s after the main pulse) caused by the positive ions which are generated by the ionization of residual gases



Time distributions of late pulses



E. Leonora, VLVnT09

Can be distinguished by the time interval that separates them from the true pulse \rightarrow use of coincidence techniques to minimize their effect

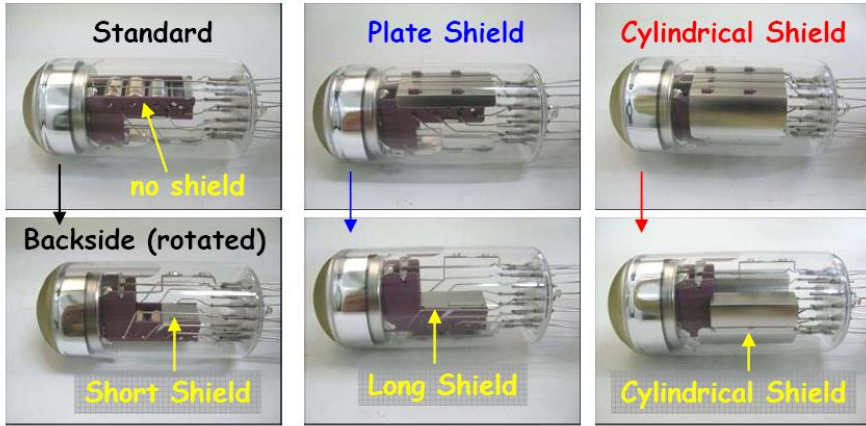
Collaboration between the PMT user and the producers → improvement of the performances

Ex: R&D in the structure of dynode chain

→ Lower after-pulse

Optimization of Dynode Shield

Dr. Mirzoyan/MPI reported that there is light emission from dynode of R11920-100. We made 2 kinds of trial tubes with different shape of dynode shield and checked the light emission.

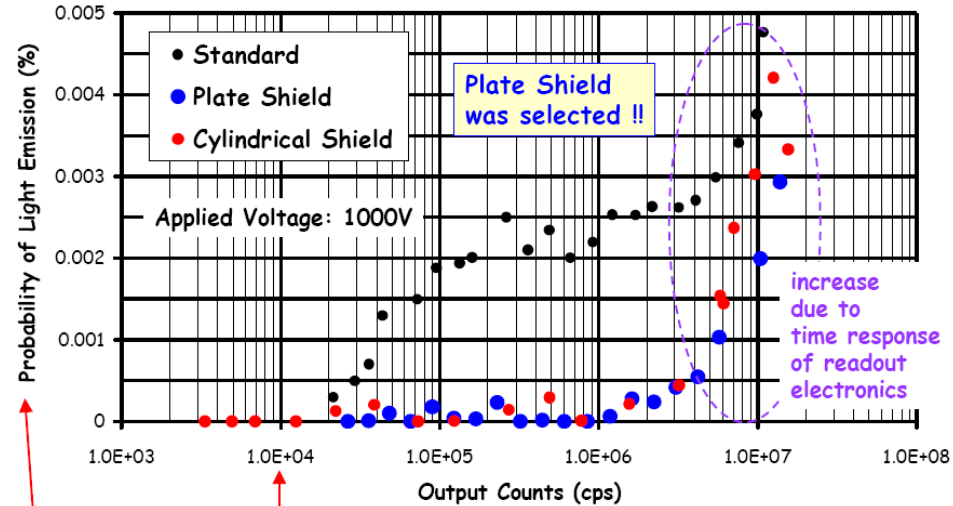


Copyright © Hamamatsu Photonics K.K. All Rights Reserved.

HPK, private communication

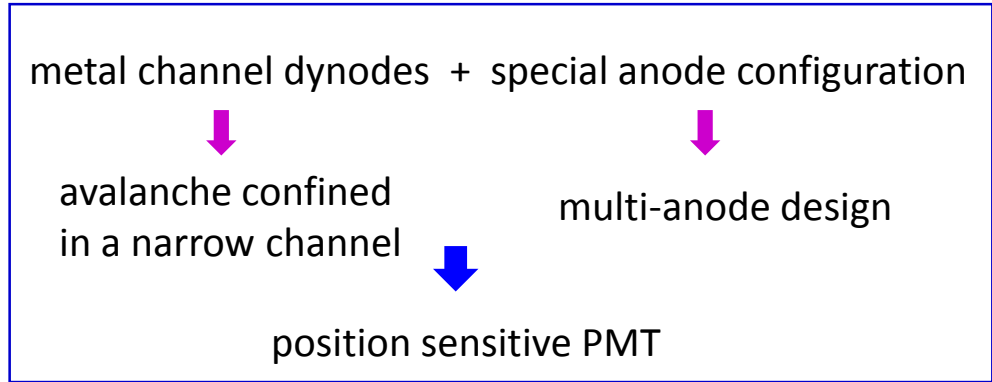
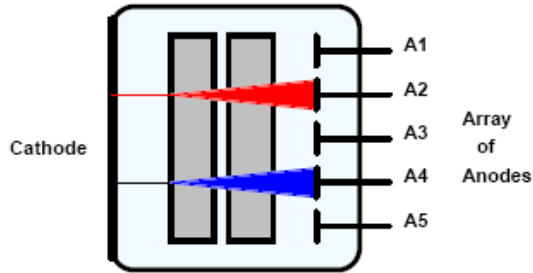
	PMT	Voltage	AP/Noise
old	R9420	850V	0.20 %
new	R11920	902V	0.013 %

Light Emission from Dynode



AP/NOISE(%) is normalized at 1.0E+04 output counts.

Need of space segmentation of the light detection



Anode Type	Single	Single	Linear (8 ch)	Linear (16 ch)	Linear (32 ch)	Matrix (2 × 2 ch)	Matrix (4 × 4 ch)	Matrix (8 × 8 ch)
Effective Area	φ8 mm	18 mm × 18 mm	21.6 mm × 2.5 mm	15.8 mm × 16 mm	31.8 mm × 7 mm	18 mm × 18 mm	18.1 mm × 18.1 mm	18.1 mm × 18.1 mm
Effective Area (per channel)	—	—	2 mm × 2.5 mm	0.8 mm × 16 mm	0.8 mm × 7 mm	8.9 mm × 8.9 mm	4.2 mm × 4.2 mm	2 mm × 2 mm

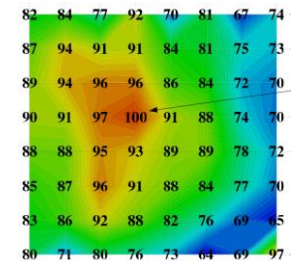


- Compact
- Good timing performances
- Good immunity to magnetic field

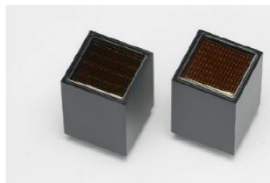


- Cross-talk
- Non uniformity across the channels

H8500 response uniformity

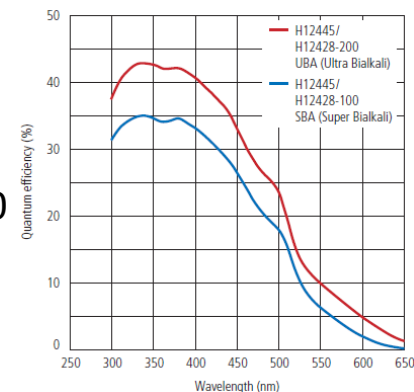


MaPMT with SBA, UBA and extended green Bialkali photocathode

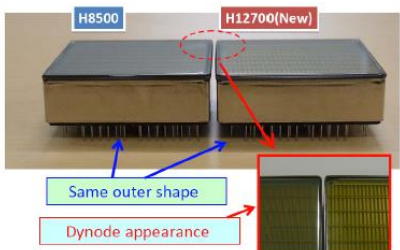


H12445-100/-200, H12428-100/-200

- Extended green bialkali PC ($Q_E = 14\%$ @ 550)
- 2 x 2 \rightarrow 8 x 8 multianode



Compact packaging multianode « flat » PMTs

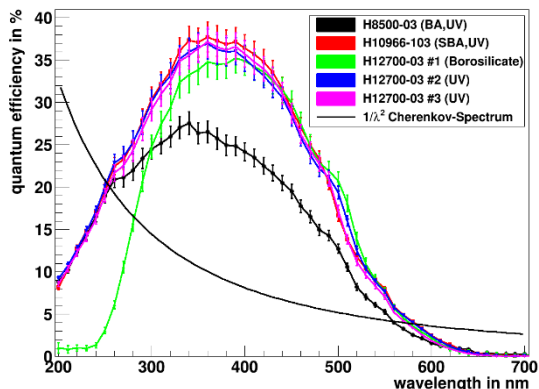


HAMAMATSU

Copyright © Hamamatsu Photonics K.K. All Rights Reserved.

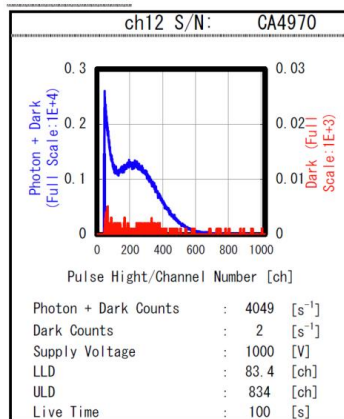
- optimized dynode structure:
- ✓ higher collection efficiency
 - ✓ better SPE resolution
 - ✓ enhanced cathode sensitivity

H12700 MaPMT

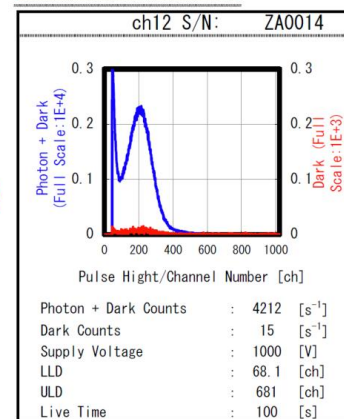


C. Pauly, RICH 2013

H8500



H12700(New)



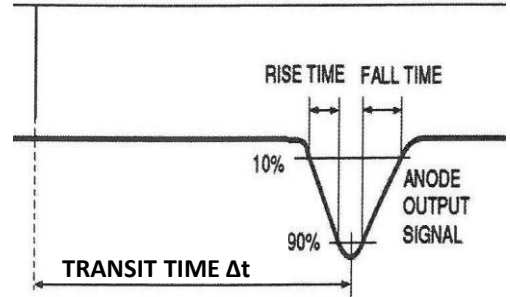
M. Contalbrigo, NDIP14

Fast time response PMTs are interesting for HEP and PET application

Need of PMTs with quite large photocathode and good TTS

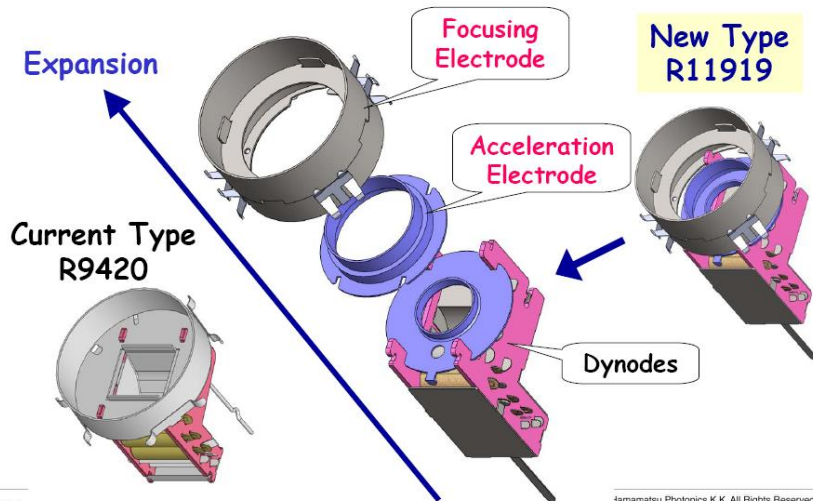


R&D in the structure of the PMT: accelerating electrode



Comparison of PMT Structure between Current Type and New Type

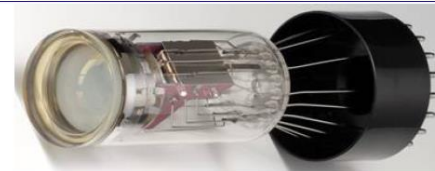
HAMAMATSU
PHOTON IS OUR BUSINESS



Better TTS: from 550 ps to 270 ps

R11919 / 1.5-inch FAST PMT

Fast Time Response with Acceleration electrode for TOF-PET and HEP experiments



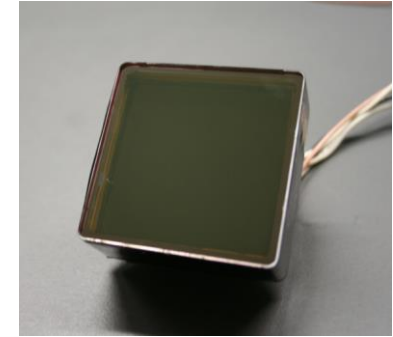
Transit Time Spread = around 270 ps

(R9420 = 550 ps, R11194 = 400 ps)

Gain = $1E+06$ (Gain is adjustable by request)

Cathode Blue Sensitivity = around 11

(SBA type could be available in future)



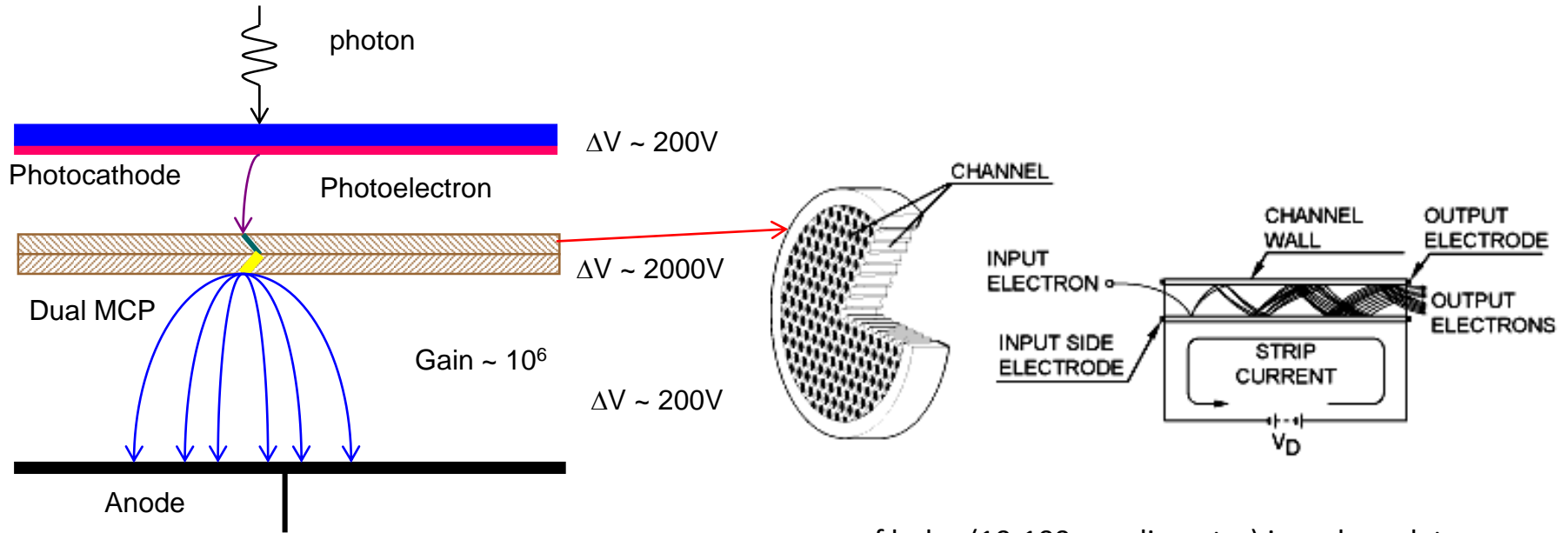
HAMAMATSU
PHOTON IS OUR BUSINESS

BURLE

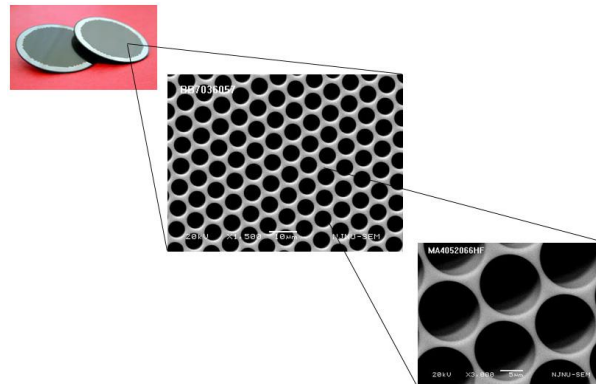
PHOTEK
ENVISAGE THE FUTURE

+ R&D in Research Institutes (BINP, Russia – IEHP, China – LAPP collaboration, USA -, ...)

Photodetector multiplication chain = Micro Channel Plate

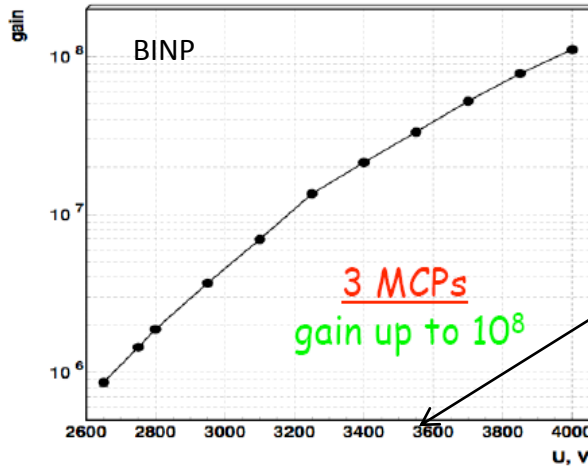


array of holes (10-100 μm diameter) in a glass plate





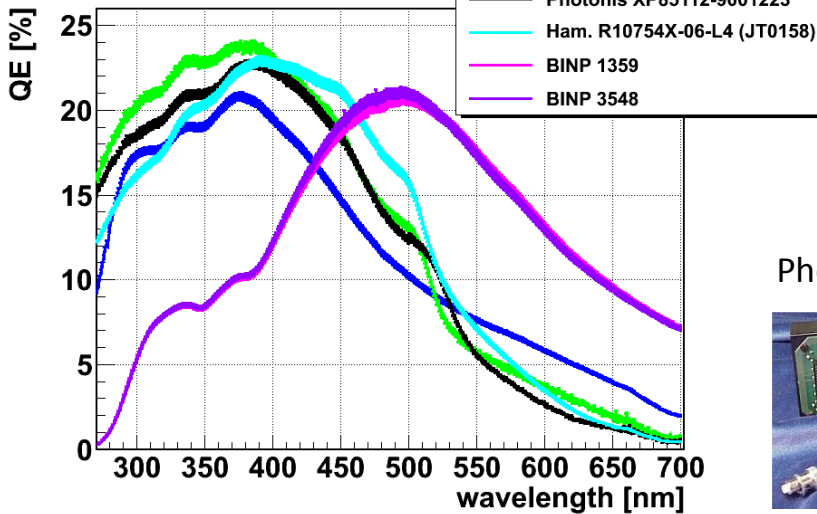
BINP



MCP-PMT bias voltage > PMT bias voltage

M. Barnyakov, AFAD 2013

Quantum Efficiency of various MCP-PMTs

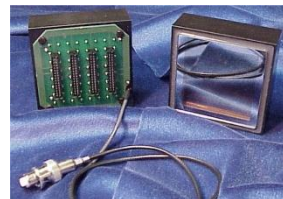


A. Lehmann, Elba Conference 2012

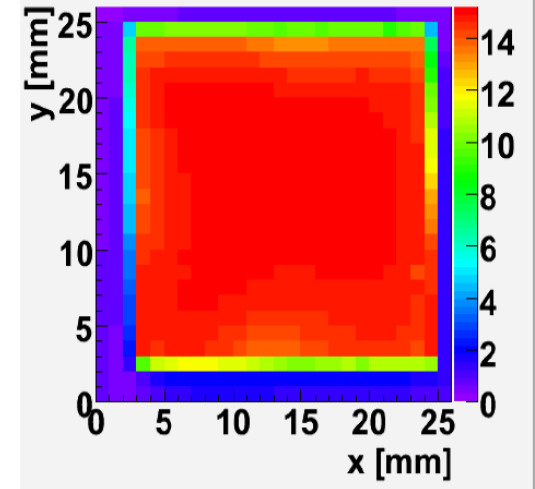


HAMAMATSU

Photonis BURLE



QE homogeneity

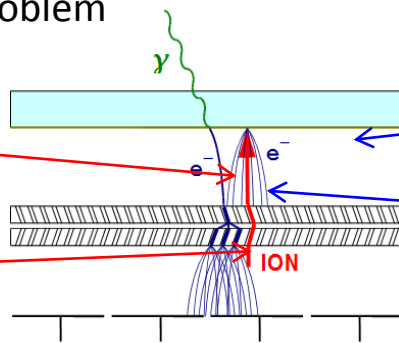


T. Inami, TIPP 2011

High photon rate \rightarrow aging problem

2 travel back toward the photocathode

1 ionisation of atoms of residual gas

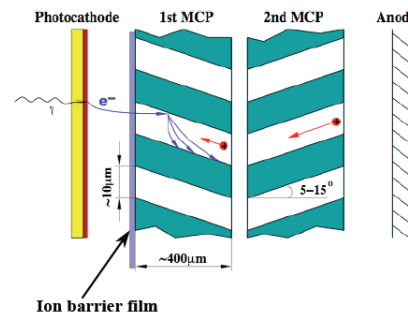


3 ion bombardment \rightarrow damages the photocathode \rightarrow reduces the $Q\epsilon$

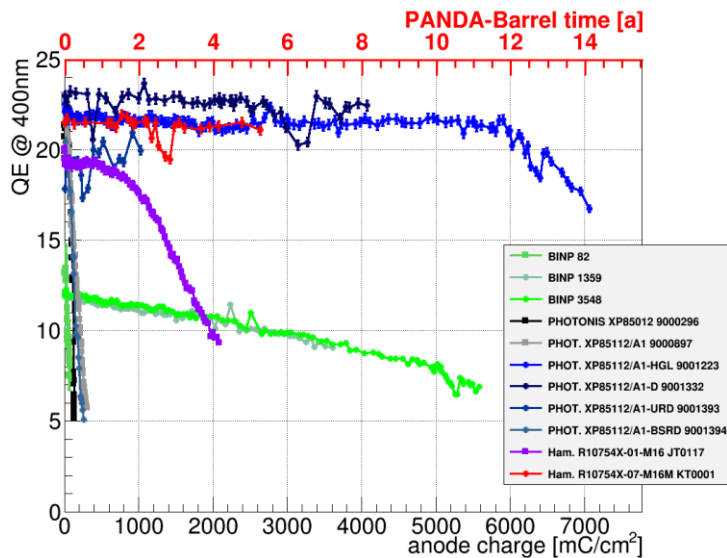
4 production of secondary pulses

Different ways of improvement (depending on the producer):

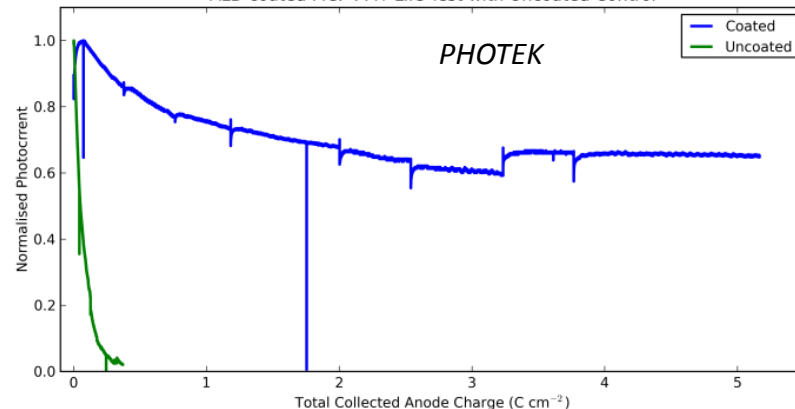
- Protection layer on the photocathode
- Improvement of the vacuum
- Treatment of the MCP surfaces (atomic layer deposition)
- New photo cathode



Lifetime of various MCP-PMTs (400nm)



ALD coated MCP-PMT Life Test with Uncoated Control

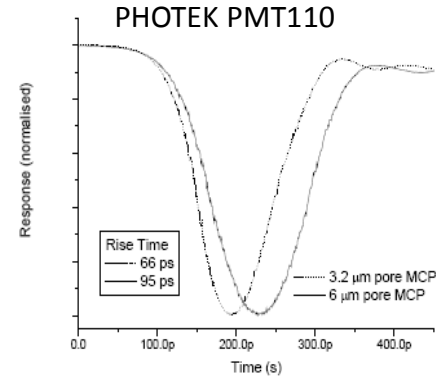


T M Conneely, PHOTEK

- high electric field between PC and MCPin and MCPout and anode → negligible effect of the angle distribution of the p.e
- e- transit time in the secondary multiplication process very short

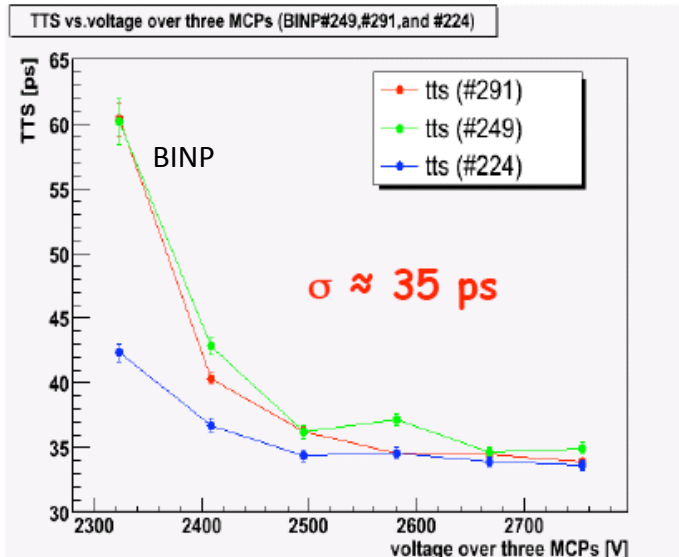


very good TTS $\approx 30\text{-}35$ ps (σ)



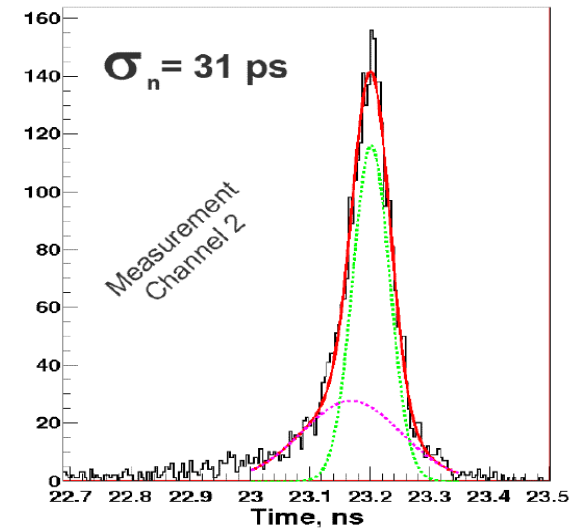
J. Milnes, PHOTEK

Single Photoelectron Timing resolution



A. Yu. Barnyakov, NIMA 598

HAMAMATSU SL10 SPTR @ 405 nm – 3.5 kV



J. Vavra, SLAC-Pub-14279

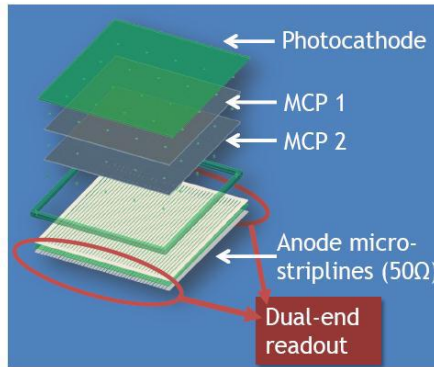
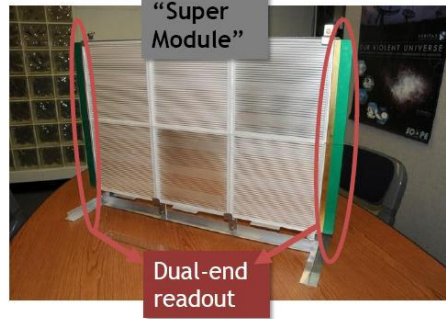
The LAPPD project

The Large-Area Psec Photo-Detector Collaboration

LAPPD Collaboration



- Development of large-area, relatively inexpensive Micro-Channel Plate (MCP) photo-detectors
 - 8" x 8" phototubes = 'tile' (large active area)
 - Gain $\geq 10^6$ with two MCP plates
 - Transmission line readout – no pins!
 - Fast pulses + low TTS ~ 30 ps



10/11/2011

ANT'11 LAPPD electronics

4

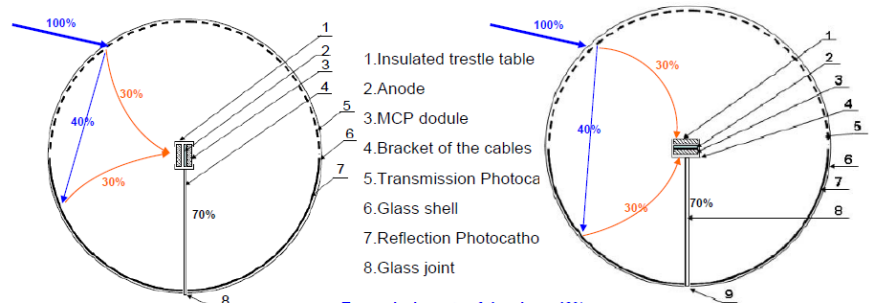
M. Sanchez, NNN14

Chinese R&D

➤ The new design of a large area PMT

High photon detection efficiency + Single photoelectron Detection + Low cost

- 1) Using two sets of Microchannel plates (MCPs) to replace the dynode chain
 - 2) Using transmission photocathode (front hemisphere) and reflection photocathode (back hemisphere)
- ~ 4 π viewing angle!



Transmission rate of the glass: 40%

Quantum Efficiency (QE) : of Transmission Photocathode 30% ; of Reflection Photocathode 30% ;

Collection Efficiency (CE) of MCP : 70% ;

$$PD = QE_{Trans} * CE + TR_{Photo} * QE_{Ref} * CE = 30\% * 70\% + 40\% * 30\% * 70\% = 30\%$$

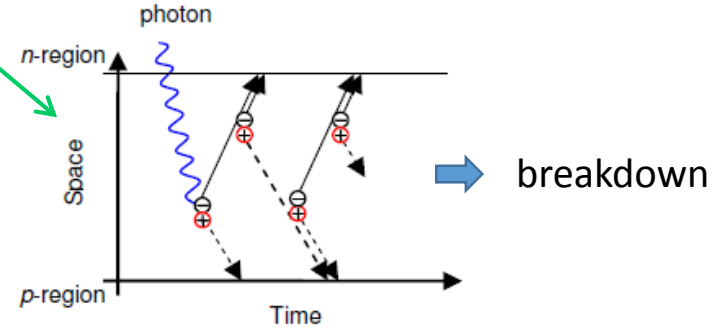
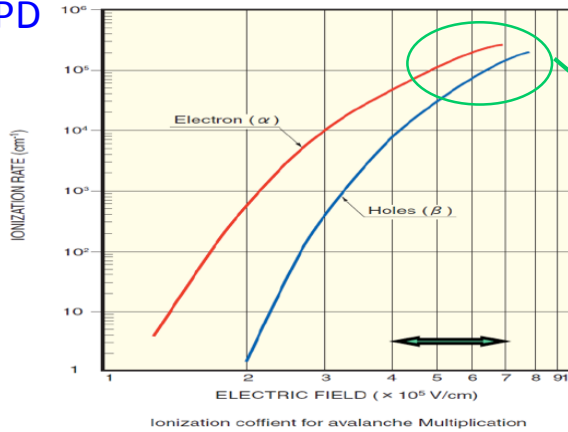
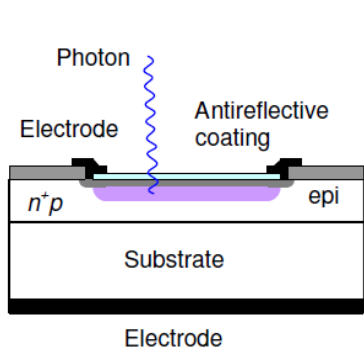
Photon Detection Efficiency: 15% \rightarrow 30% ; $\times \sim 2$ at least !

S. Quian, NDIP14

A decorative vertical element on the left side of the slide, consisting of numerous thin, overlapping lines in various colors (red, orange, yellow, green, blue, purple) that create a sense of motion and depth.

SiPM

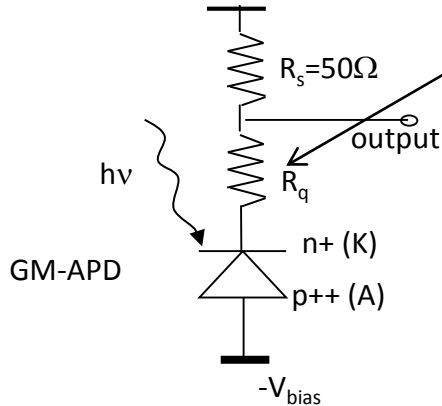
Schematic structure of a G-M APD



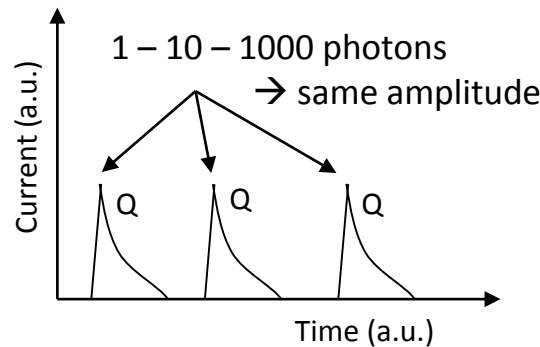
$$G = 10^5 - 10^6$$

both type of carriers participate in the avalanche process \rightarrow creation of a self-sustaining avalanche \rightarrow current rises exponentially with time and reach the **breakdown** condition. **No internal "turn-off"** \rightarrow the avalanche process must be quenched by the voltage drop across a serial resistor : **quenching resistor**

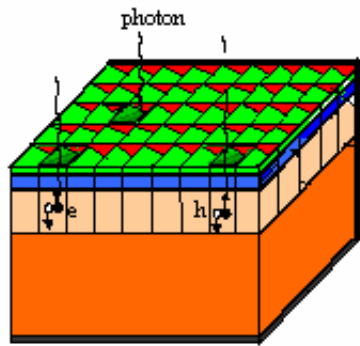
equivalent electrical circuit



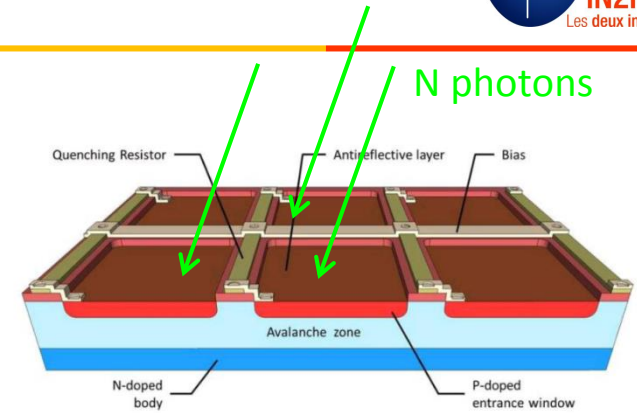
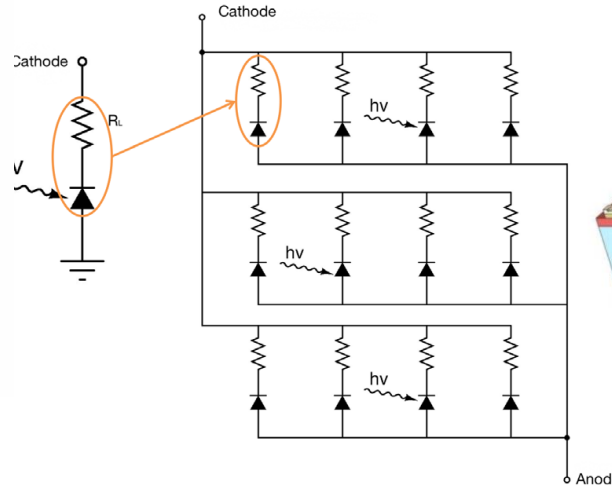
output signal



\rightarrow output charge is not proportional to the number of incident photons



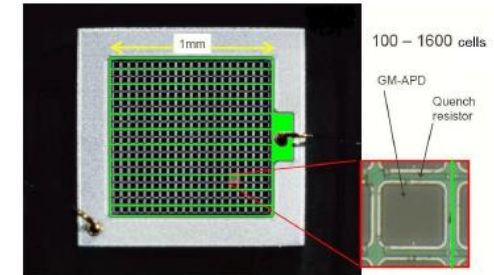
- # Microcells
- # Q.Elements
- n+
- p
- p+



KETEK web site

Valeri Saveliev, ISBN 978-953-7619-76-3

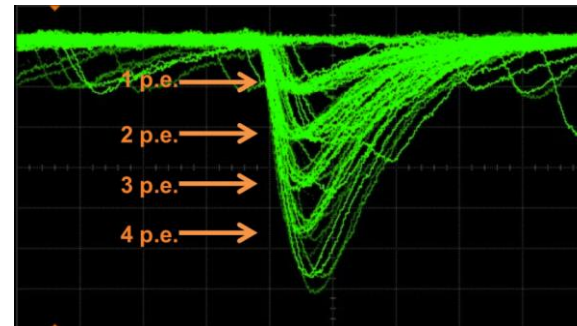
- ✓ GM-APDs (cell) connected in parallel (few hundreds/mm²)
- ✓ Each cell is reverse biased above breakdown
- ✓ Self quenching of the Geiger breakdown by individual serial resistors



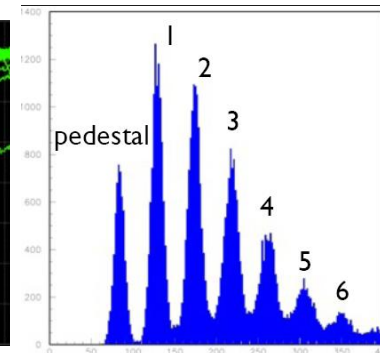
Each element is independent and gives the same signal when fired by a photon



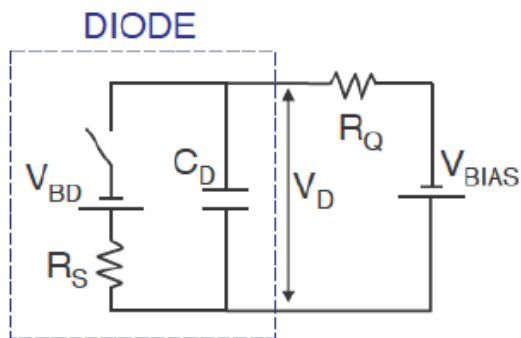
output charge is proportional to the number of incident photons



overlap display of pulse waveforms

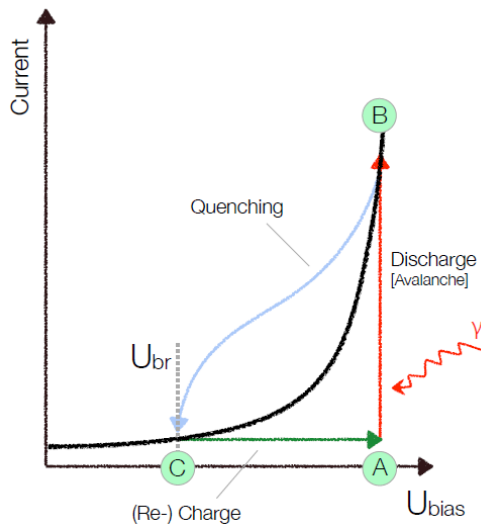


equivalent electrical circuit of a SiPM cell



V_{BD} : breakdown voltage
 R_Q : quenching resistance
 R_S : Si substrate serie resistance
 C_D : diode capacitance
 V_{BIAS} : bias voltage

$V_{bias} > V_{bd}$



quiescent mode, switch opened

If no photon or no dark event, the current stay stable

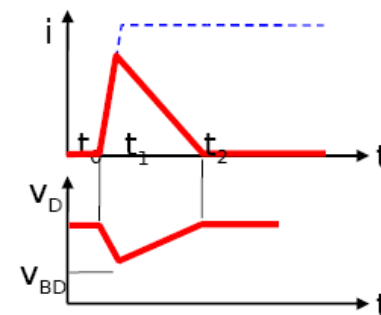
A → B : avalanche triggered, switch closed
 C_D **discharges** to V_{BD} with the time constant
 $\tau = R_S \times C_D \rightarrow$ asymptotic grows of the current

B → C : avalanche quenched, switch open

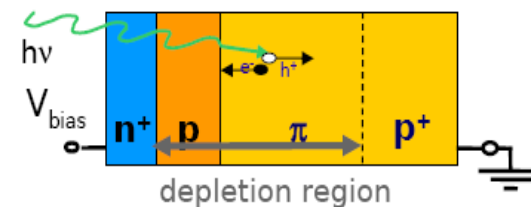
C → A : reset of the system

C_D **recharges** with the time constant $\tau' = R_Q \times C_D$

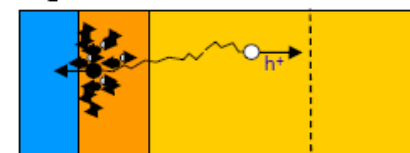
Time sequence



$t=0$: carrier initiates the avalanche



$0 < t < t_1$: avalanche spreading



$t_1 < t$: self-sustaining current limited by series R

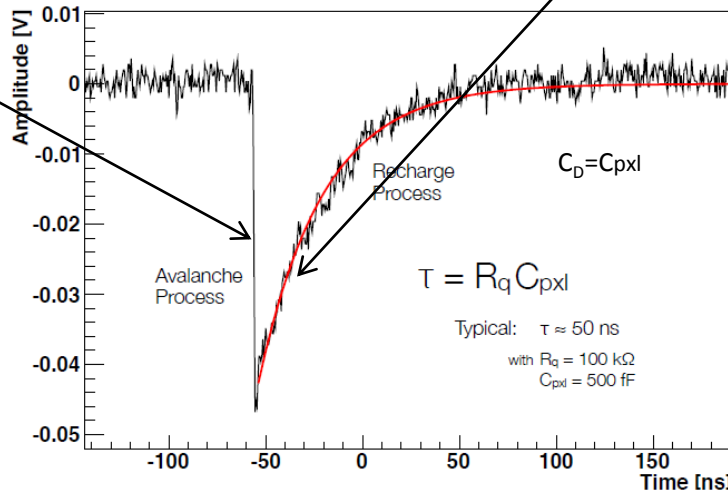
G.Collazuol, LIGHT11

Fast rise time: hundreds of ps

Recovery time: tens to hundreds of ns

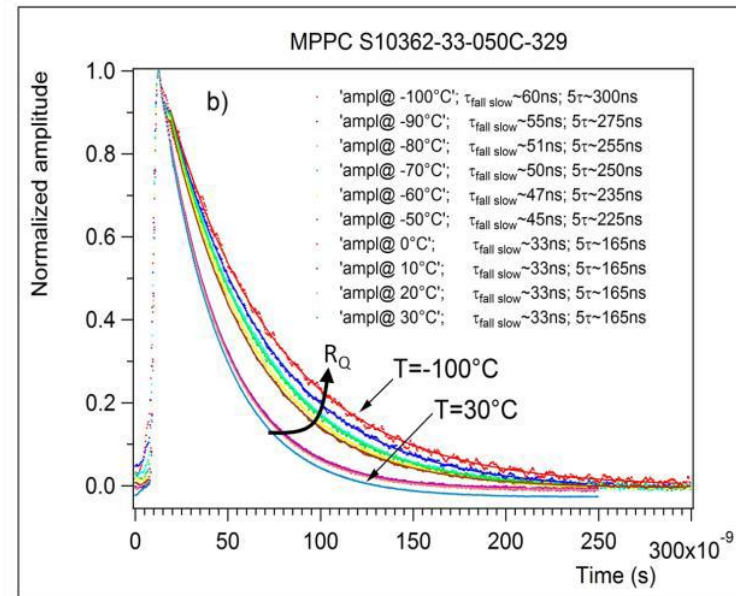
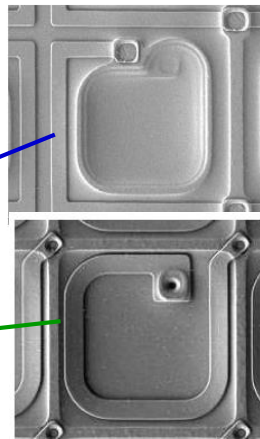
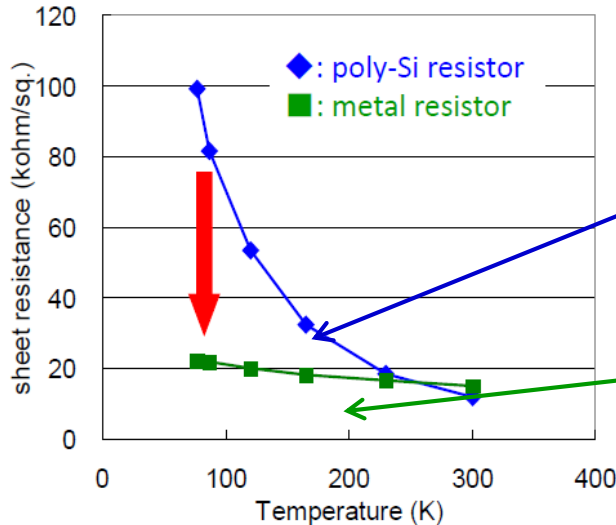
$$T_R = R_S C_D$$

Time to recharge a cell after a breakdown : $\tau = R_Q C_D$

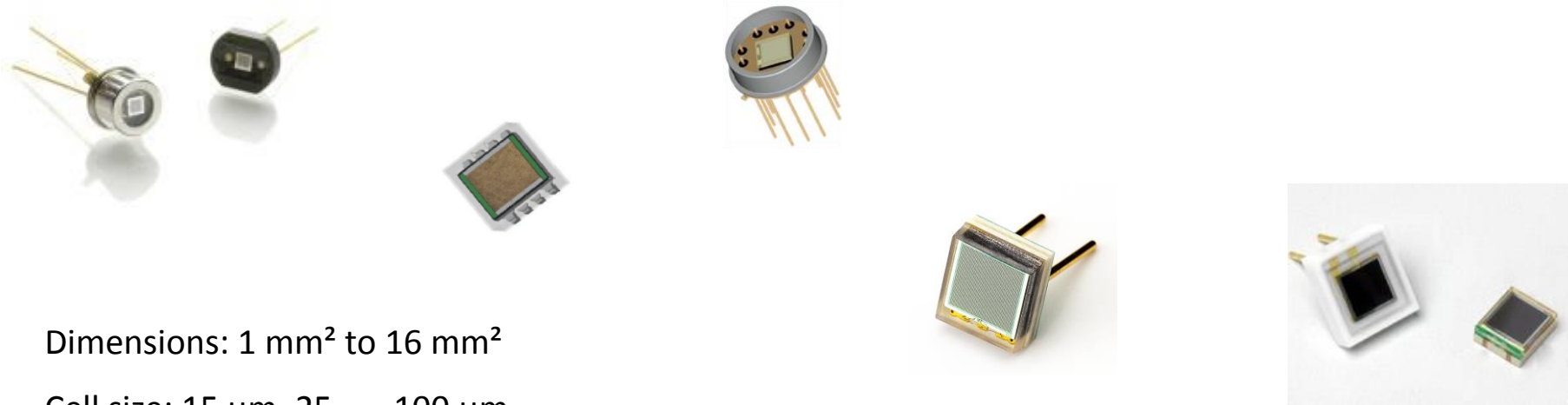


Polysilicon are temperature dependent → strong dependence of the recovery time with the temperature

Solution: Metal Quenching Resistor (MQR)



MQR with high transmittance → directly on the photosensitive surface → higher fill factor

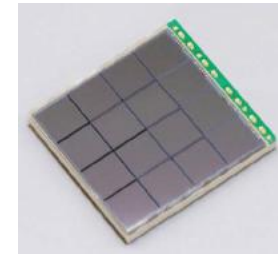
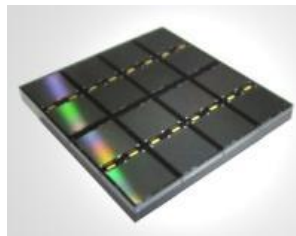


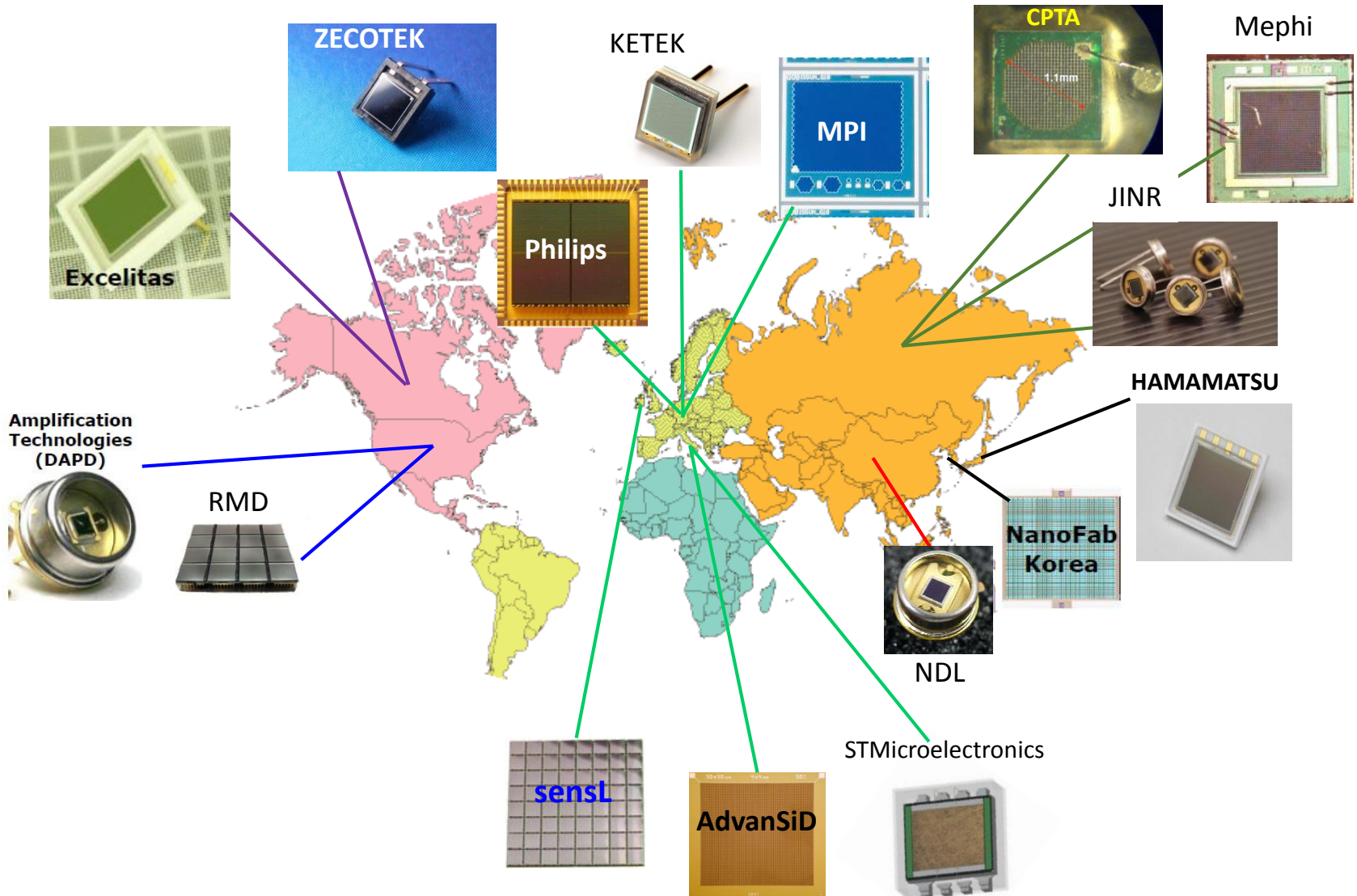
Dimensions: 1 mm² to 16 mm²

Cell size: 15 μm, 25, ..., 100 μm

Matrixes: 4 to 256 channels

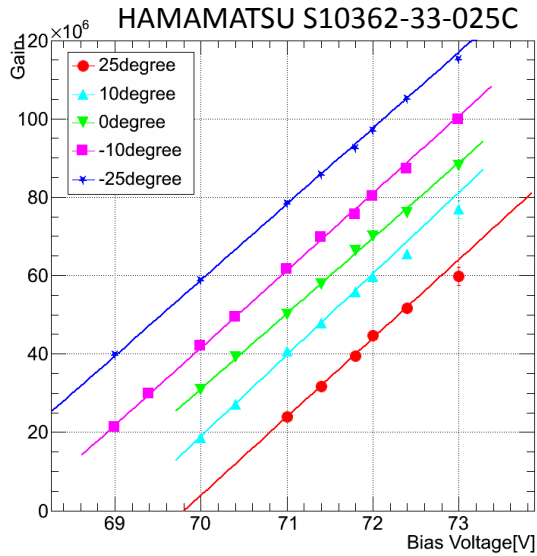
Packaging: metal (TO8), ceramic, plastic, with pins, surface mount type, matrix



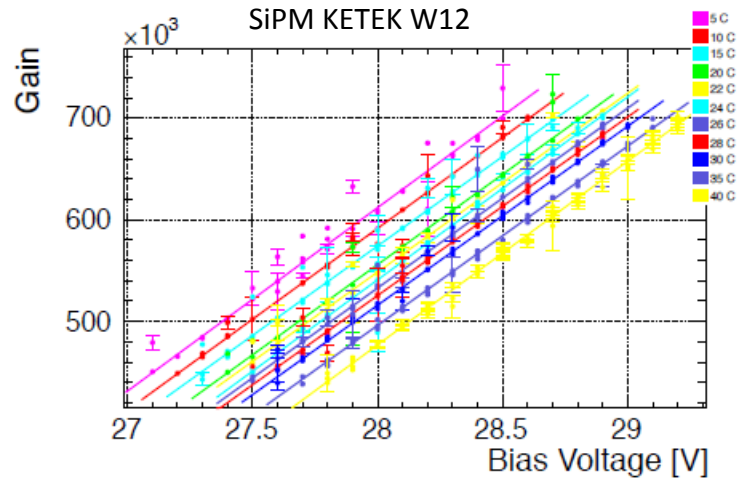


Gain: charge developed in one cell by a primary carrier

$$\text{Overvoltage } \Delta V = V_{\text{bias}} - V_{\text{BD}}$$



T. Okubo, ATHIC 2012

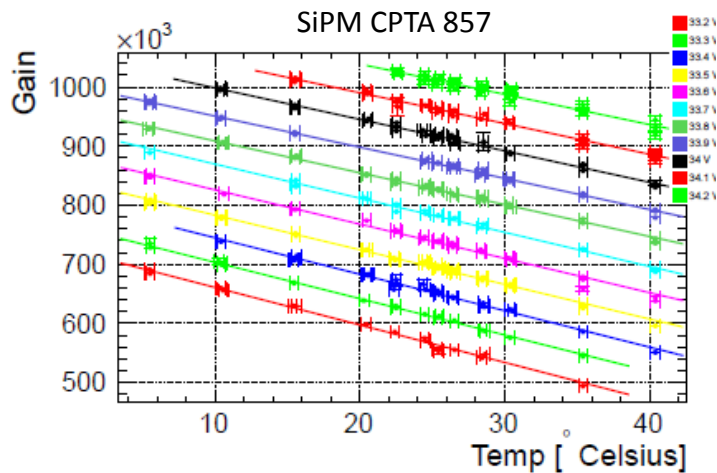


E. Van der Kraaij, AIDA 2013

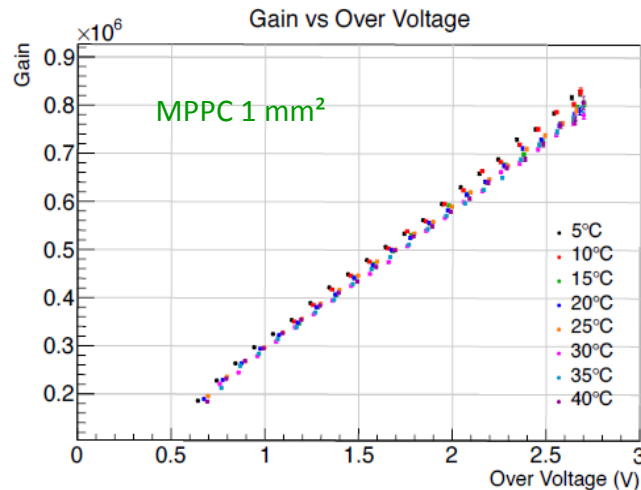
$$10^5 < \text{gain} < 10^6$$

- linear increase of the gain with V_{bias}

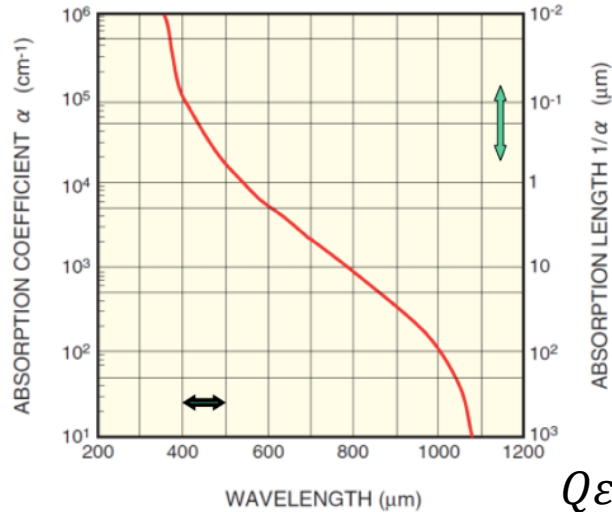
- Gain independent of the temperature at fixed ΔV



J. Cvach, arXiv:1403.8104v1]



H. Tajima, 2013 CTA SiPM meeting



$$PDE = Q_\xi \cdot P_{trig} \cdot \epsilon_{geom}$$

Q_ξ : carrier Photo-generation

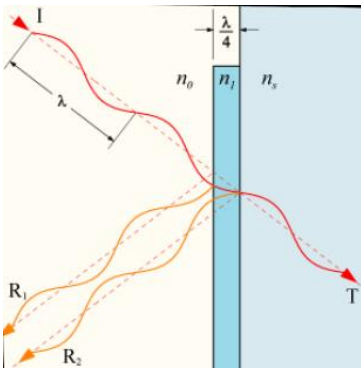
probability for a photon to generate a carrier that reaches the high field region in a cell

fraction of the photon flux absorbed in the depleted layer (sensitive region). The device should have a sufficiently large value d to maximize this factor.

$$Q_\xi = (1 - R) \xi [1 - e^{-\alpha d}]$$

effect of reflection at the surface of the device.

reflection can be reduced by the use of antireflection coatings



fraction of e-/h pairs that successfully avoid recombination at the material surface and contribute to the useful photocurrent

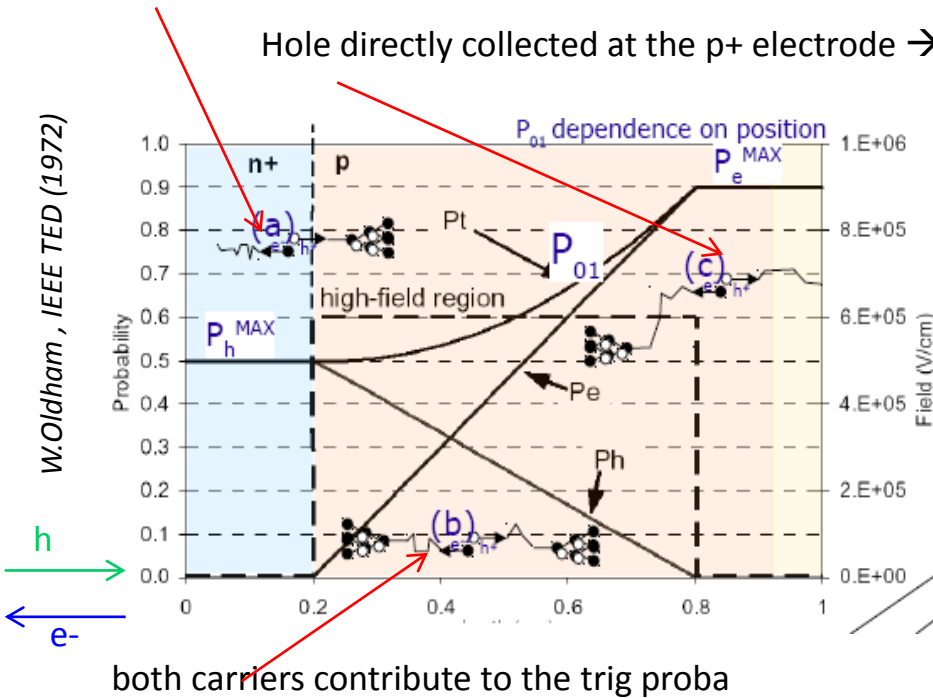
R : reflection Fresnel coefficient = 0,3 for Si

$$PDE = Q_{\epsilon} \cdot P_{trig} \cdot \epsilon_{geom}$$

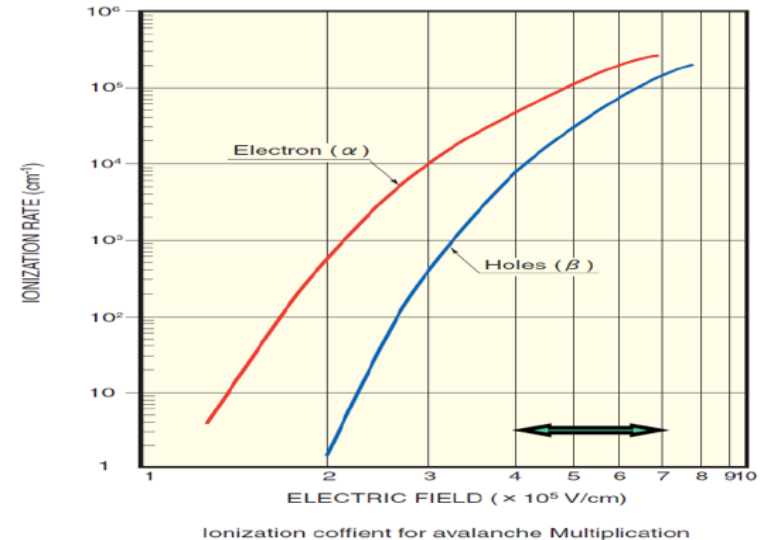
P_{trig} : avalanche triggering: probability for a carrier traversing the high-field to generate the avalanche
 Depends on the position where the primary e/h pair is generated

e- directly collected at the n+ electrode → only the holes contribute to the trig proba

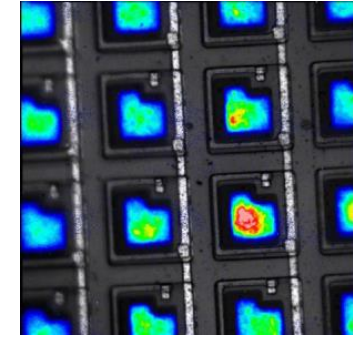
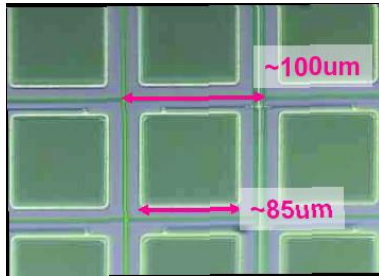
Hole directly collected at the p+ electrode → only the e- contribute to the trig proba



Ionization coefficients α for electrons and β for holes



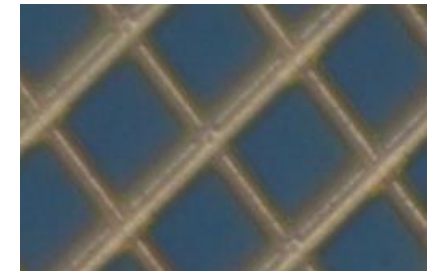
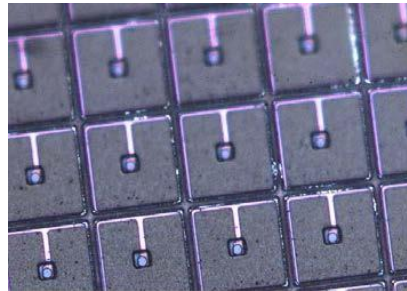
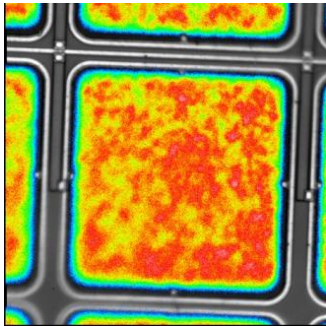
Ionization coefficient of e- > coeff of holes → the triggering probability is max when the charge carriers p_{MAX} generation happens in the p side of the junction → the e- pass through the high field region



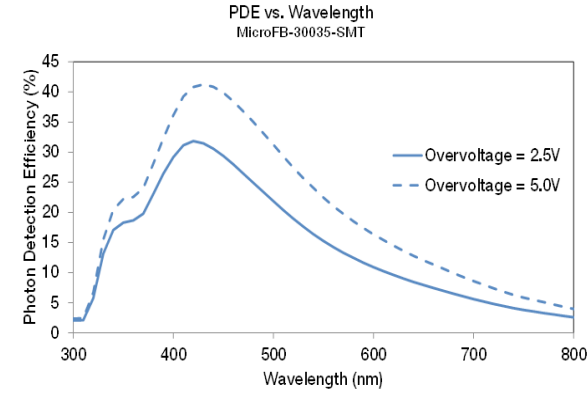
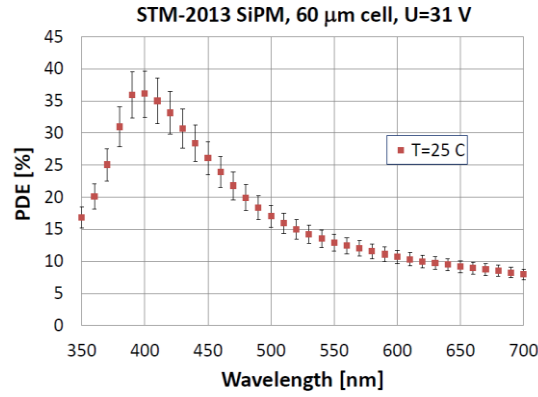
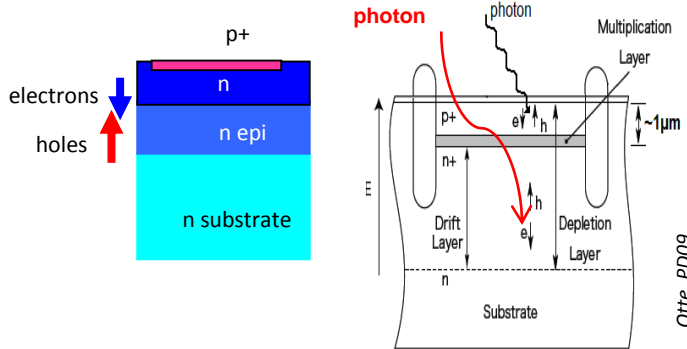
$$\text{PDE} = Q_{\epsilon} \cdot P_{\text{trig}} \cdot \epsilon_{\text{geom}}$$

ϵ_{geom} : geometrical Fill Factor

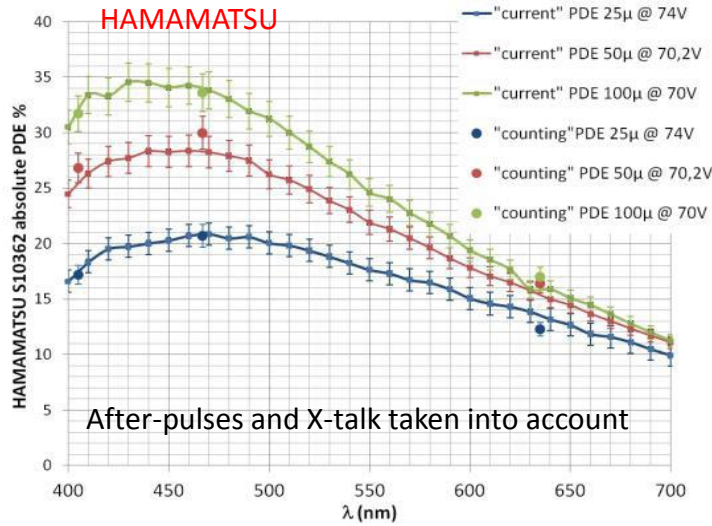
fraction of the sensitive to insensitive area. Only part of the area occupied by the cell is active and the rest is used for the quenching resistor and other connections



p-on-n SiPM with shallow junction exhibits higher PDE value in the blue region (e- trigger avalanches at short λ)

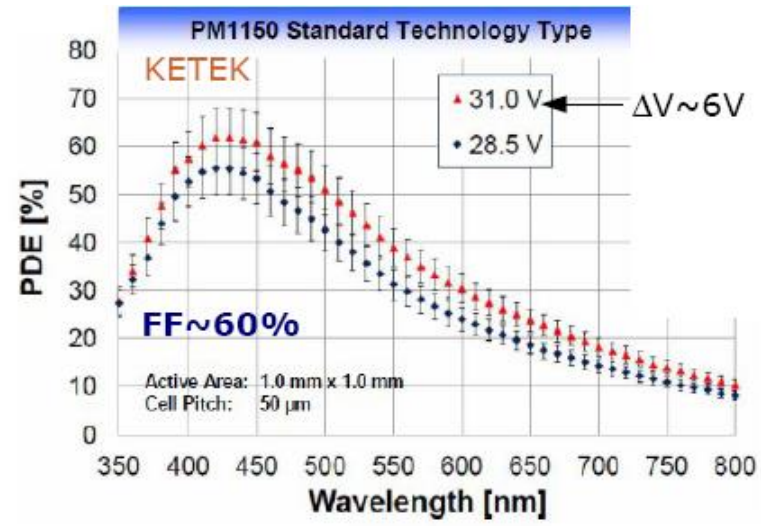


Y. Musienko, INSTR14



After-pulses and X-talk taken into account

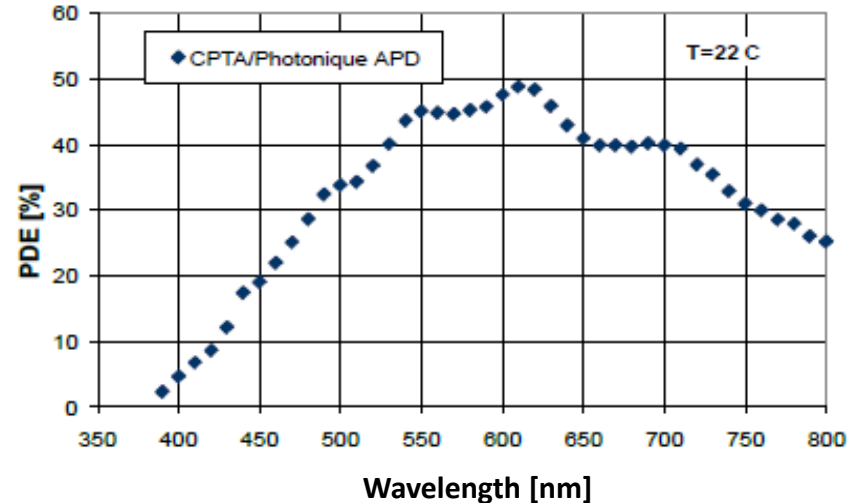
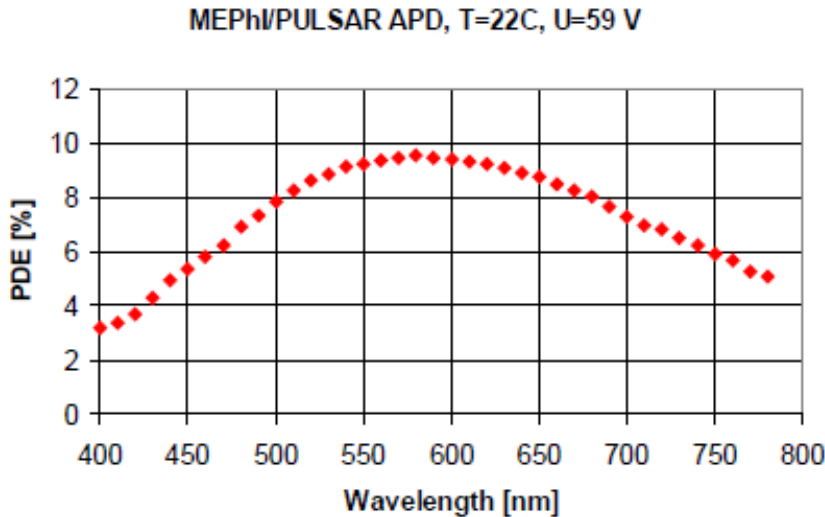
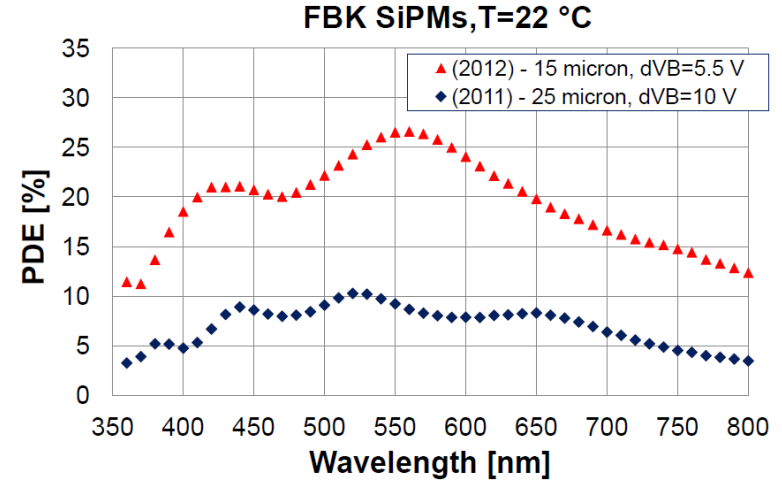
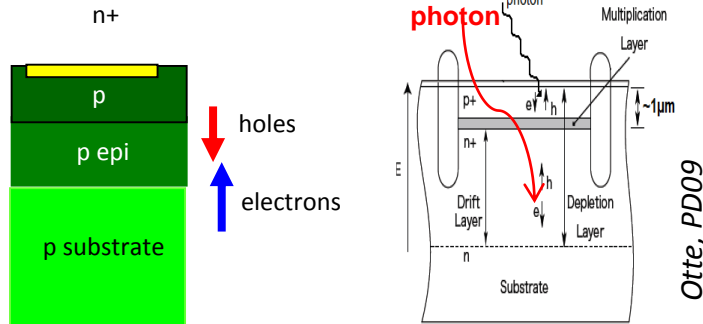
V. Chaumat, PoS (PhotoDet 2012) 058



F.Wiest – AIDA 2012

PDE in the blue region : 35 – 60 %

n-on-p SiPM with larger depletion depth have higher sensitivity in the red

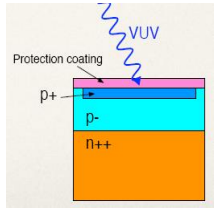


Y. Musienko, INSTR14

PDE in the green region : 25 – 50 %

Almost no detection of the UV light → limitation of the suitability of SiPMs for Noble-gas detectors

PDE for VUV is ≈ 0 for commercial devices because of the low transmission for VUV of the sensitive layer due to:



- ❖ protection coating (epoxy resin/silicon rubber)
- ❖ insensitive layer (p+ contact layer with \sim zero field)
- ❖ absorption length in Si for VUV photon: $\sim 5\text{nm}$
- ❖ high reflectivity for VUV on Si surface



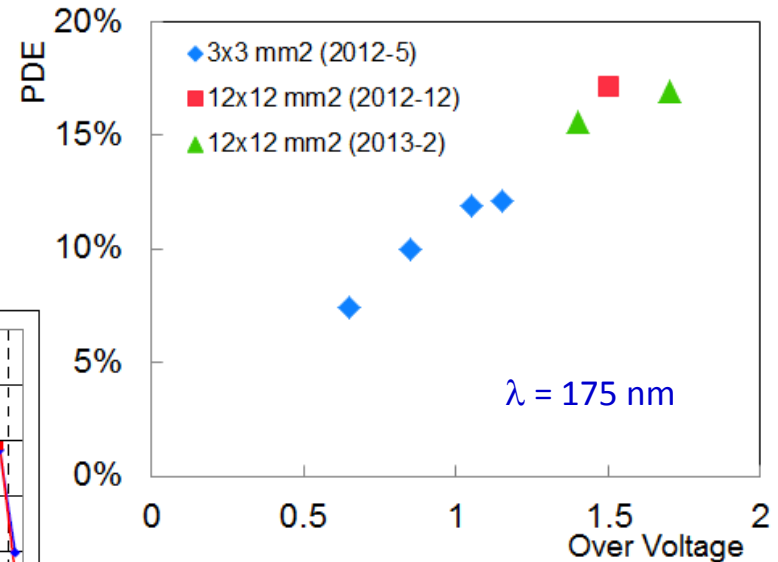
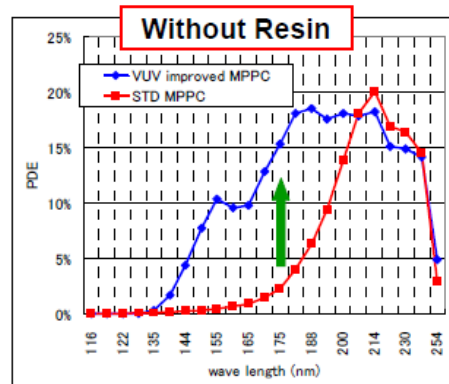
Possible solutions:

- ❖ Remove protection coating
- ❖ Thinner p+ contact layer
- ❖ Optimize reflection/refractive index on sensor surface

HAMAMATSU

UV-enhanced MPPC under development (collaboration between Hamamatsu, ICEPP and KEK) : removal of the protection coating and optimization of the MPPC parameters → currently sensor size: $12 \times 12 \text{mm}^2$ (cell size = $50 \mu\text{m}$)

- ❖ PDE (175 nm) = 17 % (best sample)
- ❖ Gain $\approx 10^6$ @ 165 K
- ❖ DCR = 0 @ 165 K
- ❖ decay time $\approx 30 - 60 \text{ ns}$



D. Kaneko at al, IEEE NSS 2013 Proceedings

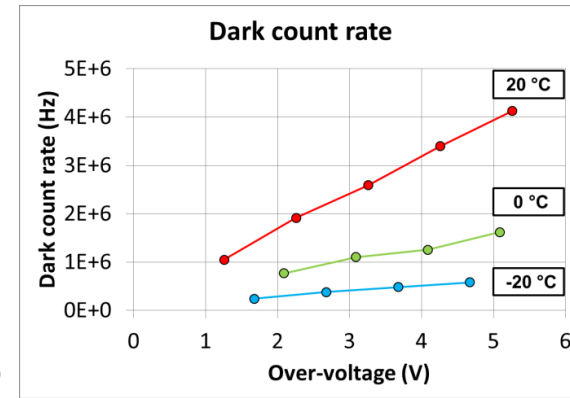
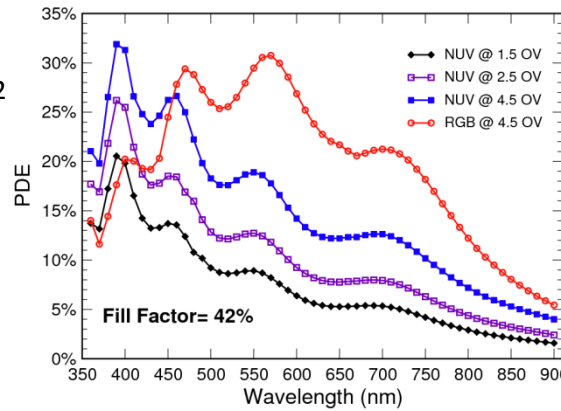
FBK NUV-SiPM (Near-UV SiPM)

1x1mm² 50x50 μm² cell

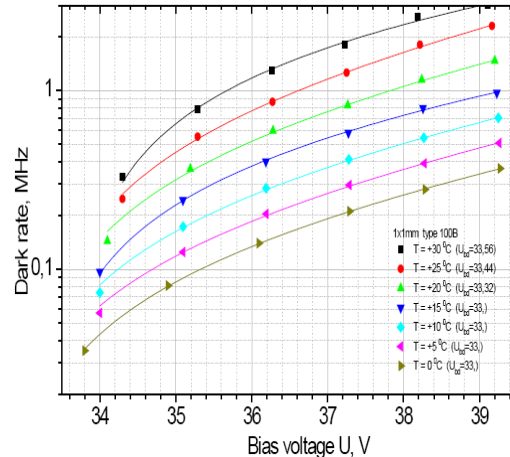
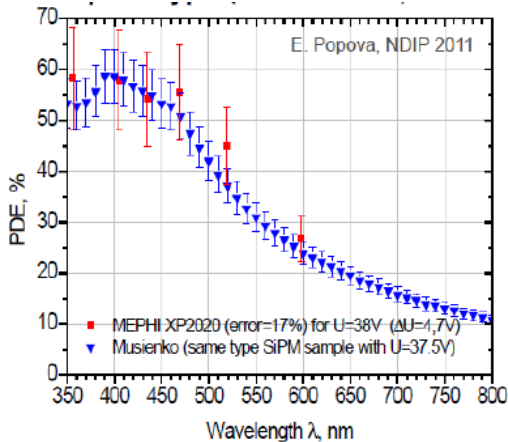
Designs available: 1x1, 2x2, 3x3, 4x4mm²

Results (FBK measurements):

- ✿ PDE (350 nm) = 20 %
- ✿ DCR = 4 MHz @ 20°C (ΔV = 5V)

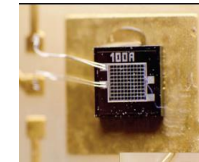


A. Ferri, NIMA 718 (2013)



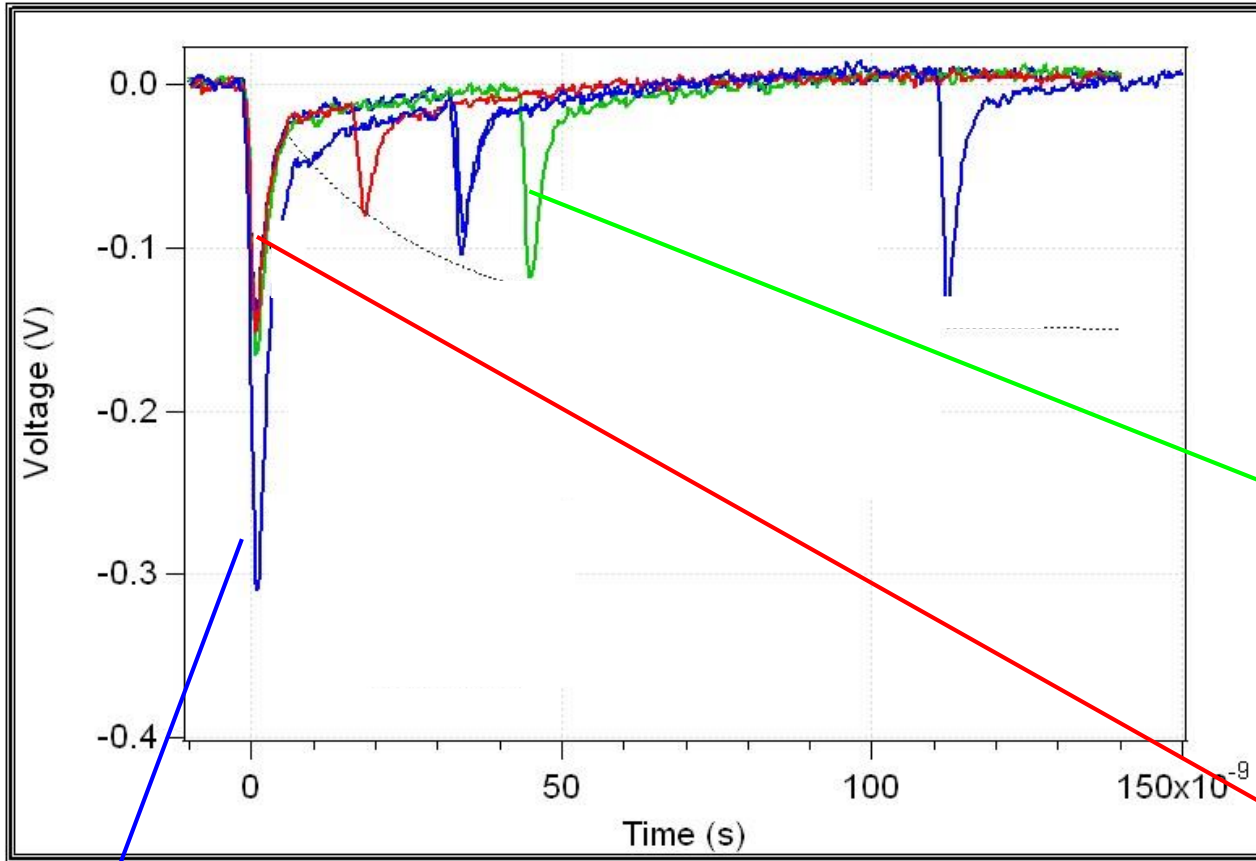
E. Popova, NDIP2011

Excelitas



Collaboration between Excelitas, MEPHI and MPI : 1x1 mm² (cell size = 100 μm)

- ✿ PDE (350 nm) = 50 %
- ✿ DCR = 800 kHz @ 20 °C (ΔV = 4V)



Cross-talk : amplitude = 2 p.e

avalanche in one cell → proba that a photon triggers another avalanche in a neighboring cell without delay

After-pulses

carriers trapped during the avalanche can produce delayed secondary pulses

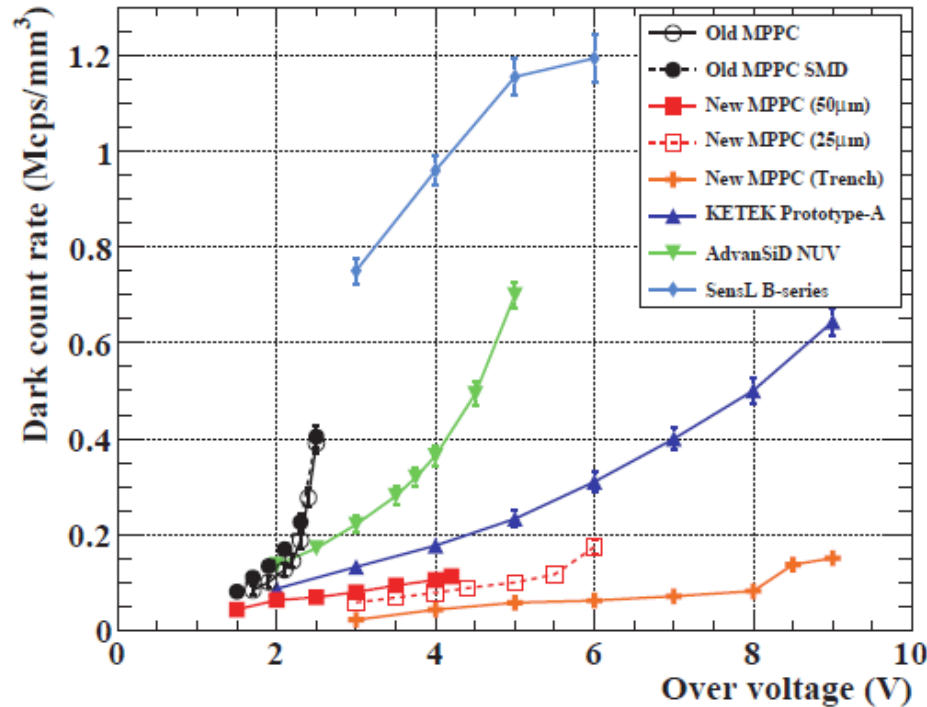
Dark counts

pulses triggered by non-photo-generated carriers (thermal / tunneling generation in the bulk or in the surface depleted region around the junction)

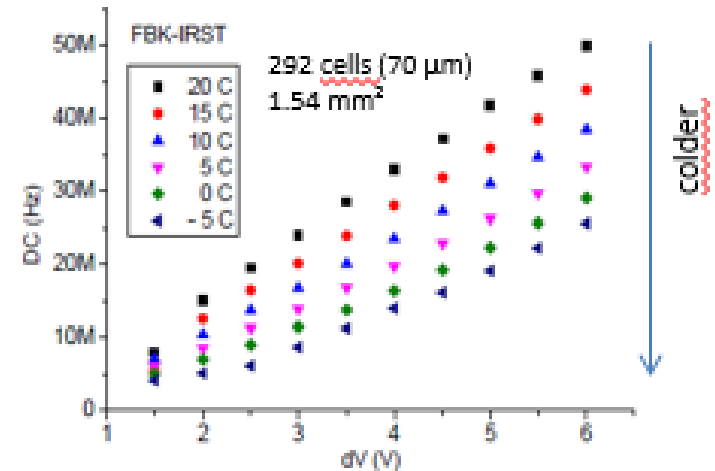
Average frequency of the **thermally generated avalanches breakdown process** that result in a current pulse indistinguishable from a pulse produced by the detection of a photon.

Few 100kHz/mm² < DCR < 1 MHz/mm² till 2013

DCR of most recent devices \approx few 10 kHz/mm²



Y.Uchiyama et al, IEEE NSS 2013



O. Starodubtsev, PoS 2012

Best way to decrease the Dark Count rate:

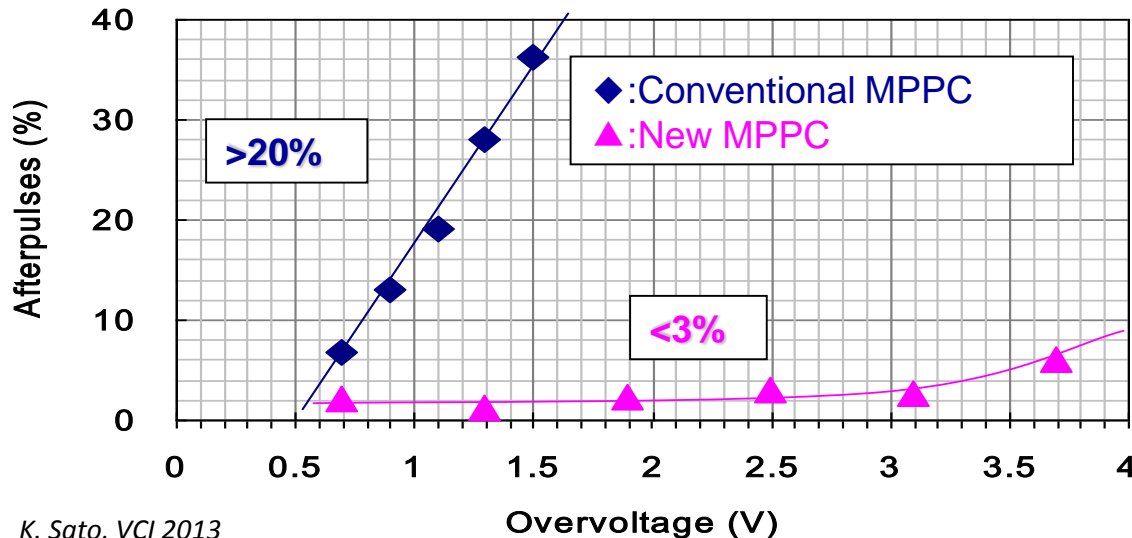
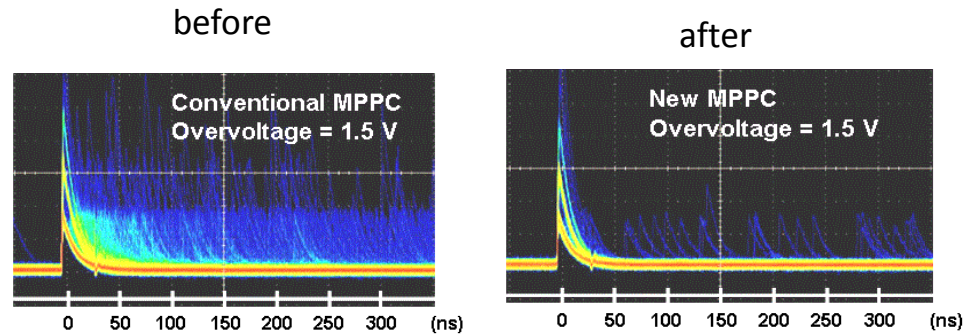
- ✓ operate the SiPM at lower voltage
- ✓ cooling (factor \approx 2 reduction of the dark counts every 8°C)

Breakdown → production of a large number of charge carriers → some of them are trapped in deep trap levels created by impurities (Iron, Gold) and defects (point, dislocation)

These carriers may be released at some time and trigger a new breakdown avalanche event : afterpulse (described in term of probability)

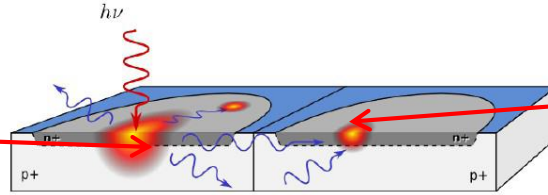


Minimization of the amount of impurities in the avalanche region employing pure Si wafers and new process conditions.



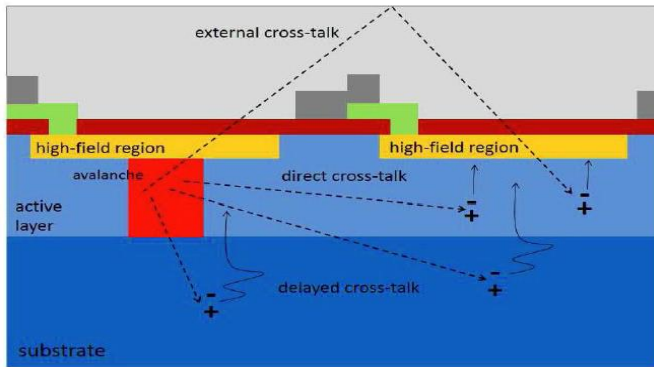
After-pulse proba < 10 % for most of the SiPMs on the market

avalanche in one cell
probability than 1 carrier
emits $\approx 3 \cdot 10^{-5}$ photons
with $E > 1.12$ eV



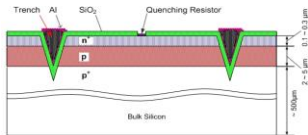
these photons (≈ 30 for a gain of 10^6) can trigger another avalanche in a neighboring cell without delay

A. Lacaita, et al., *IEEE Trans. Electron Devices ED-40* (1993) 577

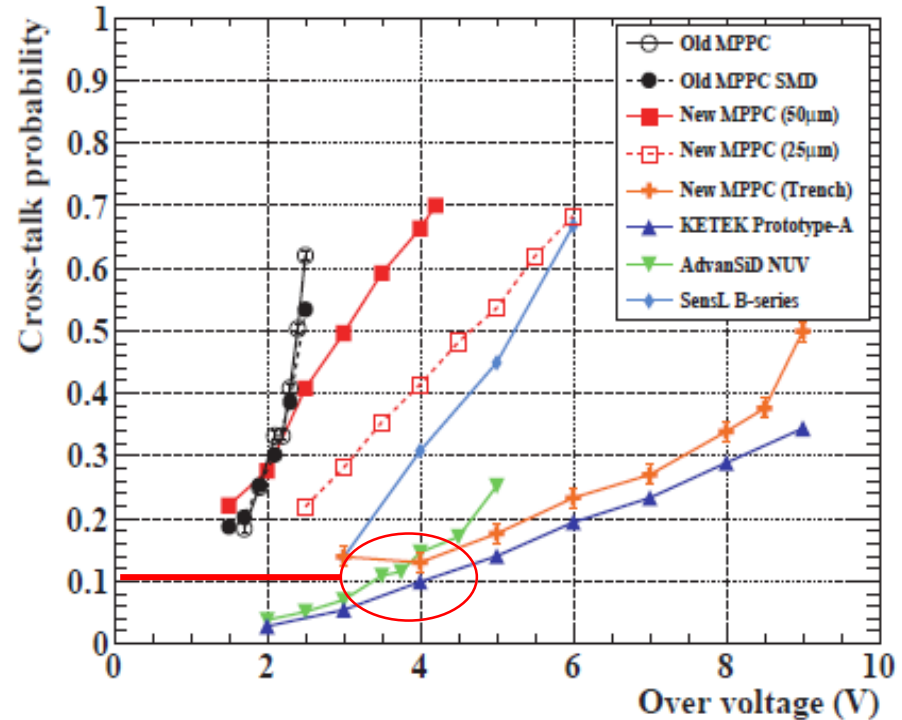
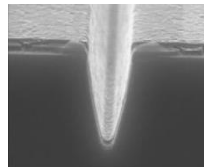


A. Ferri, *IPRD13*

One solution to decrease the CR is to improve the optical isolation between the cells: etching trenches filled with opaque material



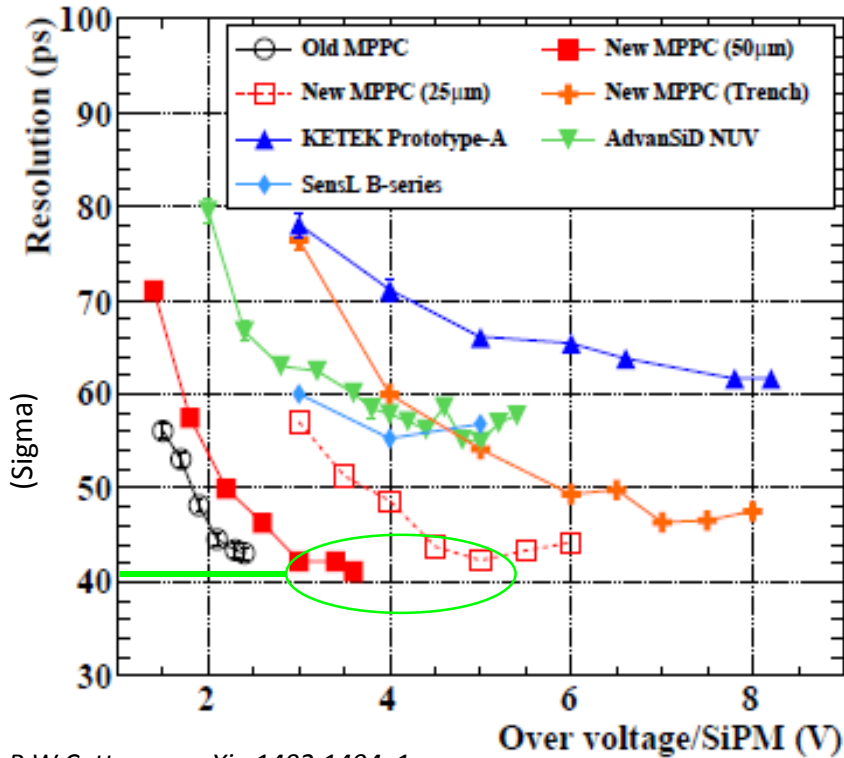
D. McNally, *G-APD workshop* (2009)



Y. Uchiyama et al., *IEEE NSS 2013*

less than 15 % of crosstalk for low overvoltage which is at least a factor 2 better than with the old geometries

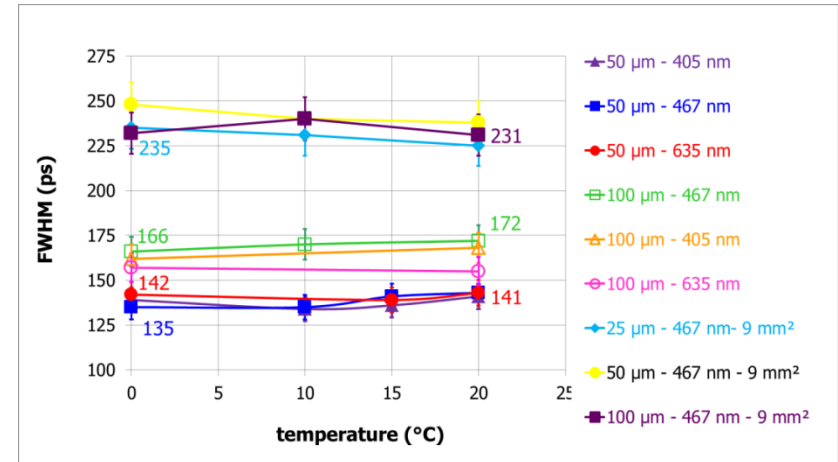
active layer is very thin (few μm) + breakdown development is very fast + big signal amplitude \rightarrow very good timing properties even for single photons can be expected



P.W Cattaneo, arXiv:1402.1404v1

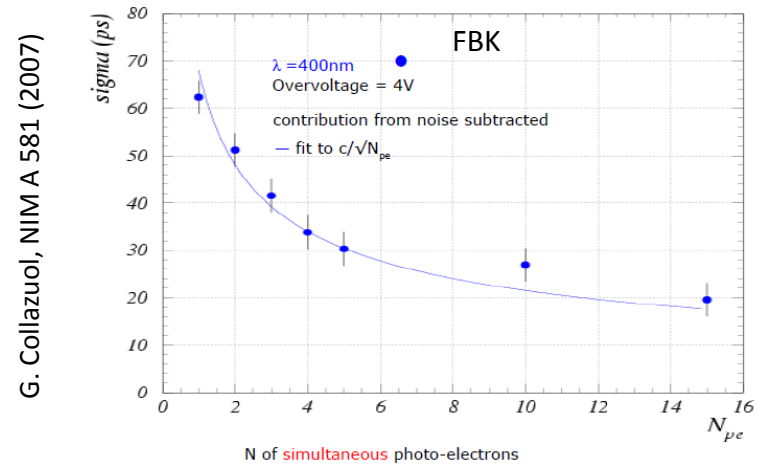
40 ps < SPTR (σ) < 60 ps

No variation of the SPTR with the temperature



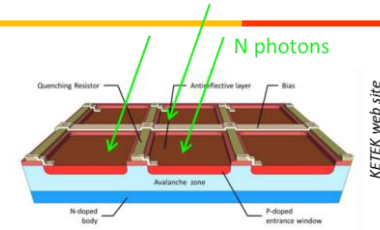
V. Puill, NIMA 695, 2012

Timing resolution as a function of the incident number of photons



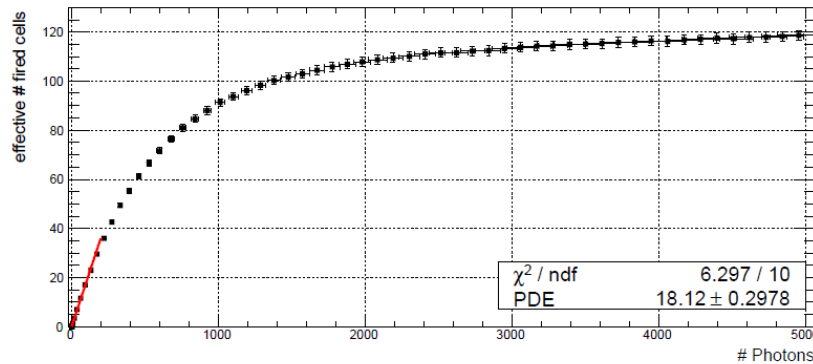
G. Collazuol, NIM A 581 (2007)

2 or more photons in 1 cell look exactly like 1 single photon



Output signal: proportional to the number of fired cells as long as $N_{\text{photon}} \times \text{PDE} \ll N_{\text{total}}$

SiPM response as a function of the number of instantaneous incident photons



T. Kowalew Thesis

$$A \approx N_{\text{firedcells}} = N_{\text{total}} \cdot \left(1 - e^{-\frac{N_{\text{photon}} \cdot \text{PDE}}{N_{\text{total}}}}\right)$$

$N_{\text{firedcells}}$: number of excited cells

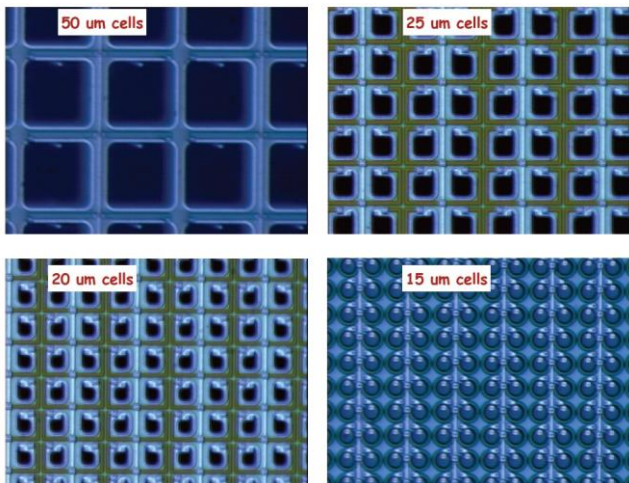
N_{total} : total number of cells

N_{photon} : number of incident photons in a pulse

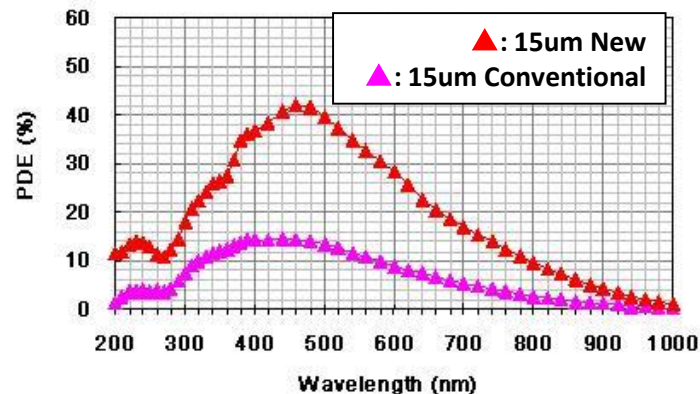
The saturation is a limiting factor for the use of SiPM where large dynamic range of signal (5000 – 10000 photons/pulse) has to be detected (calorimetry)

high density SiPM : device with more than 1000 cells/mm² + short recovery time

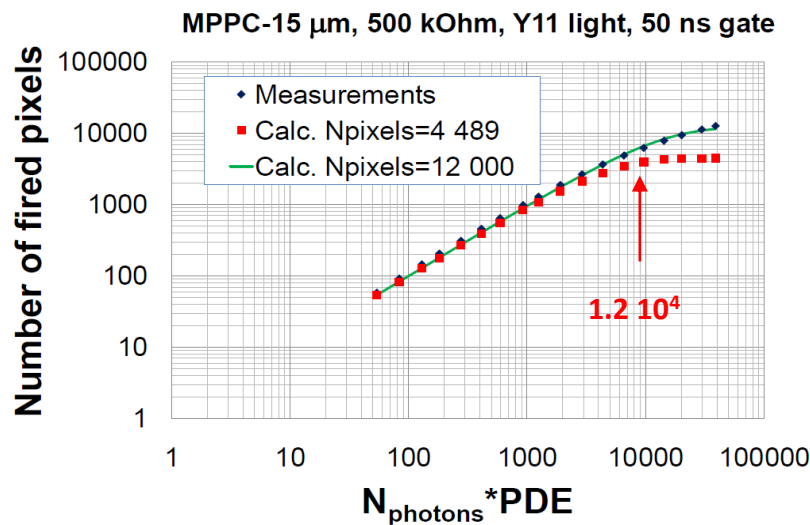
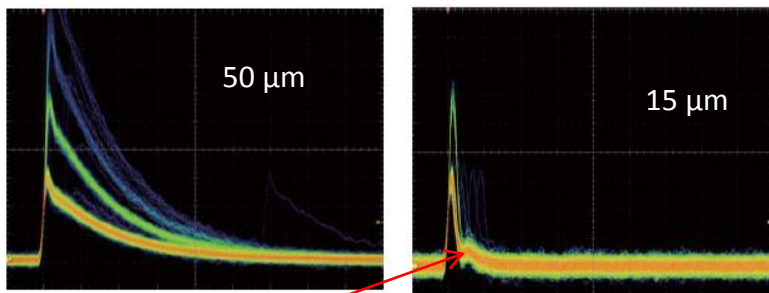
HAMAMATSU



1 mm²
4489 cells
cell size : 15 μm
gain = 2x10⁵



HPK, private communication



Y. Musienko, NDIP-2011

fast cell recovery time (~4ns) → the linearity for Y11 (WLS fiber) light of 4489 cells/mm² MPPC corresponds to a SiPM with ~ 12000 cells/mm²

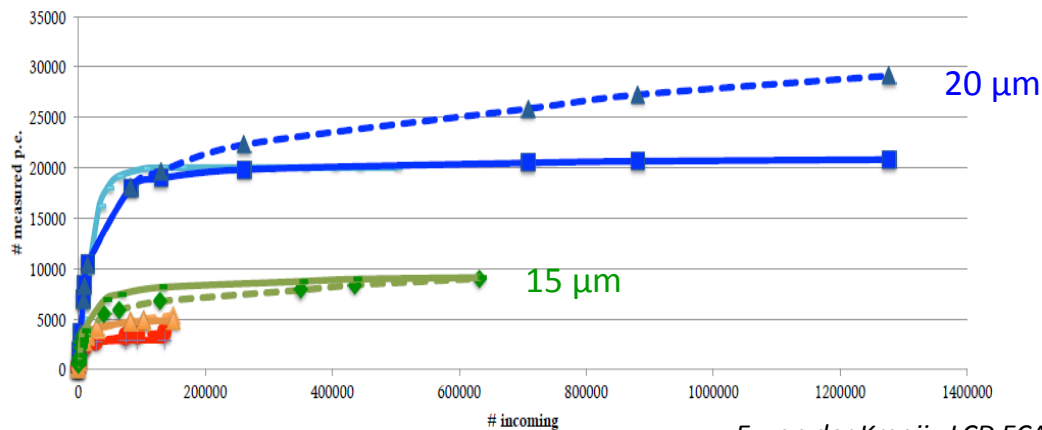
KETEK

high density SiPM : device with more than 1000 cells/mm²

MP15 V6 W8:
1.2x1.2 mm²
Cell size = 15 μm
12800 cells



MP20 V4 W12:
3x3 mm²
Cell size = 20 μm
22500 cells



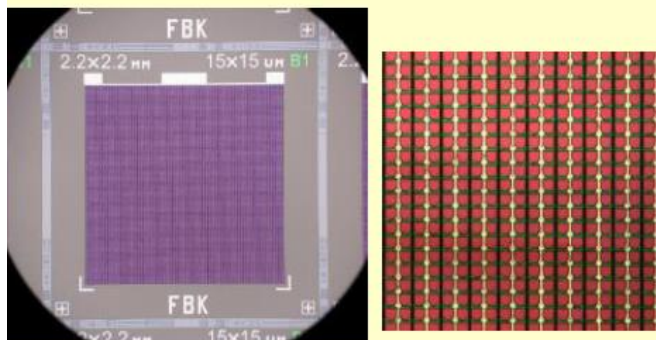
E. van der Kraaij, LCD ECAL meeting 2014

FBK

Active area: 2.2x2.2 mm²
cell size: 15x15 μm²
cells: ~ 21300
Fill factor = 48%

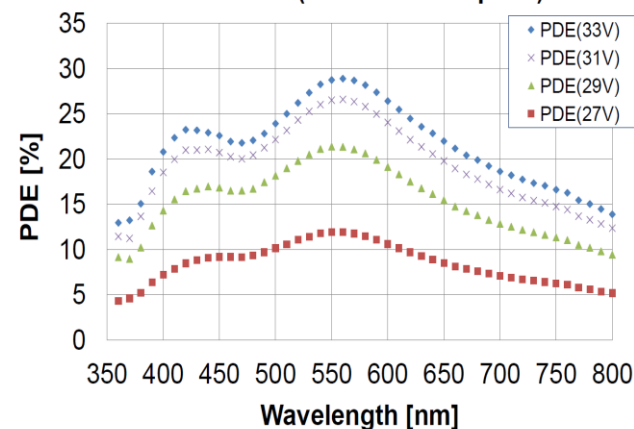
RGB-SiPM-HD

2.2 x 2.2 mm²
gain = 8x10⁵
DCR = 2MHz/mm²
recovery time = 9 ns



A. Ferri

FBK SiPM (15 micron cell pitch) *



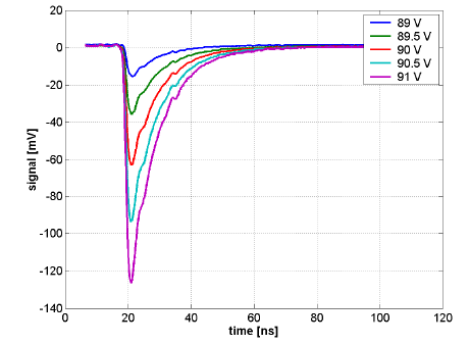
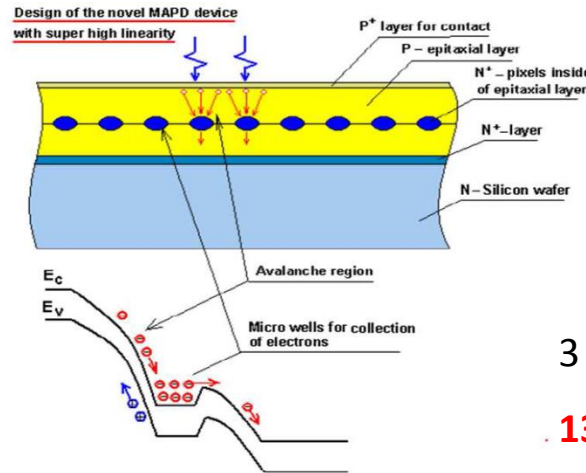
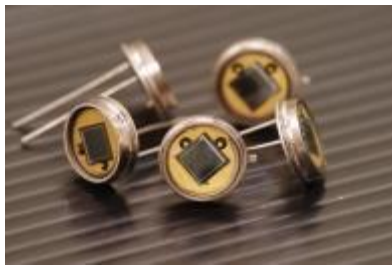
** measurements by Y.Musienko @ CERN*



ZECOTEK

MAPD-3N

Special design: both the matrix of avalanche regions and the individual quenching elements are created inside the Si substrate with a special distribution of the inner electric field

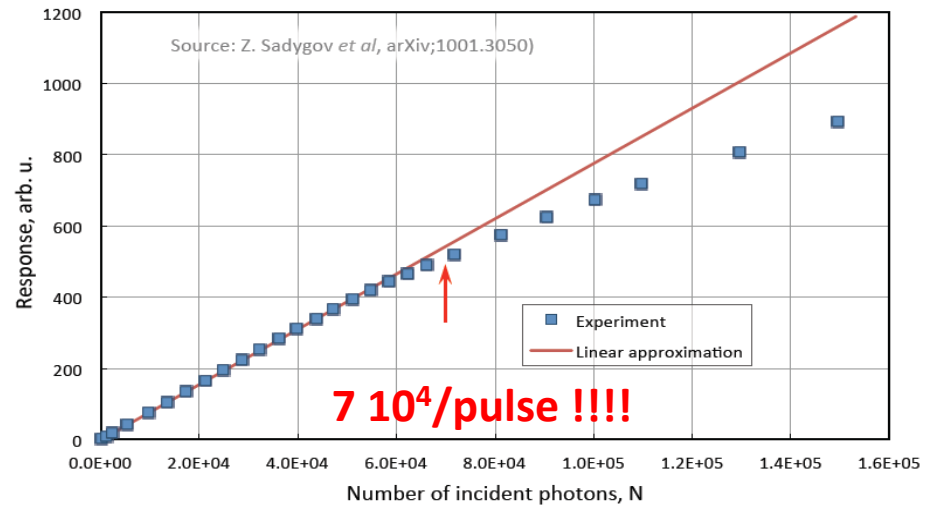
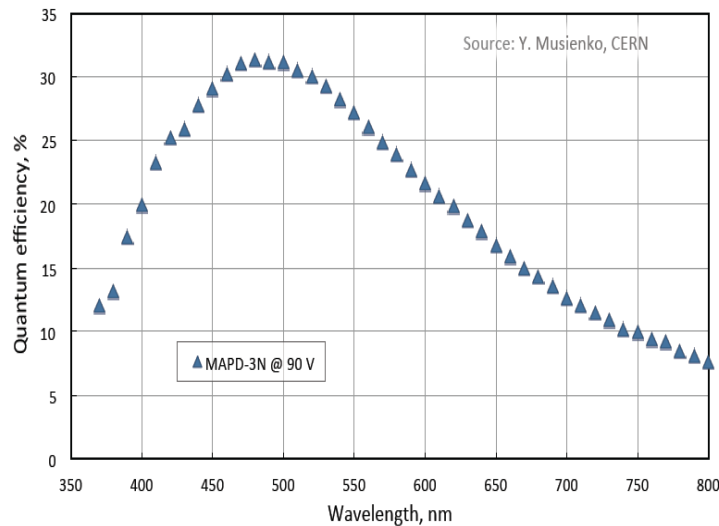


3 x 3 mm²

1350000 cells (15000/mm²)

gain = 10⁵

slow cell recovery time : 80 ns



protons / neutrons

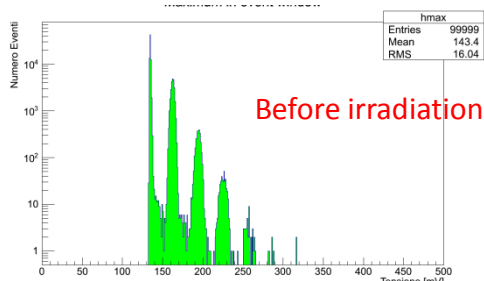
bulk damages caused by lattice defects

γ -rays, X-rays

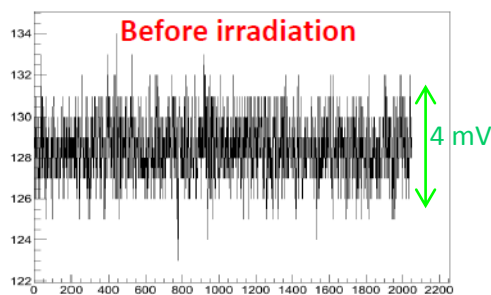
creation of trapped charges near the Si-insulator interface

- increase of the dark current and the DCR
- change of the breakdown voltage
- change of the gain and PDE dependence as a function of bias voltage

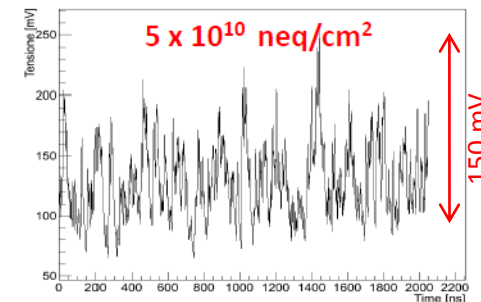
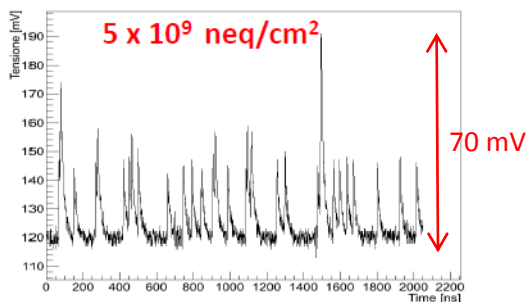
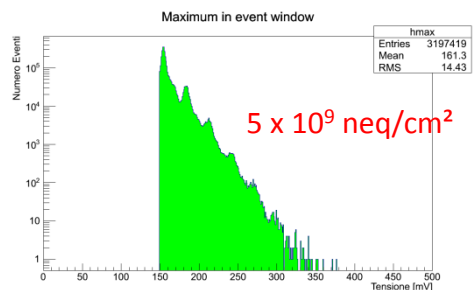
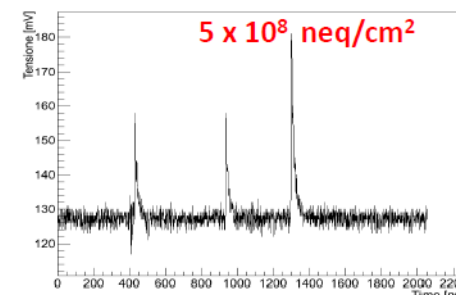
→ high dark noise → large size cells (we need them for high PDE!!) are permanently fired → significant drop of the SiPM PDE and gain → SiPM has low PDE, gain and it is useless as a photodetector for the calorimetry... (Y. Musienko, NDIP14)



DCR

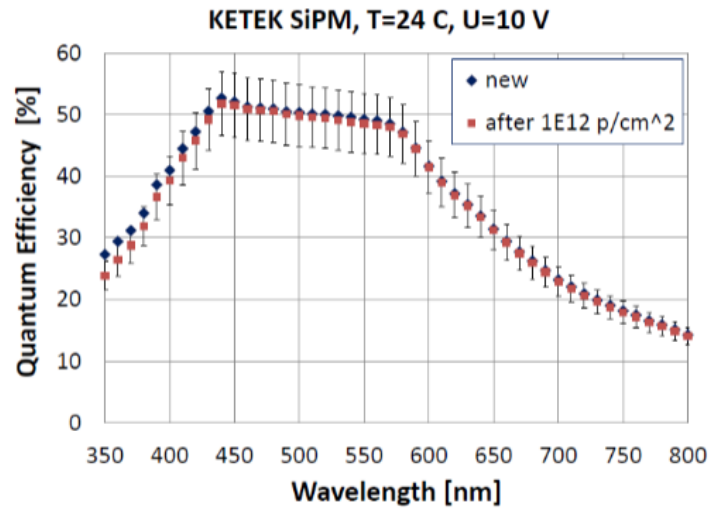
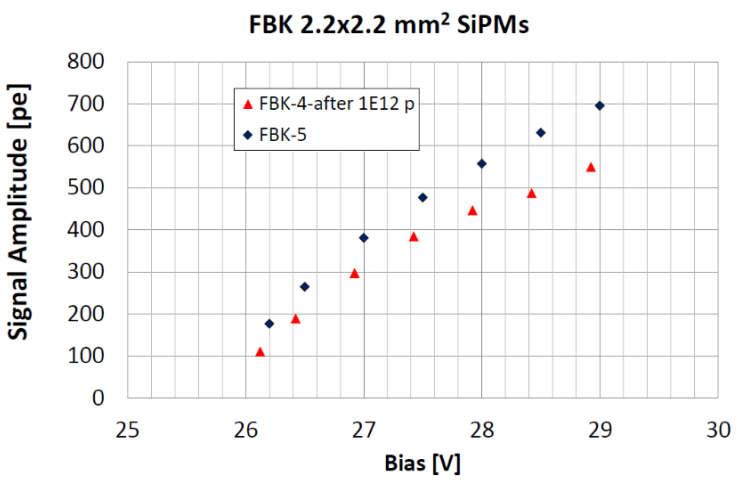


DCR

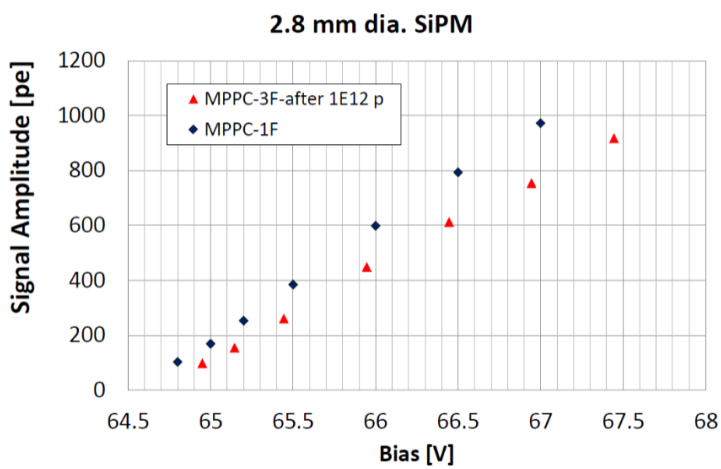


HAMAMATSU , FBK, NDL, ZECOTEK, KETEK developed devices with improved radiation hardness

HAMAMATSU, KETEK and FBK SiPMs survive 10^{12} n/cm² 1 MeV equivalent neutron flux (it was 10^8 n/cm² 3 years ago)



Y. Musienko, NDIP 2014



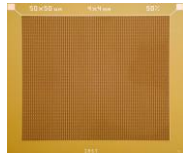
At high neutron fluence a decrease of the Gain*PDE is observe → can be recovered by bias voltage increase.

Large SiPMs: large sensitive area but high DCR ...

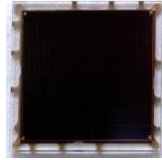
Excelitas C30742-66



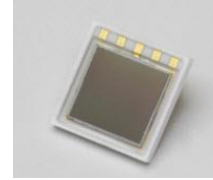
ASD-SiPM4S



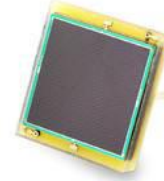
sensL C-series



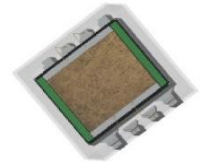
HAMAMATSU S10985



KETEK PM6060



STMicroelectronics



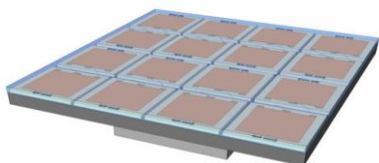
Producer	Reference	Area (mm ²)	PDE max @ 25 °C *	Dark Count Rate max (Hz) @ 25°C *	Gain *
EXCELITAS	C30742	6 x 6	30% @ 420 nm	10 .10 ⁶	1.5 10 ⁶
FBK - AdvanSiD	ASD-SiPM4S	4 x 4	30% @ 480 nm	9.5 10 ⁷	4.8 10 ⁶
HAMAMATSU	S10985-50C	6 x 6	50% @ 440 nm (includes afterpulses & crosstalk)	10.10 ⁶	7.5 10 ⁵
SensL	C-series	6 x 6	40 % @ 420 nm	4.5 10 ⁶ (21 °C)	3 10 ⁶
KETEK	PM6060	6 x 6	40% @ 420 nm	18.10 ⁶	10 ⁷
STMicroelectronics	SPM35AN	3,5 x 3,5	16% @ 420 nm	7.5 10 ⁶	3.2 10 ⁶

* datasheet data

Segmentation of the light detection + need of larger active area → SiPM matrix

FBK

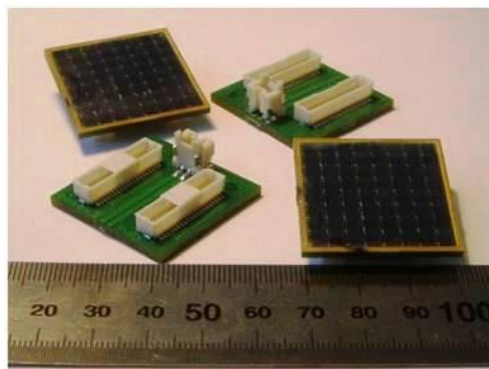
ASD-SiPM4S-P-4x4T-50



4x4 channels

1 channel = $4 \times 4 \text{ mm}^2$
6400 cells ($50 \times 50 \text{ }\mu\text{m}^2$)
/channel

Zecotek

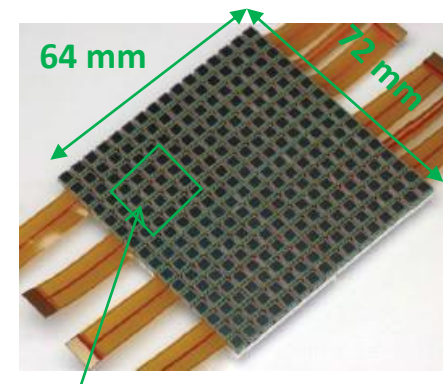


8x8 channels

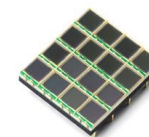
1 channel = $3 \times 3 \text{ mm}^2$
15000 cells /channel

HAMAMATSU

S11834-3388DF



S11064-025

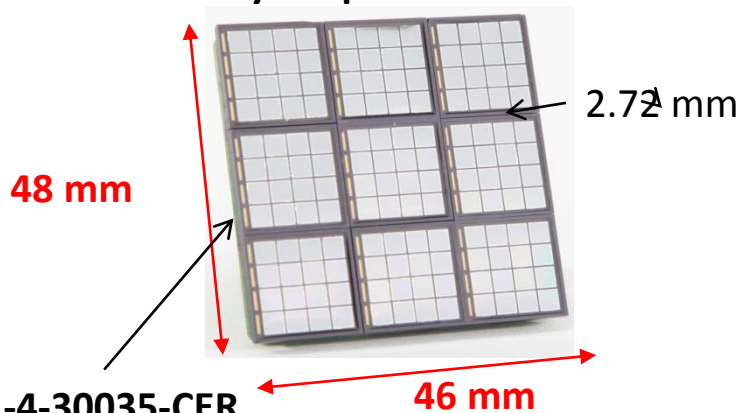


4x4 channels

1 channel = $3 \times 3 \text{ mm}^2$
14400 cells ($25 \times 25 \text{ }\mu\text{m}^2$) /channel

Sensl

ArraySL-4p9-30035



SL-4-30035-CER

4x4 channels

1 channel = $3 \times 3 \text{ mm}^2$

4774 cells ($35 \times 35 \mu\text{m}^2$) /channel

ArrayB-600XX-64P



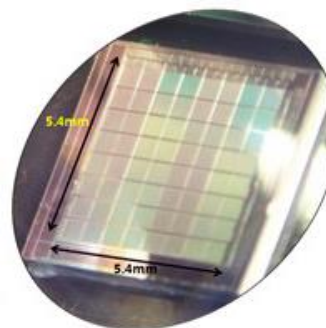
8x8 channels

1 channel = $6 \times 6 \text{ mm}^2$

18980 cells /channel

new surface mount package

Sungkyunkwan University (Korea)



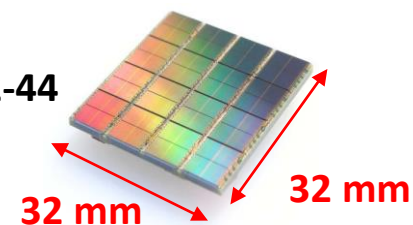
8x8 channels

1 channel = $0.5 \times 0.5 \text{ mm}^2$

1024 cells ($32 \times 32 \mu\text{m}^2$) /channel

Philips Digital Photon Counting

DLS-6400-22-44



8x8 channels

1 channel = $3.9 \times 3.2 \text{ mm}^2$

6396 cells ($59 \times 32 \mu\text{m}^2$) /channel

Electronics embedded

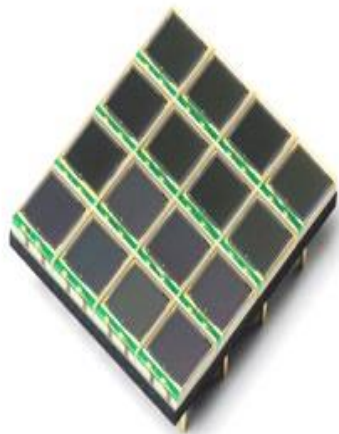
Requirements for the SiPM matrixes:

- improvement of the spatial resolution and PDE
- simplification of the assembly for the building of detectors with large surface and large active area

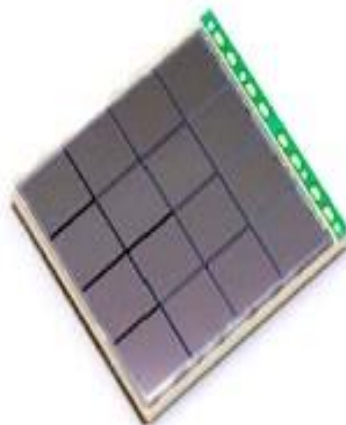


- ✓ Important efforts on the packaging: matrix tileable on almost all their sides + small dead space between them
- ✓ Development of monolithic SiPM matrices: all the channels are on the same substrate → small dead spaces, simplification of the assembly

Discrete Array



Monolithic Array



3-side buttable Tiling

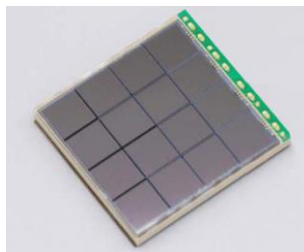


HAMAMATSU

4x4 channels

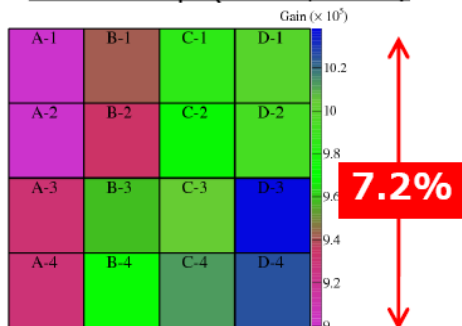
1 channel = 3x3 mm²

3600 cells (50x50 μm²)/channel



S11828-3344

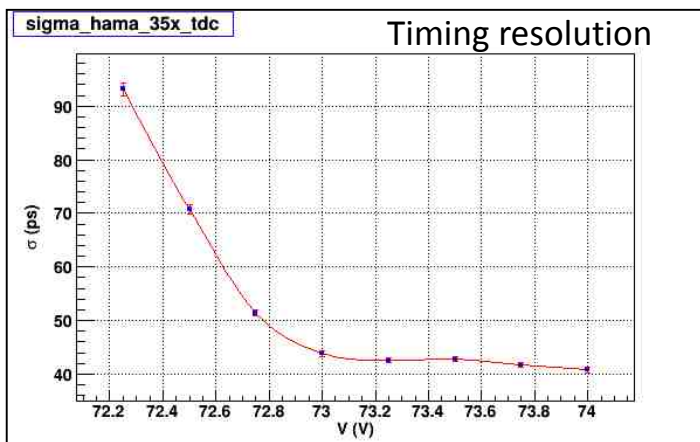
Gain map (71.9V, 0 °C)



ave. gain = 9.7x10⁵

3 sides tileable
1 cathode – 16 anodes

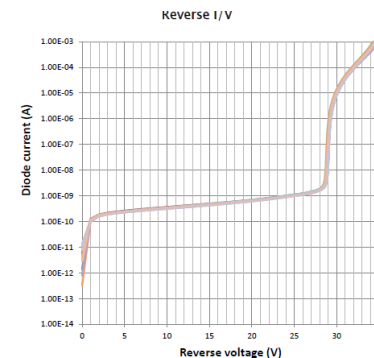
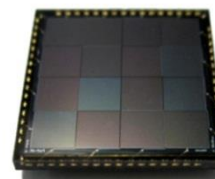
Kato et al, NIMA 638 (2011) 83–91



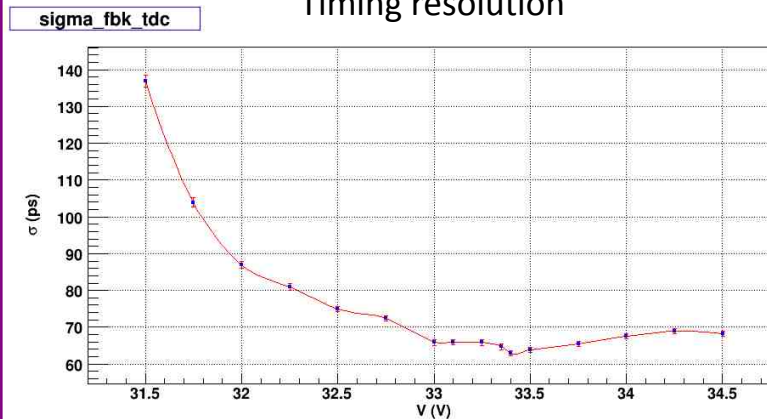
M. Bonesini, IPRD13

FBK - AdvanSiD

ASD-SiPM3S-P-4x4A

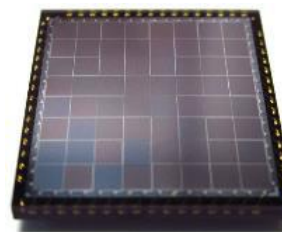


Timing resolution



M. Bonesini, IPRD13

ASD-RGB1.5S-P-8x8A



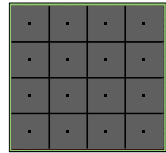
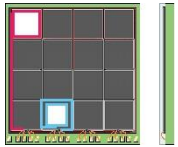
8 x 8 channels

4 sides tileable

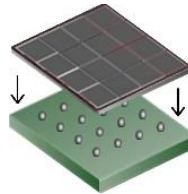
HAMAMATSU development: another way to improve the fill factor and therefore the PDE

Through Silicon Via Technology: each anode is connected by the shortest distance possible to the substrate

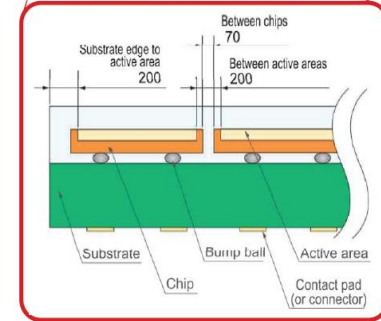
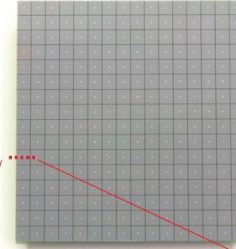
with wire bonding (traces to the bonding pads)



with TSV (No traces)

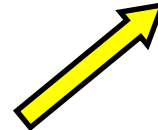
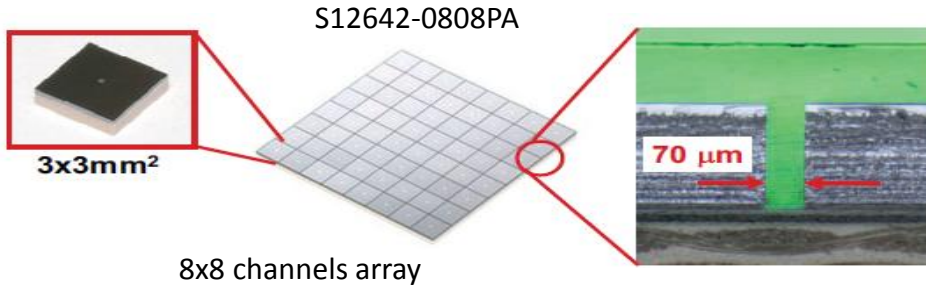


16x16 channels array

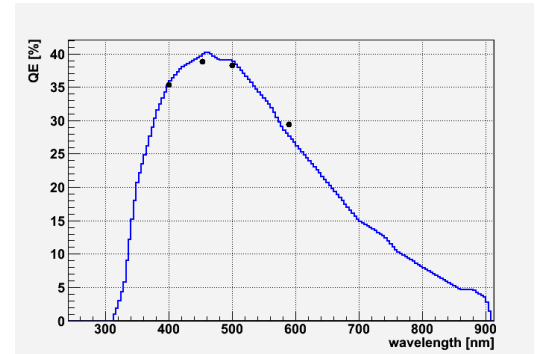


K. Sato, IEEE NSS 2013

+ high precision assembly → Discrete Array like monolithic array !



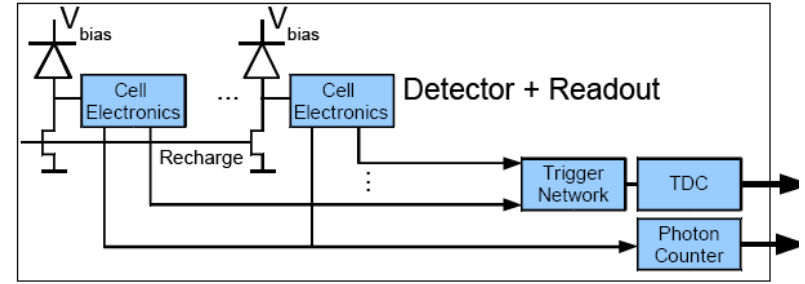
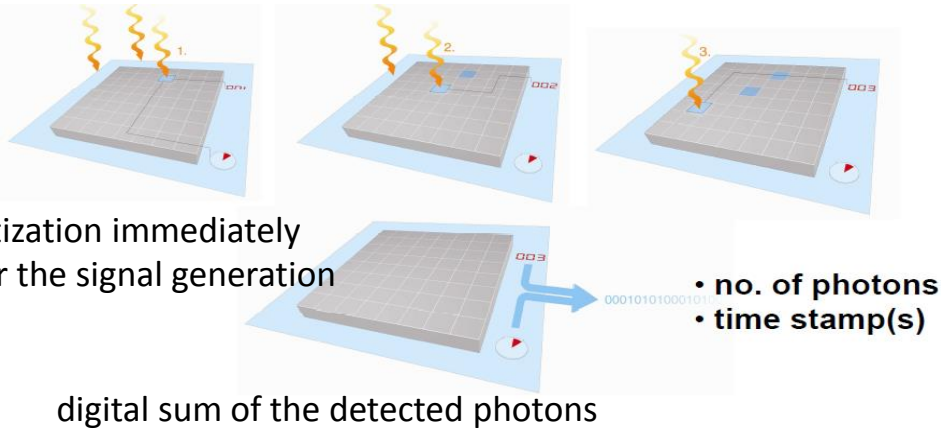
4 side tileable configuration with very narrow gap between neighboring active areas (200 μm) equivalent to the gap in traditional monolithic type devices



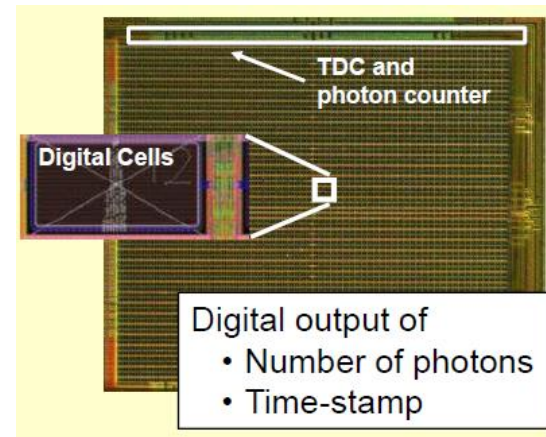
N. Otte, NDIP14

Array of G-APDs integrated in a standard CMOS process. The signal from each cell is digitized and the information is processed on chip:

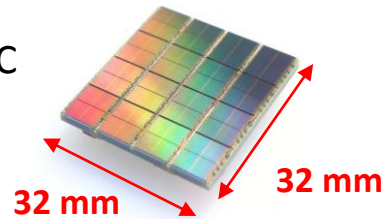
- time of first fired cell is measured
- number of fired cells is counted
- active control is used to recharge fired cells



York Hämisch, TIPP 2011



Example of a matrix of DPC



DLS-6400-22-44

8x8 channels

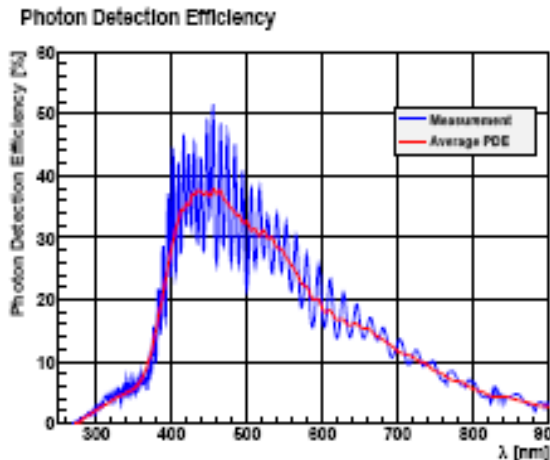
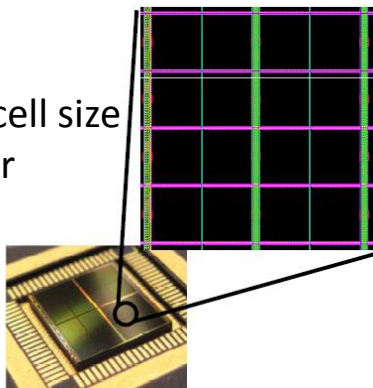
1 channel = 3.9 x 3.2 mm²

Electronics embedded

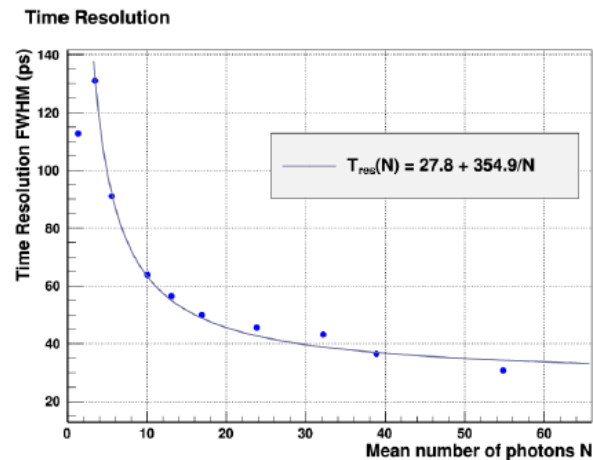
Early Designs in 2005

DLS-3200-22-44

- 3200 cells
- $59 \times 64 \mu\text{m}^2$ cell size
- 78% fill-factor



T. Frach, 2012 JINST 7 C01112



T. Frach, Hereaus seminar 2013

- *afterpulsing* $\sim 18\%$ (20 °C)
- *DCR* = 200 kHz/mm² (20 °C)
- *temperature sensitivity* $\sim 0.33\%$ /°C
- *timing resolution (SPTR)* = 140 ps (FWHM)
- *recovery time* : 5 – 40 ns

Radiation hardness ?

→ still working for 10^{11} n/cm² (producer communication)



Drawback:

➤ requires a dedicated readout provided by Philips

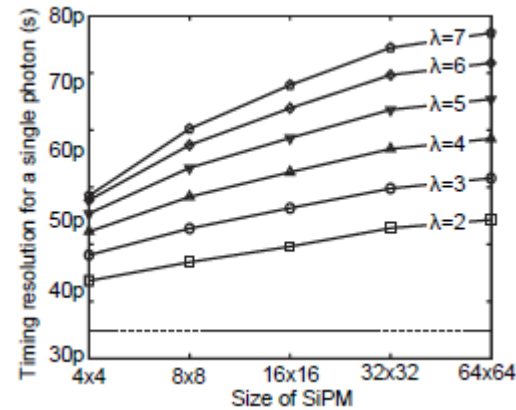
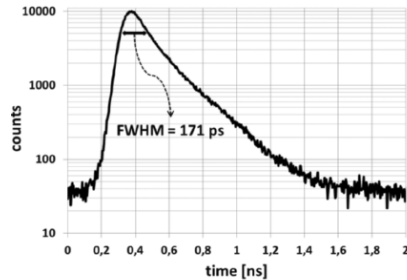
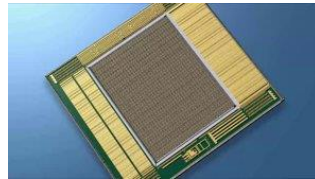
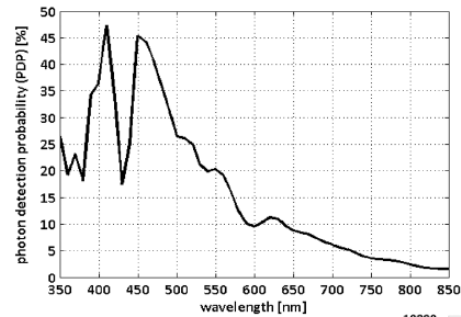
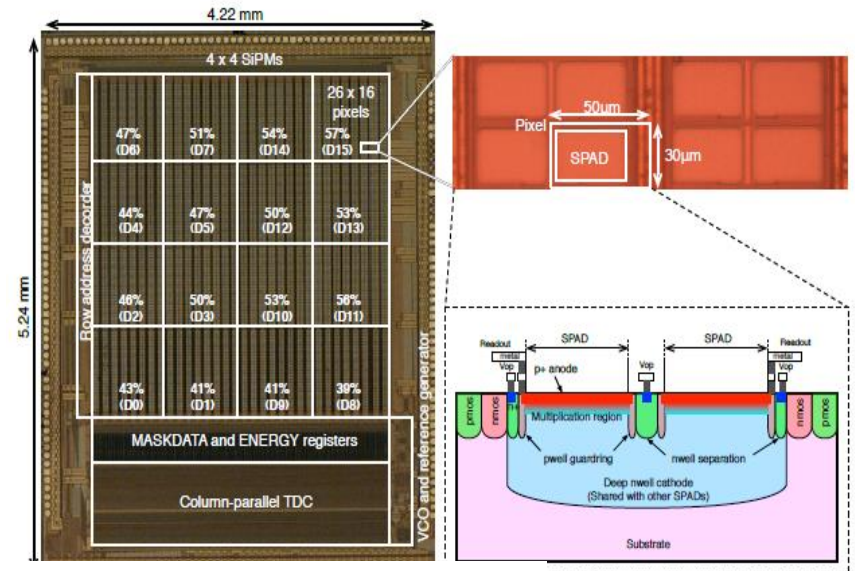
FBK – ST micro – Edimburg University



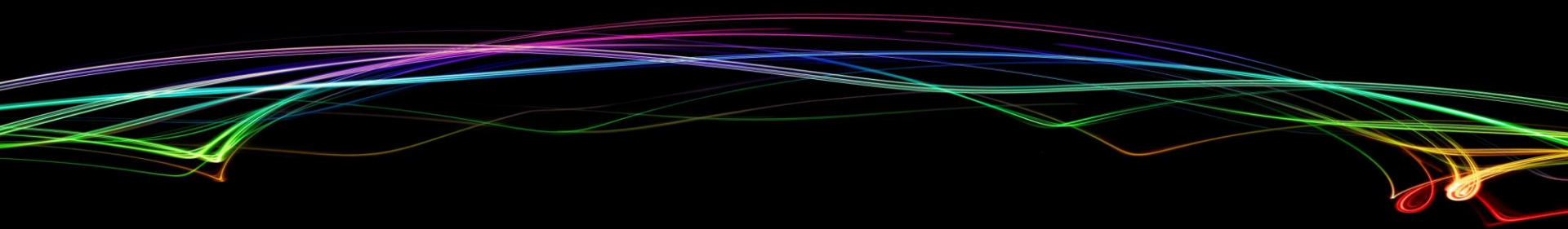
L. H. C. Braga, *IEEE Journal of solid state circuit* vol. 49, 2014.

Faculty of Electrical Engineering, TU Delft



Area of the chip: 22.1 mm² with a sensitive area of 3.2 x 3.2 mm²



S. Mandai, 2013 JINST P05024



Conclusion

	 (max value)	
PMT	<ul style="list-style-type: none"> ▪ High gain (10^6) with 1000 – 2000 V ▪ Low noise ▪ High quantum efficiency (30 % in blue) ▪ Large area ($> 10000 \text{ mm}^2$) ▪ Large number of configurations ▪ Commercial products since 70 years 	<ul style="list-style-type: none"> ▪ Non linearity ▪ Non response uniformity ▪ Affected by magnetic field ▪ Fragility ▪ Only 2 producers on the market !!
MCP-PMT	<ul style="list-style-type: none"> ➤ High gain (10^7- 10^8) ➤ High quantum efficiency ➤ Very good timing properties (SPTR = 30 ps) 	<ul style="list-style-type: none"> ➤ Fragility ➤ Cost
SiPM	<ul style="list-style-type: none"> • High gain (10^5-10^6) with low voltage ($< 100 \text{ V}$) • Single photo detection • Good timing resolution (SPTR = 40 ps) • Insensitivity to magnetic field (up to 7 T) • High photon detection efficiency (50 % in blue) • Mechanically robust • A lot of R&D and different producers • Low cost mass production possible (ex: T2K) 	<ul style="list-style-type: none"> • High dark count rate @ room temperature for large device ($\geq 9 \text{ mm}^2$) • High temperature dependence of the breakdown voltage, the gain • Small devices • Few geometrical configurations available

Lectures and Revues :

- **IEEE NSS 2012:** Vacuum based photodetector, **Katsushi Arisaka**
- **PhotoDet 2012 workshop**, LAL Orsay: The SiPM Physics and Technology - a Review , **Gianmaria Collazuol**
- **Summer School INFIERI 2013, Oxford:** Intelligent PMTs versus SiPMs, **Véronique Puill**
- **RICH 2013:** Status and Perspectives of Solid State Photo-Detector, **Gianmaria Collazuol**
- **NDIP14:** MCPs and Vacuum Detectors Review, **Thierry. Gys**

Reference articles:

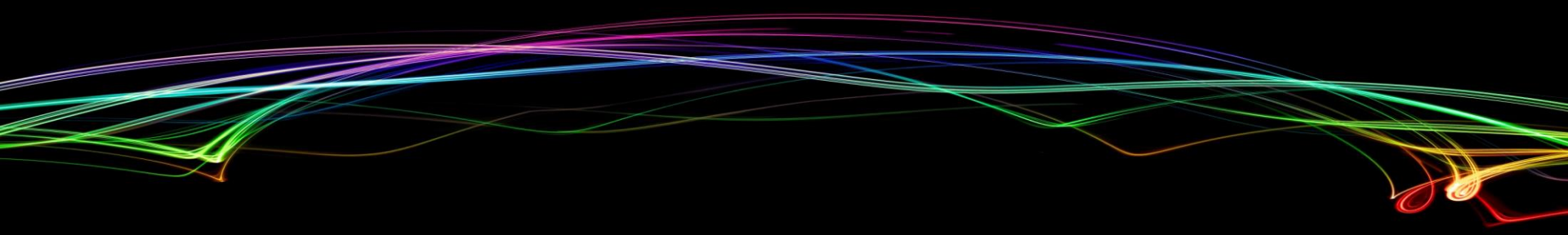
- **Photomultipliers** from S.Donati
- **Silicon Photomultiplier - New Era of Photon Detection** from Valeri Saveliev
- **Advances in solid state photon detectors** from D. Renker and E. Lorenz
- **Silicon Photo Multipliers Detectors Operating in Geiger Regime: an Unlimited Device for Future Applications** from G. Barbarino, R. de Asmundis, G.a De Rosa, C. M Mollo, S. Russo and D. Vivolo

Books:

- ❖ **Hamamatsu PMT Handbook**
- ❖ **Burle PMT book**

Articles and presentations:

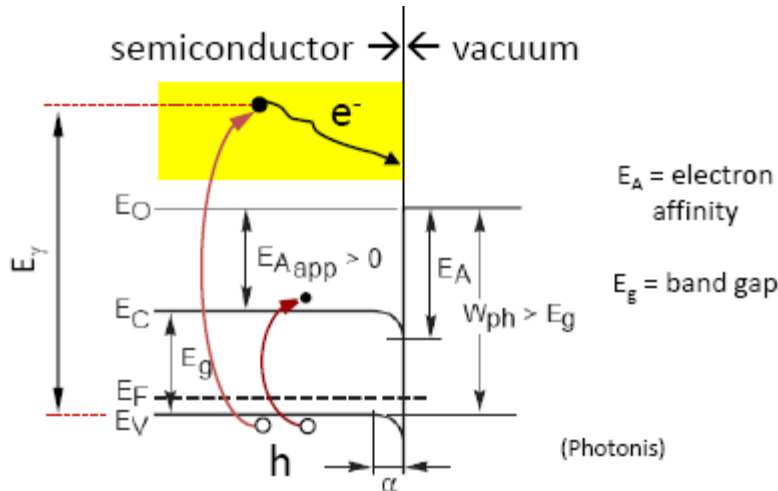
All quoted under the figures and plots of this presentation (my apologies if I forgot some of them)



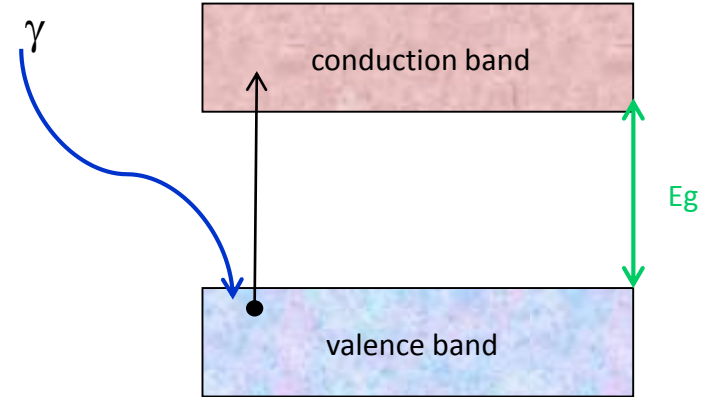
The End

Thanks for your attention

in vacuum devices



in semiconductor devices



1 or 3 steps process:

Step 1: Absorption of the photon (γ) in the material and generation of electrons. If $E_\gamma > E_g$, electrons are lifted to conduction band

→ for Si-photodetector this leads to a photocurrent: **internal photoelectric effect**

→ for vacuum device (PMT, MCP-PMT, ...), 2 more steps are needed to detect a signal:

external photoelectric effect

Step 2: diffusion of the electrons through the material toward the boundary to vacuum. The escape depth L depends on the material.

Step 3: electrons with sufficient excess energy (larger energy than the work function) reaching the surface escape from it

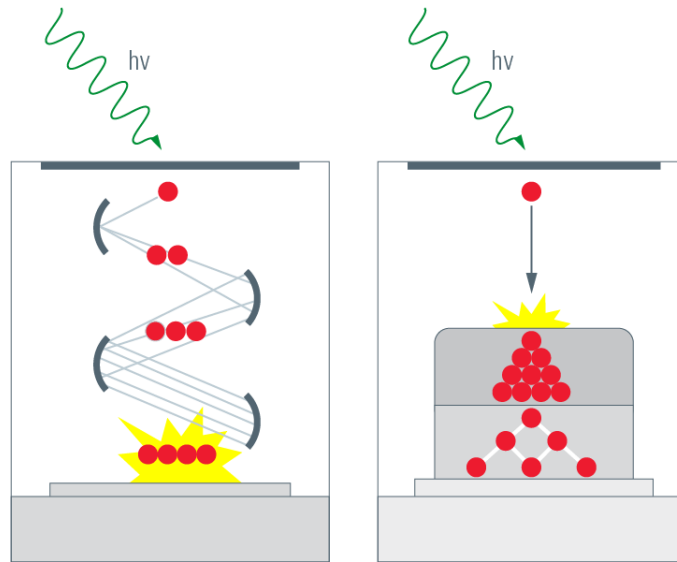
Once created, the photo-electrons (vacuum devices) or electron/hole pair (Si photodetector) can be lost (absorption, recombination)

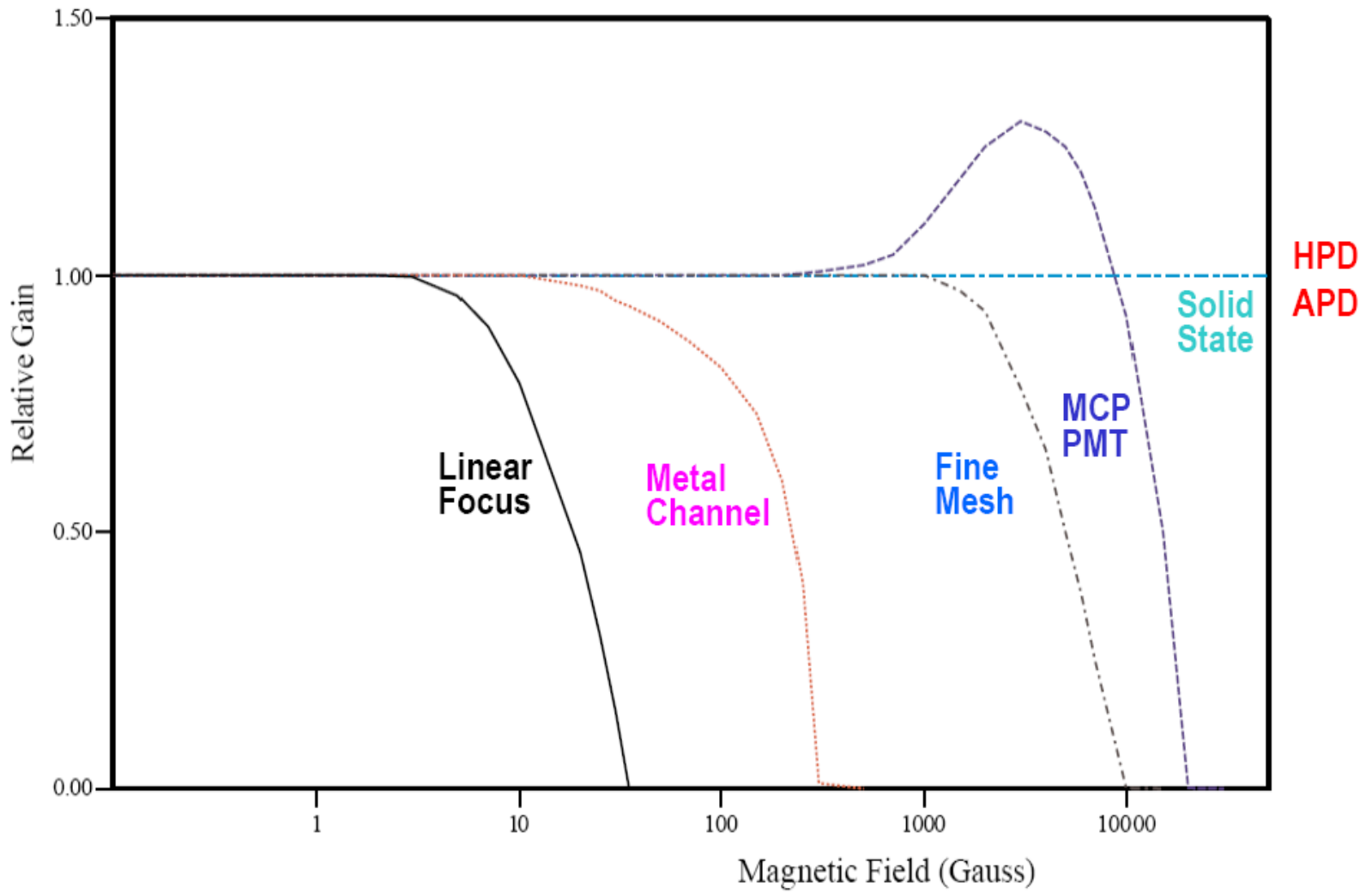


Need of a good **collection efficiency (C_E)**: probability to transfer the primary p.e or e/h to the amplification region or readout channel

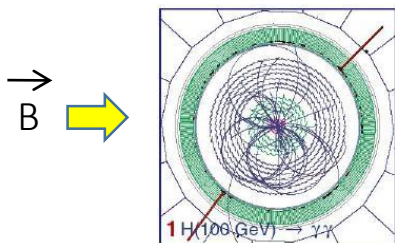
Step 3: the signal multiplication

The primary photo-electron or electron/hole pair is amplified (photodetector with **internal gain**)

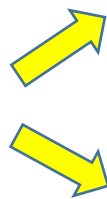




★ earth magnetic field = 30-60 mT



curves the trajectory of charges particles



separate the particles



easier analysis

reduce the detector size



reduce the detector price

PMT

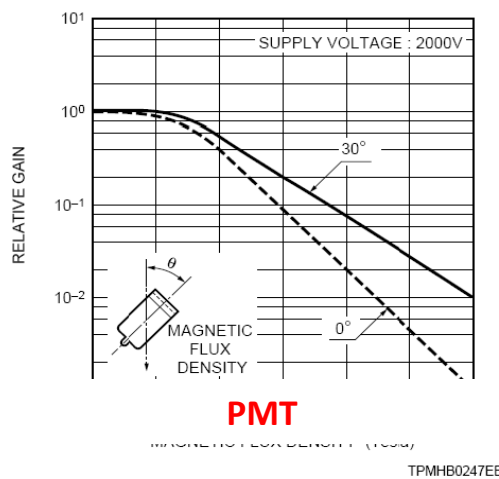
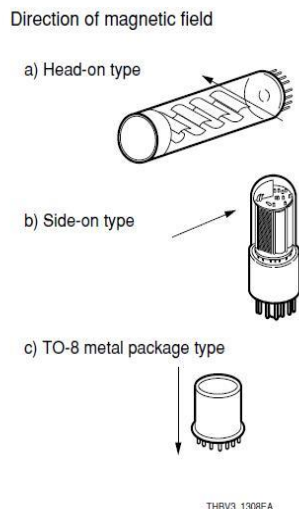
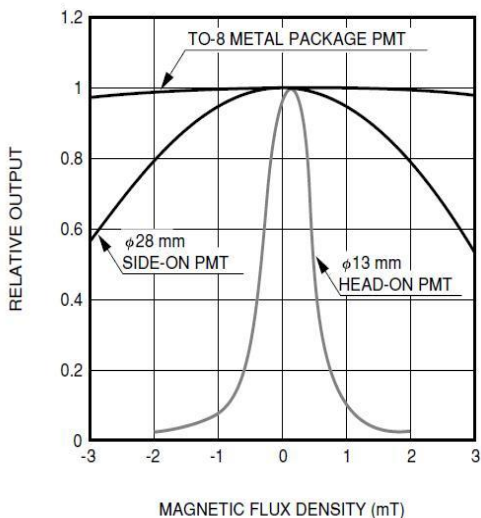
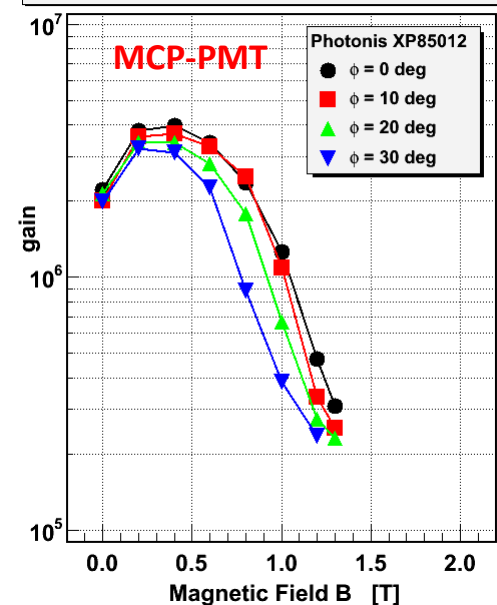


Figure 6-25: Gain vs. magnetic flux density

Figure 13-8: Magnetic characteristics of typical photomultiplier tubes

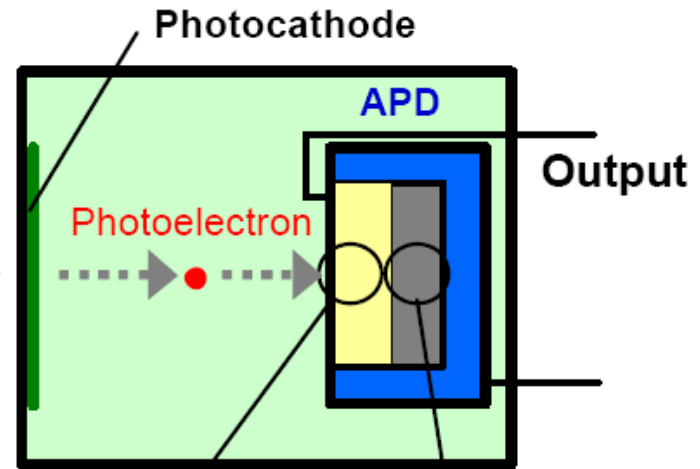
HAMAMATSU PMT book

Gain Dependence on Tilt Angle ϕ



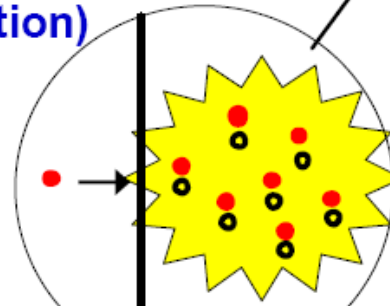
Albert Lehmann RICH 2010

PMT very sensitive to magnetic field → shielding required (μ metal)

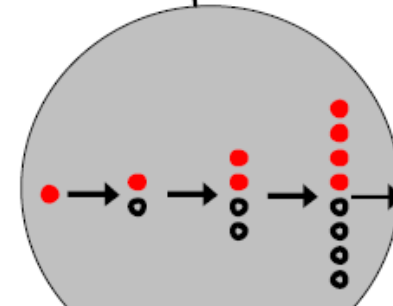


- Good PHD (Pulse Height Distribution)
- Good Uniformity
- Immunity to Magnetic Field
- Fast Time Response
- Compact (16mm in dia x 16mm)

<Photocathode>
Multi-Alkali, GaAsP, GaAs



Electron Bombardment
X 1200



Avalanche Gain
X 50

Combination of EB and avalanche gain

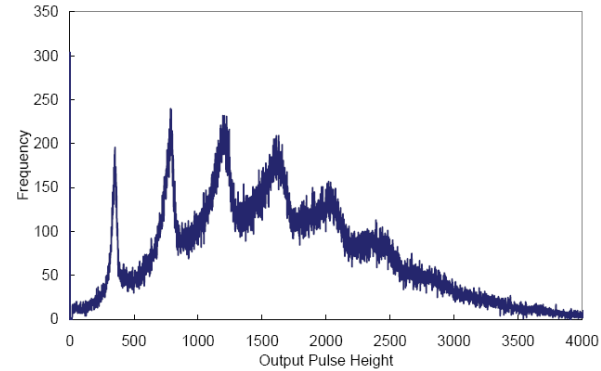
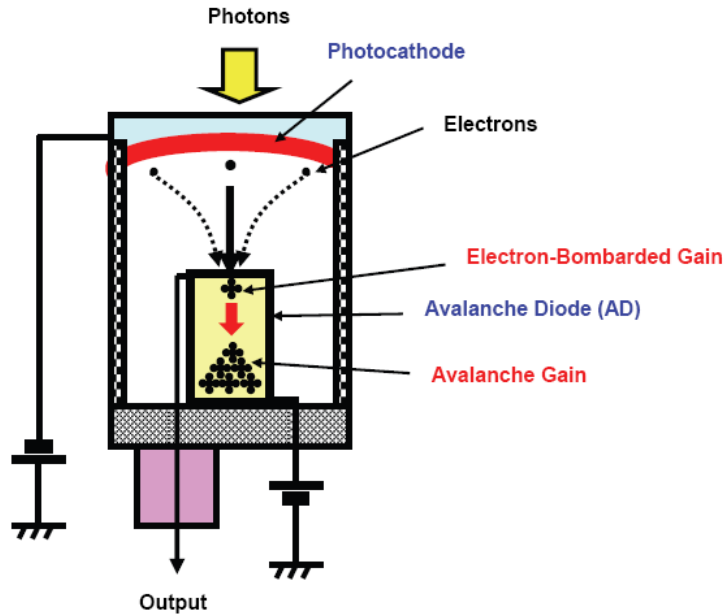
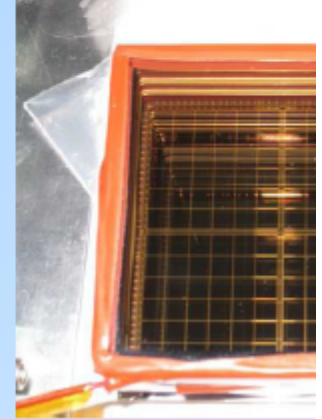
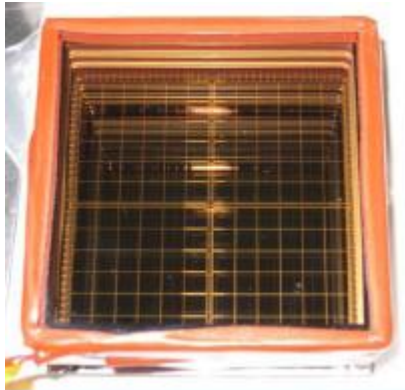
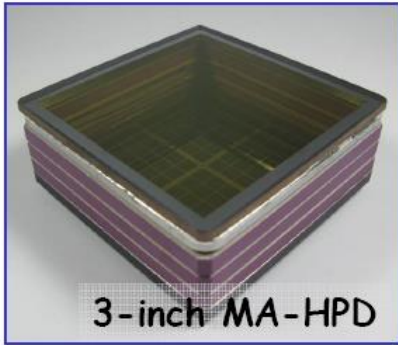


Figure 13: The pulse height spectrum for multi photons clearly shows peaks corresponding up to 6 photoelectrons.

Belle II aerogel RICH HAPD

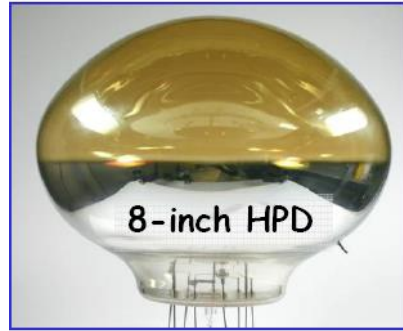
- proximity focusing configuration → operation in magnetic field
- HV ~8kV, gain ~100k (2000x50)
- 144 channels
- ~ 65% effective area
- tested up to 1000 Gy and 10^{12} n(1MeV)/cm²
- Belle + Hamamatsu





3-inch MA-HPD

RICH/Belle upgrade

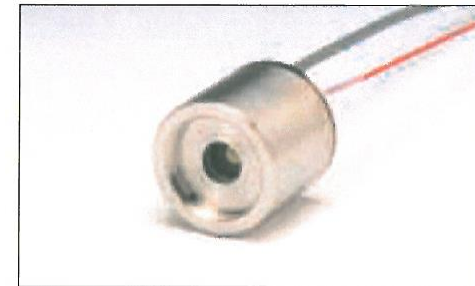


8-inch HPD

Water Tank Detector

The HPD (Hybrid Photodetector) utilizes the "electron bombardment" method in which photoelectrons are accelerated in a strong electric field to directly strike an avalanche diode (AD) in a vacuum tube. This mechanism achieves excellent quality of amplification.

Using a new AD with very low capacitance, we have developed a compact HPD with an excellent time resolution.



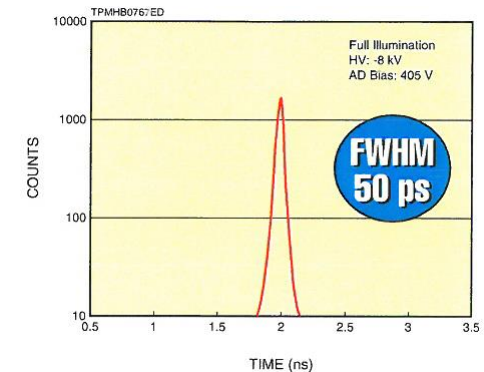
R10467U series

Parameter		R10467U-06	R10467U-40	R10467U-50	Unit
Spectral Response		220 to 650	300 to 720	380 to 890	nm
Photocathode	Material	Bialkali	GaAsP	GaAs	—
	Effective Area	$\phi 6$	$\phi 3$		mm
Quantum Efficiency		28 ^①	45 ^②	14 ^③	%
Gain ^④		1.2 × 10 ⁵			—
Rise Time		400			ps
T.T.S. (Transit Time Spread) ^⑤ (FWHM)		50	90	130	ps

① At 350 nm ② At 500 nm ③ At 800 nm

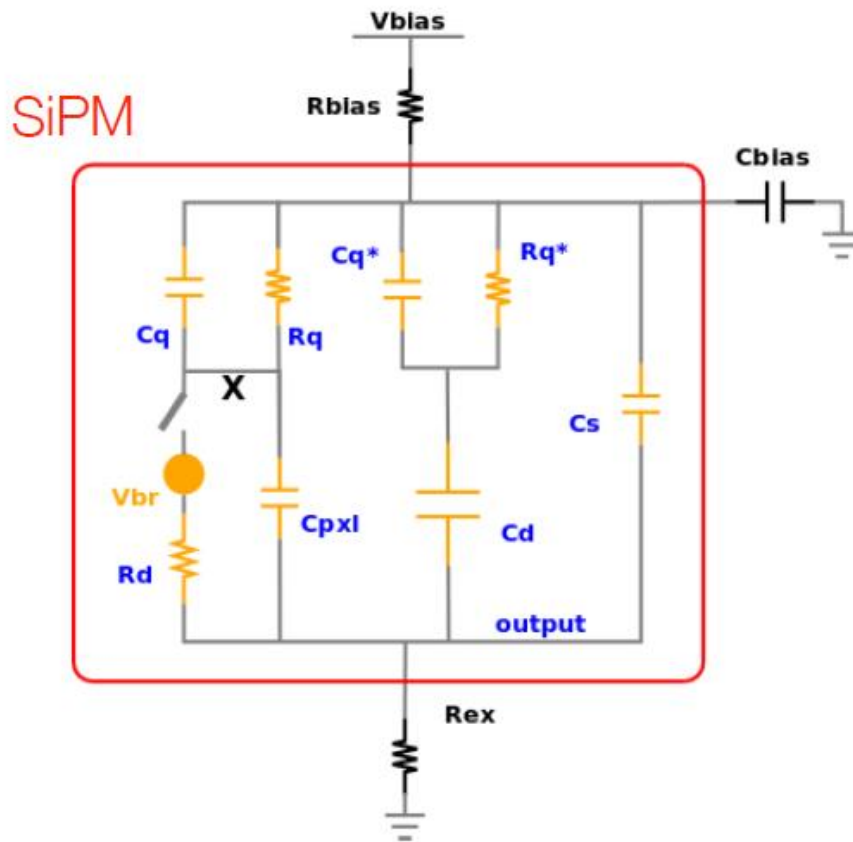
④ At the photocathode voltage of -8 kV and the AD bias voltage of V_b -10 V

⑤ At the single photon state and full illumination on the photocathode, specified as FWHM (Full Width at Half Maximum). These values include the jitter of the electronics of about 30 ps

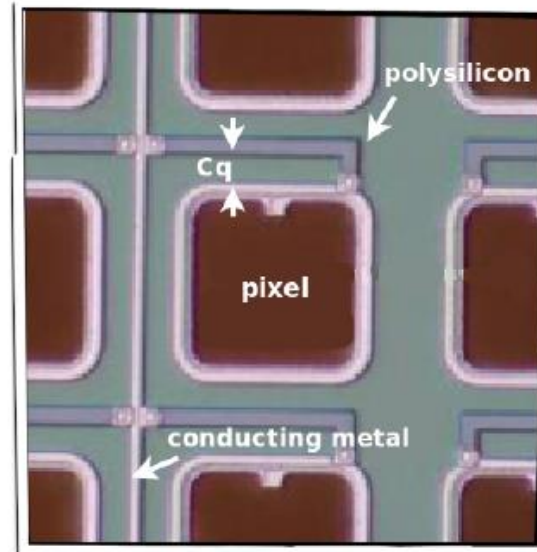


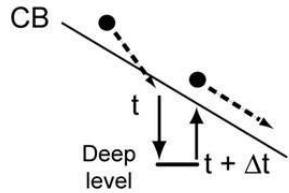
SiPM – Electrical Model

[source: W. Shen]



- C_{pxl} Pixel capacitance
- C_q Parasitic capacitance
- C_d Capacitance of inactive pixels
- C_s Stray capacitance
- R_q Quench resistor
- R_d Space charge resistance



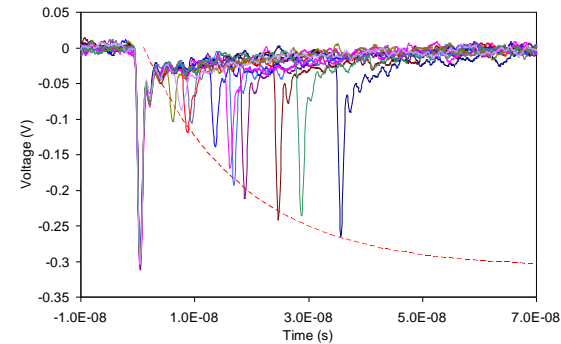
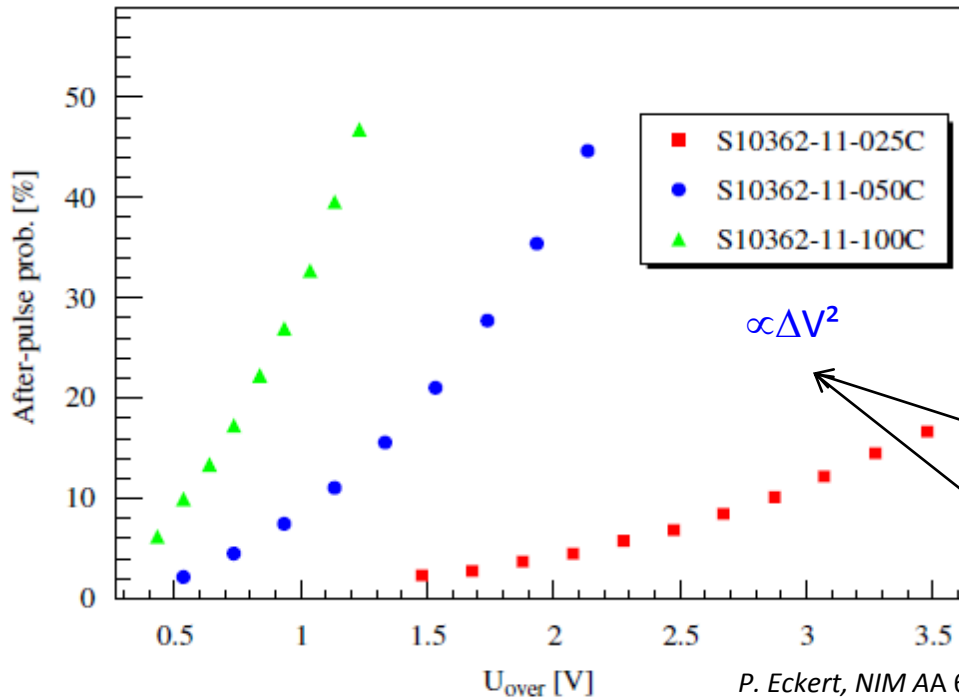


Breakdown \rightarrow production of a large number of charge carriers \rightarrow some of them are trapped in deep trap levels

These carriers may be released at some time and trigger a new breakdown avalanche event : afterpulse (described in term of probability)

$$P_{afterpulse}(t) = P_{trig} \times P_{capture} \frac{e^{-t/\tau}}{\tau}$$

$P_{capture}$: trap capture proba
 P_{trig} : avalanche triggering proba
 τ : trap lifetime



Number of carriers produced in the avalanche $\propto \Delta V$

Triggering proba $\propto \Delta V$

P. Eckert, NIM AA 620 (2010)

Proposal to Test Improved Radiation Tolerant Silicon Photomultipliers

F. Barbosa, J. McKisson, J. McKisson, Y. Qiang, E. Smith, D. Weisenberger, C. Zorn

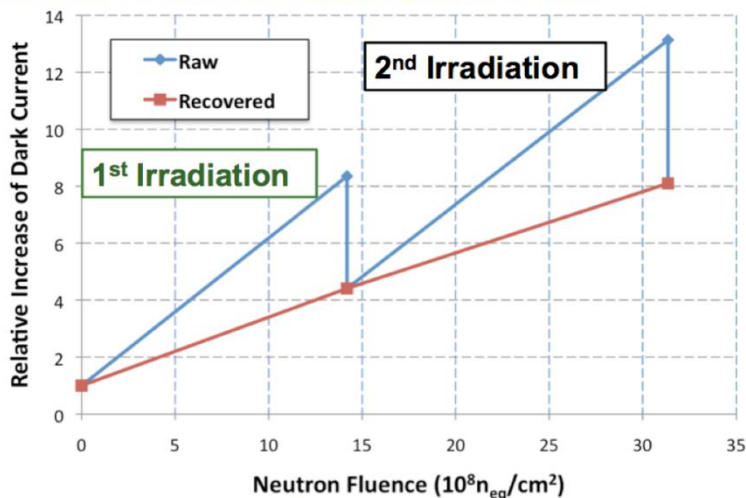
Jefferson Laboratory

How to Extend the Lifetime?

SiPMs cooled to 5°C during the beam → reduction of the dark noise by a factor 3 and minimization of the effects of neutron irradiation

Beam down period : SiPMs heated to ~40°C (post-irradiation annealing) → bring the noise down to a residual level

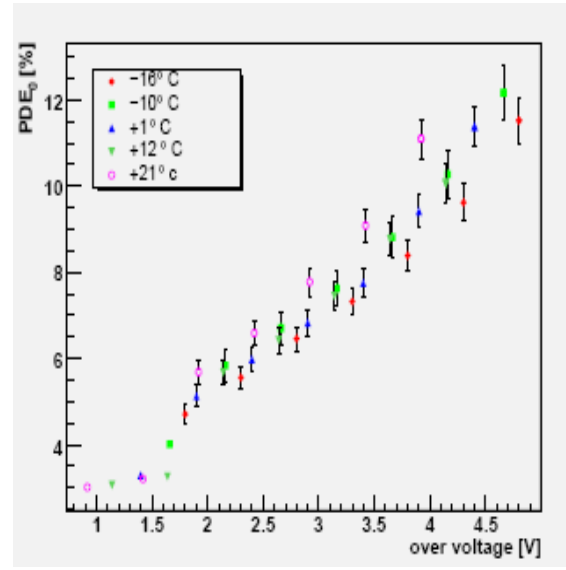
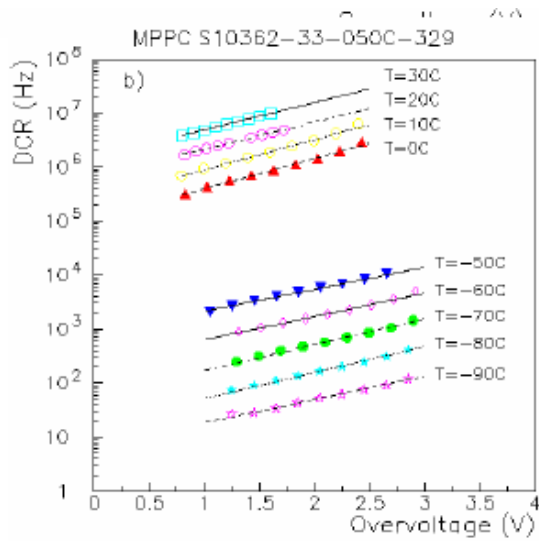
SiPM Neutron Radiation Test



At 25°C, annealing requires at least 5 days

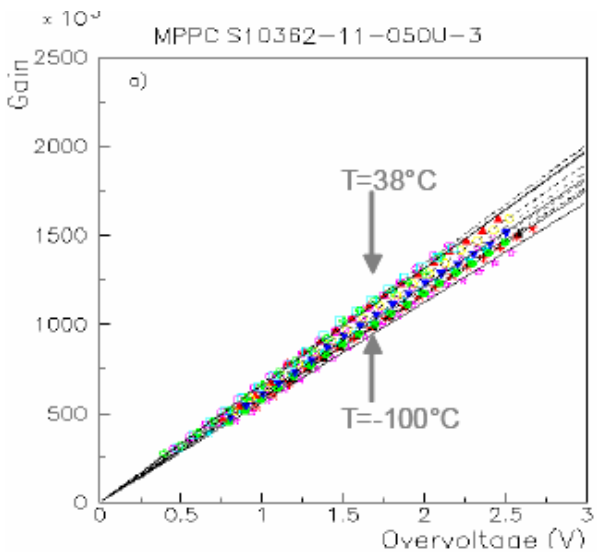
Heating to above 40°C can reduce the annealing time to less than 24 hours

Neutron Fluence with 10^8 g/s on LH_2 Target with 1/3 efficiency
 → $3 \times 10^8 n_{eq}/cm^2/year$



M. Ramilli

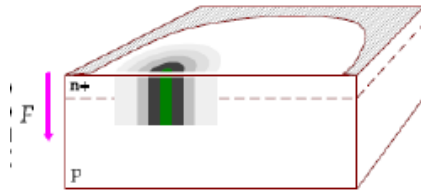
no temperature dependence of the PDE



Dinu, IEEE NSS 2010

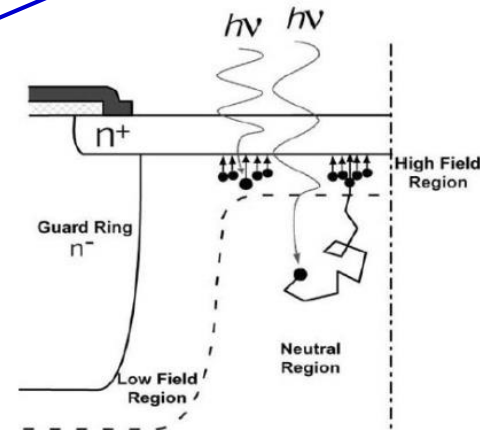
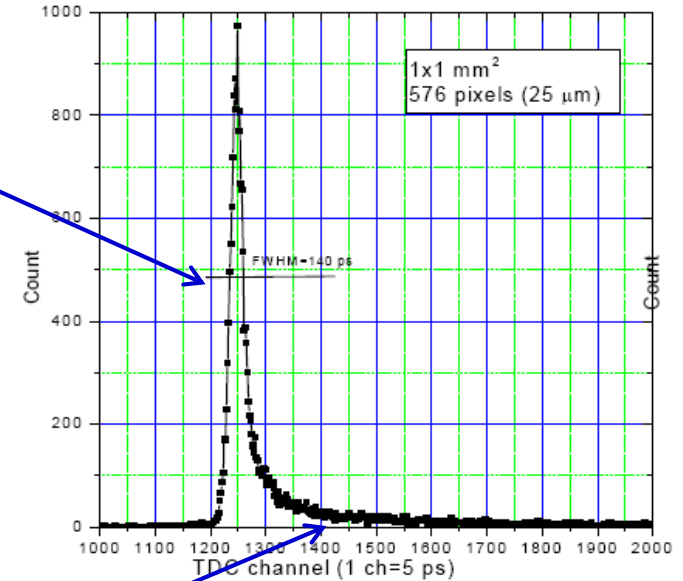
Two components :

fast component of Gaussian shape with $50 \text{ ps} < \sigma < 150 \text{ ps}$
 The fluctuation are due to the variance of the transverse diffusion speed and the variance of transverse position of photo-generation.



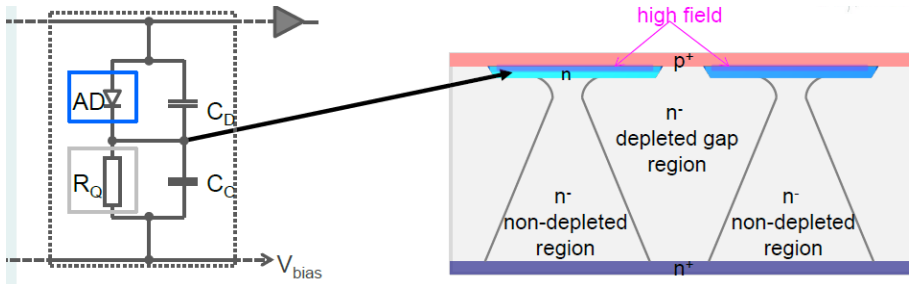
Transverse multiplication

slow component: minor non Gaussian tail with time scale of several ns due to minority carriers, photo-generated in the neutral regions beneath the depletion layer that reach the junction by diffusion.

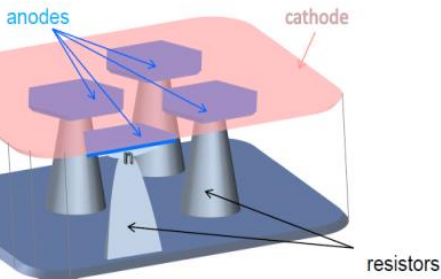
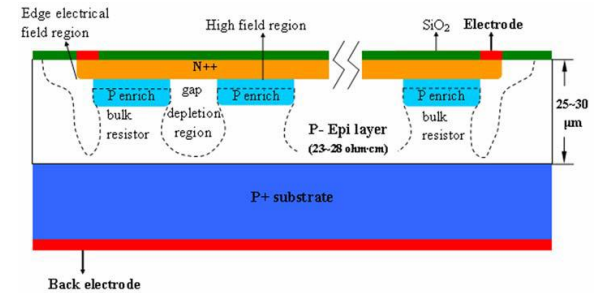


The quenching resistors are formed in the Si bulk rather than on the surface of the device

MPI



NDL

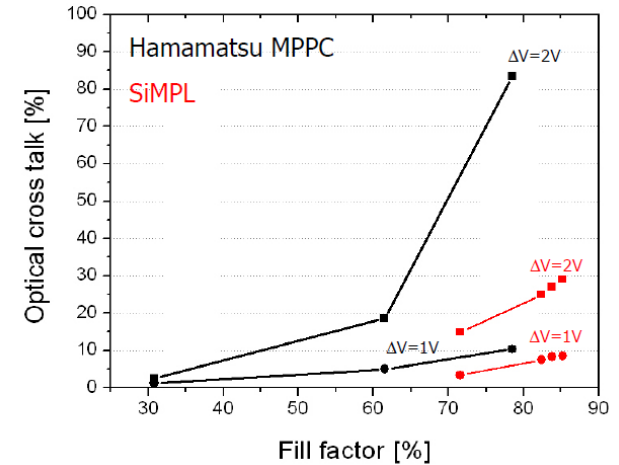
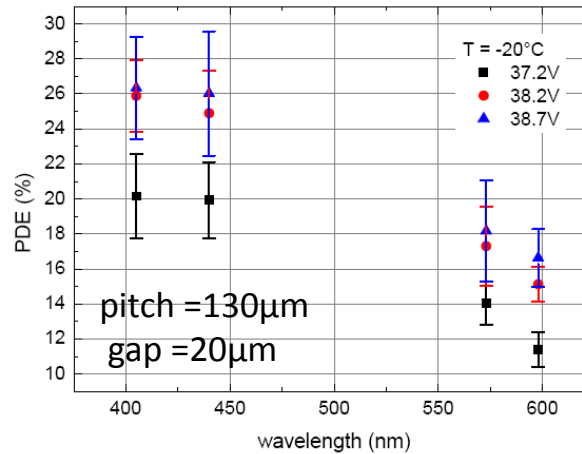


Advantages

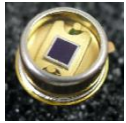
- simple fabrication process
- no obstacles in entrance window
- possible high geometrical fill-factor
- possibility of antireflective coating
- possible high cell density

MPI

- Pitch : 100 – 160 μm
- Gap : 5 – 20 μm
- Gain = 2 – 10×10^6
- Cross-talk = 15 – 30 % (-20°C)
- DCR = 10 MHz/mm² (25 °C)
- PDE (440 nm) = 26 % (-20°C)

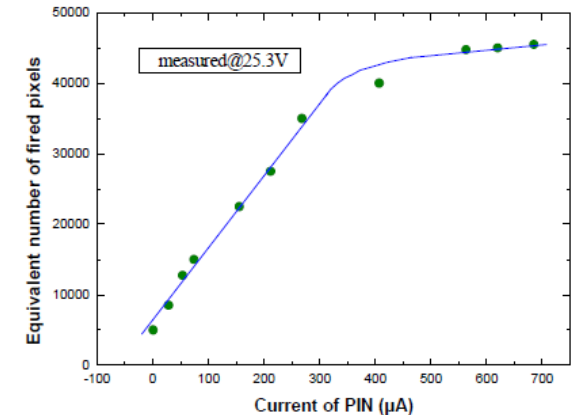
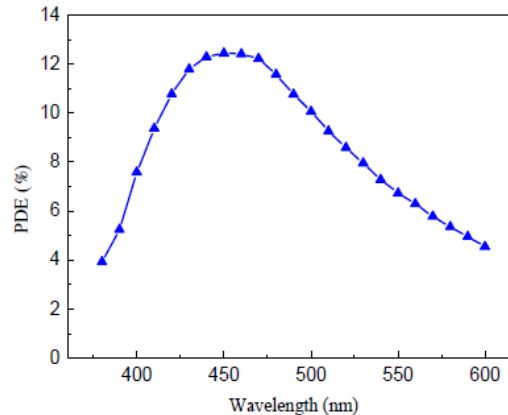


C. Jendrysik, NIM A 718 (2013)



NDL

- 2.2 × 2.2 mm² cell size : 42 μm
- 43400 cells
- DCR = 8 MHz/mm² (21 °C)
- Gain = 2 × 10⁵ (21 °C)
- PDE (460 nm) = 12 %
- recovery time : 5.8 ns



C. Li, IEEE NSS 2013

Promising results

R&D on going at MPI and NDL to improve the structure and the performances

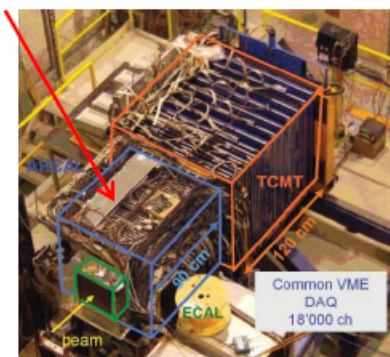
High granularity hadronic calorimeter optimised for the Particle Flow measurement of multi-jets final state at the ILC

Photodetector requirements:

- insensitive to magnetic field ($\sim 4T$)
- good sensitivity in blue-green
- cheap (10 millions channels)

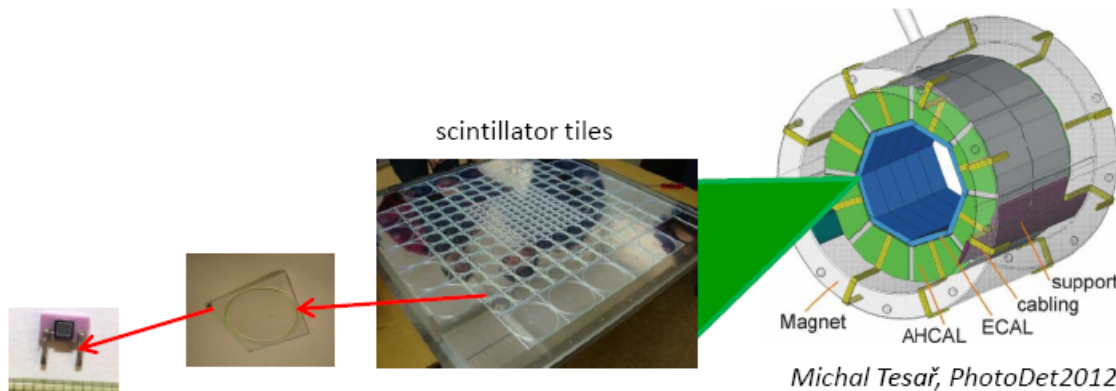
studied SiPMs : MePHI/PULSAR, CPTA

HCAL prototype (from 2007 to 2011)



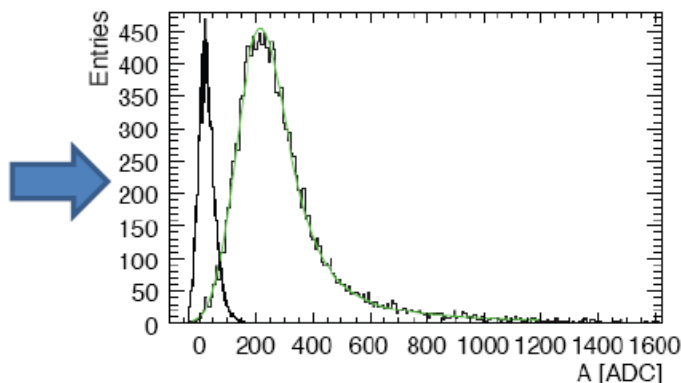
38 layers - ~ 7600 SiPMs from MePHI/PULSAR

temperature dependence (variation of PDE x Gain : $3.7\%/^{\circ}C$ %) \rightarrow correction of response variations



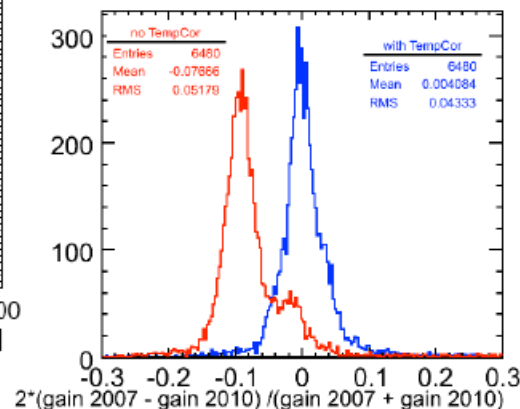
Michal Tesař, PhotoDet2012

HCAL test beams at SPS H8



MIP distribution of muons

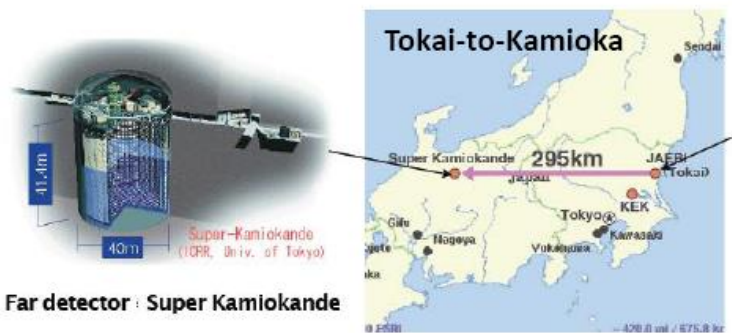
CALICE Collaboration, 2010 JINST 5 P05004



S. Lu, LCWS11

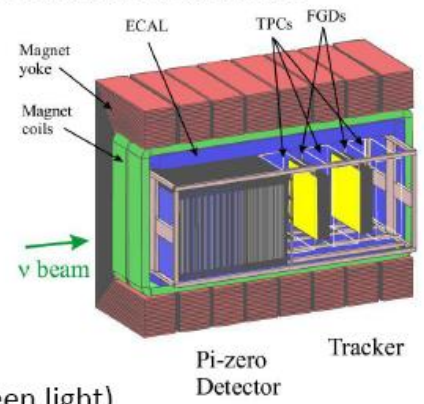
Ongoing activity : engineering prototype is now under construction with SiPM from CPTA

SiPMs for neutrino oscillation experiment: T2K



Far detector: Super Kamiokande

ND280: near detector complex - neutrino beam flux and spectrum measurements



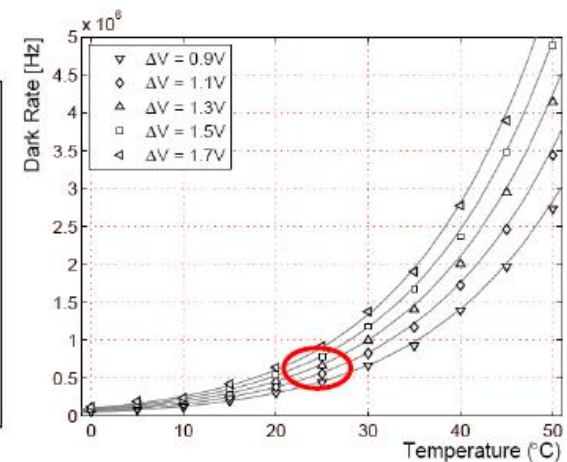
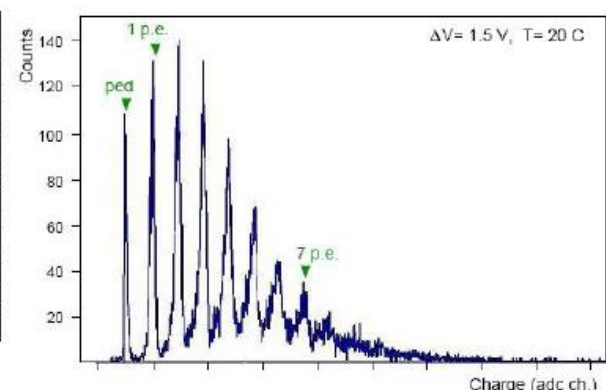
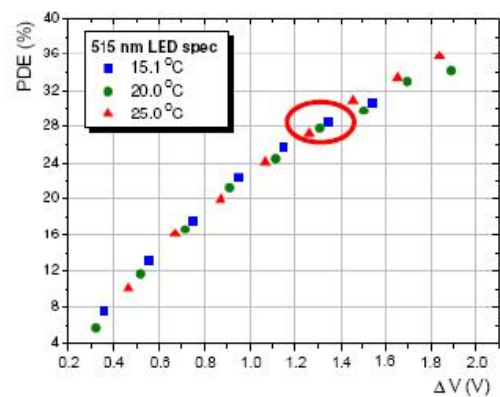
HAMAMATSU MPPC customized device



1.3 x 1.3 mm²
667 cells (50 x 50 μ m²)

Photodetector requirements:

- insensitive to magnetic field
- coupling with a scintillator + WLS fiber (PDE > 20 % for green light)
- DCR < 1 MHz
- compact



A. Vacheret, arXiv:1101.1996

55996 MPPC tested : only 0,16 % rejected



SiPMs for Cherenkov light detection (IACT)



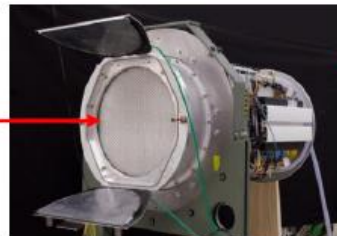
FACT: First G-APD Cherenkov Telescope



MPPC S10362-33-50C
coupled to a cone light
concentrator



1440 channels



Th. Krähenbühl, Photodet
2012

Photodetector requirements:

- PDE > 20 % for blue light
- ability to detect single photons
- stable
- robust
- compact

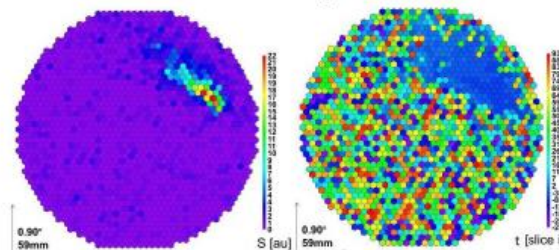
problem with the SiPM V_{BD} temperature dependence
→ regulation of the bias voltage with a feedback system

First operation on the night of October 11, 2011

After one year of routine operation:

- no indication of any problem or ageing in any SiPM
- temperature as well as ambient-light dependence of SiPM well under control
- operation under very different ambient conditions shows no problem

an Event Seen by FACT



P. Voqler, TWEPP 2012